Robotic Arm Design

Joseph T. Wunderlich, Ph.D.

“Lunar Roving Vehicle” (LRV) *Robotic Arms*

Image from: Young, A.H. ***Lunar and planetary rovers: the wheels of Apollo and the quest for mars***, S

Human Arms do the dexterous “manipulation” work on manned missions

"Lunar Roving Vehicle" (LRV) *Robotic Arms*

1971

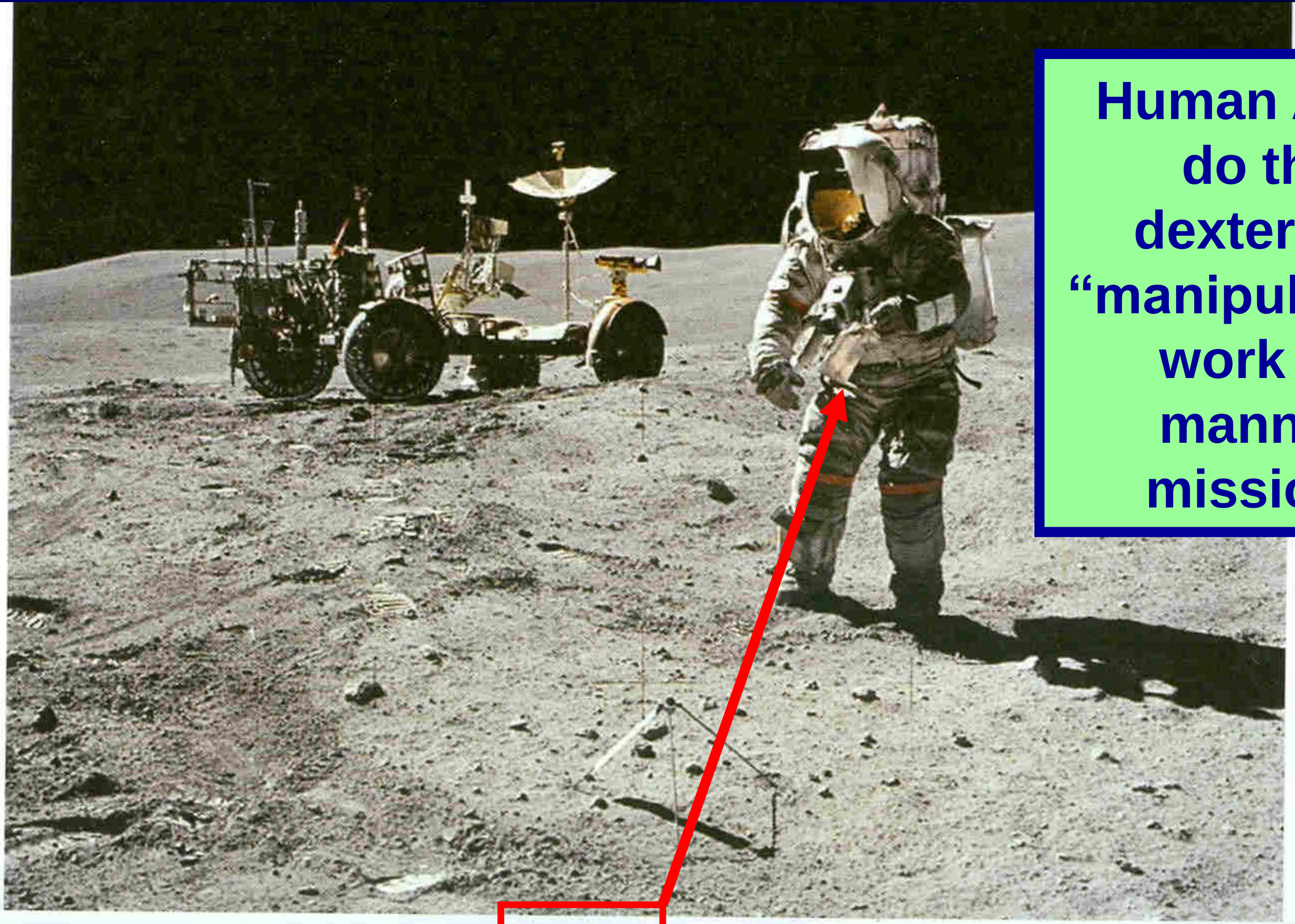

Human Arms do the dexterous "manipulation" work on manned missions

Plate 40 Charlie Duke photographed John Young as he took a sample at the Station 10 stop. Young remarked that driving conditions as a result of Sun angle and direction of the traverse made it nearly impossible to detect surface hazards in front of the LRV. (NASA)

Image from: Young, A.H. ***Lunar and planetary rovers: the wheels of Apollo and the quest for mars***, Springer; 1 edition, August 1, 2006.

Mars Rovers

Robotic Arms

Mars Pathfinder "Sojourner"

1996

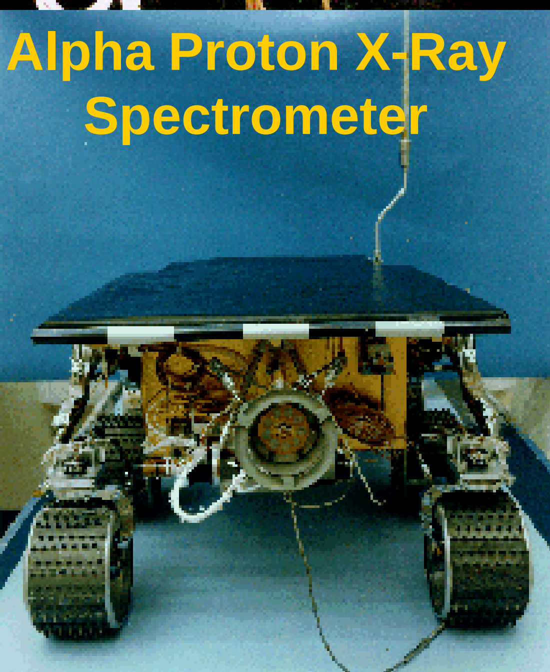

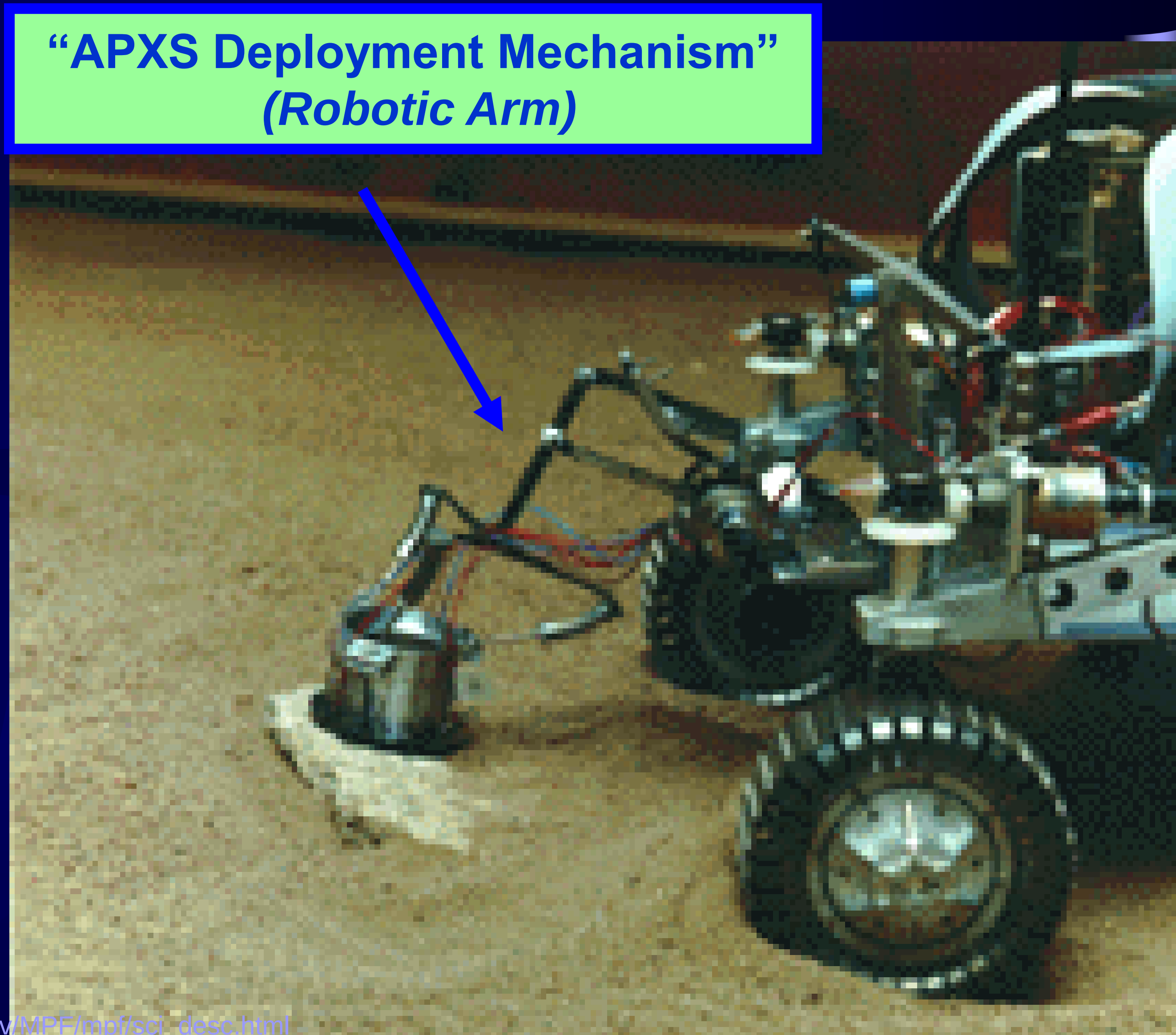

Image from: http://marsprogram.jpl.nasa.gov/MPF/mpf/sci_desc.html

Mars Rovers

"Spirit" & "Opportunity"

Robotic Arms

2004

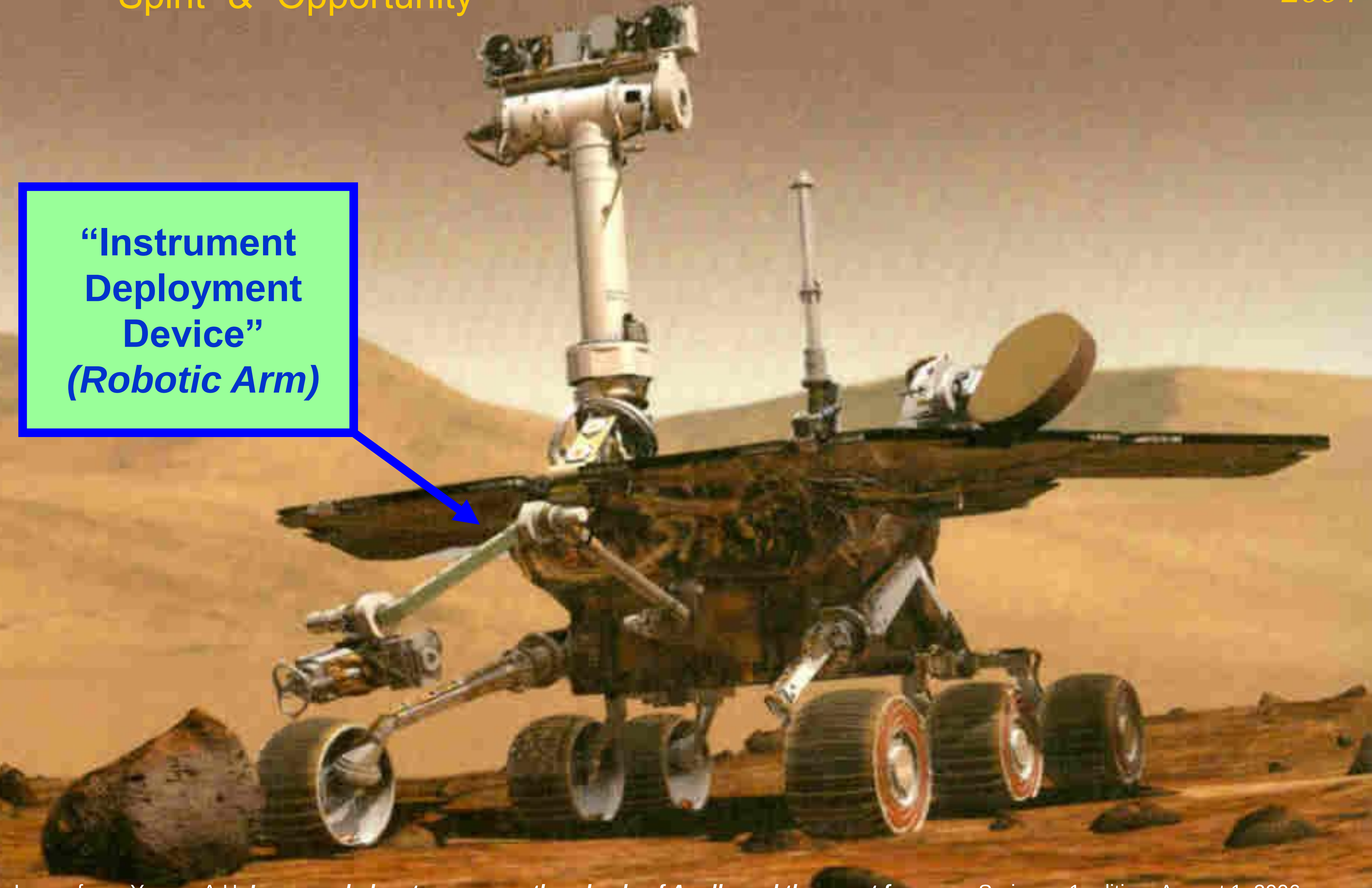

Image from: Young, A.H. ***Lunar and planetary rovers: the wheels of Apollo and the quest for mars***, Springer; 1 edition, August 1, 2006.

Mars Rovers

Robotic Arms

“Spirit” & “Opportunity”

2004

“Instrument Deployment Device”
(Robotic Arm)

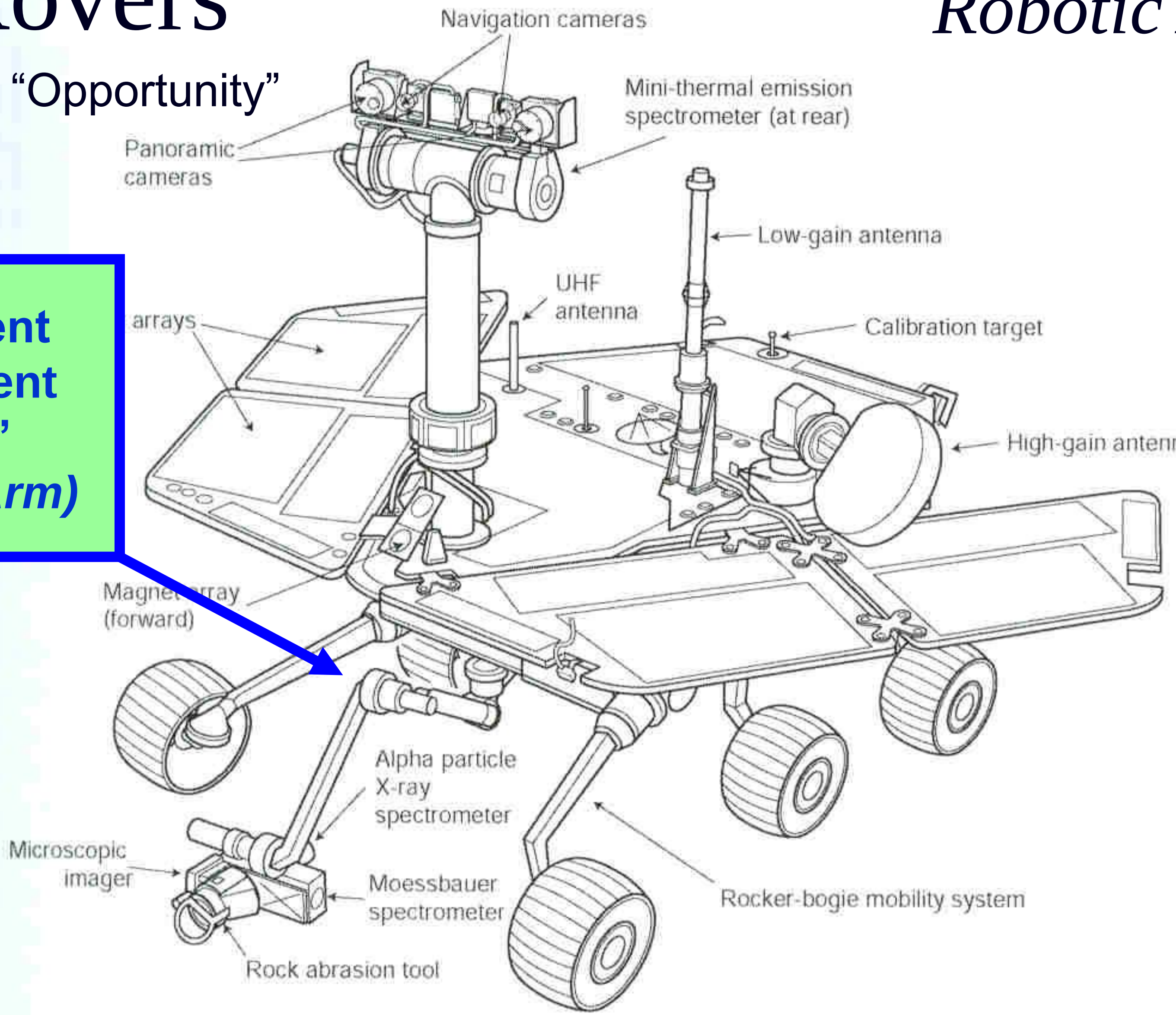

This illustration shows key components of the MER rover from the top but does not show the bulk of the electronic equipment inside the body of the rover. (NASA/JPL)

Image from: Young, A.H. ***Lunar and planetary rovers: the wheels of Apollo and the quest for mars***, Springer; 1 edition, August 1, 2006.

Mars Rovers

"Spirit" & "Opportunity"

Robotic Arms

2004

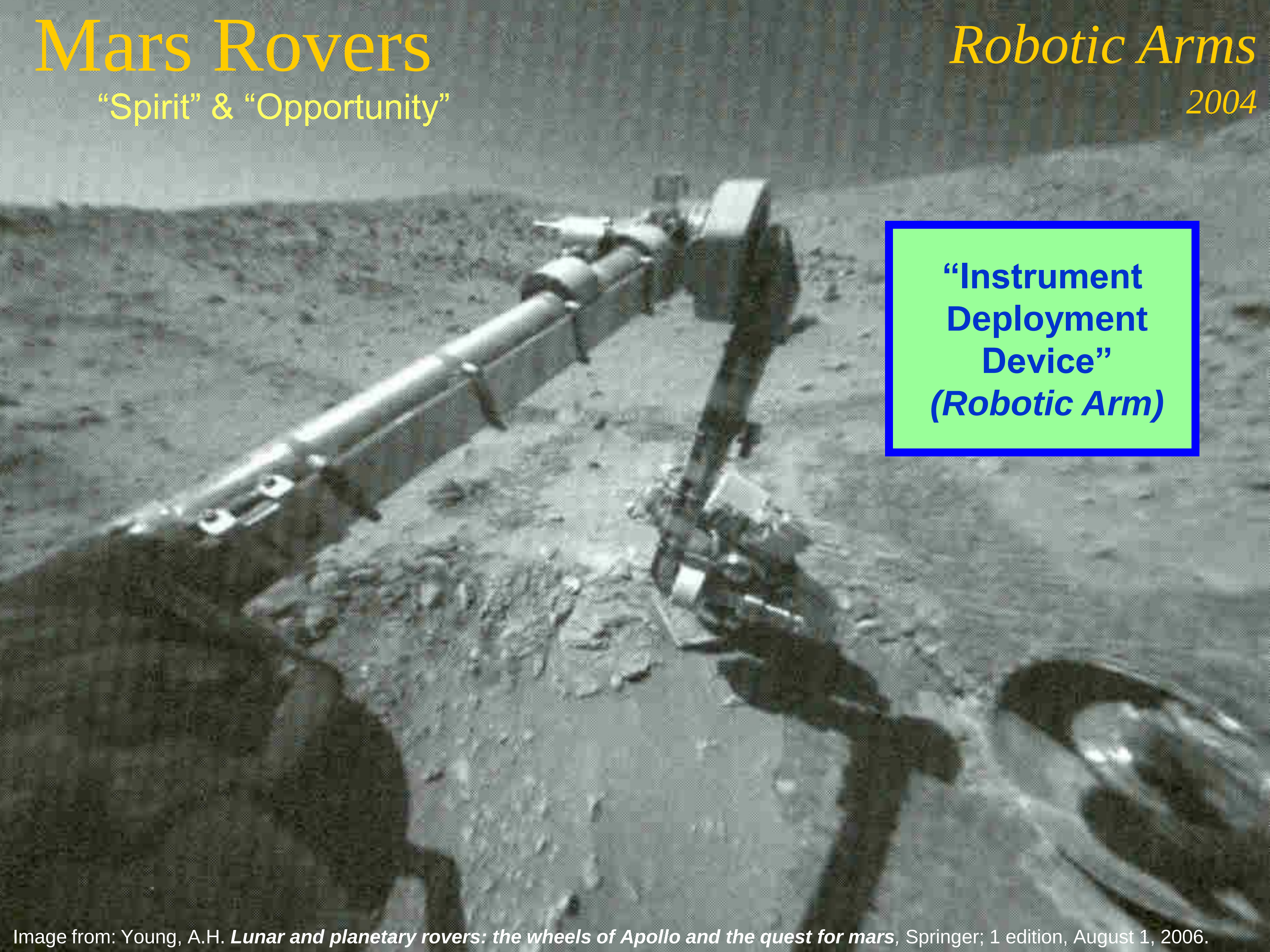

Image from: Young, A.H. ***Lunar and planetary rovers: the wheels of Apollo and the quest for mars***, Springer; 1 edition, August 1, 2006.

Mars Rovers

Mars Science Lab

Robotic Arms

2000's

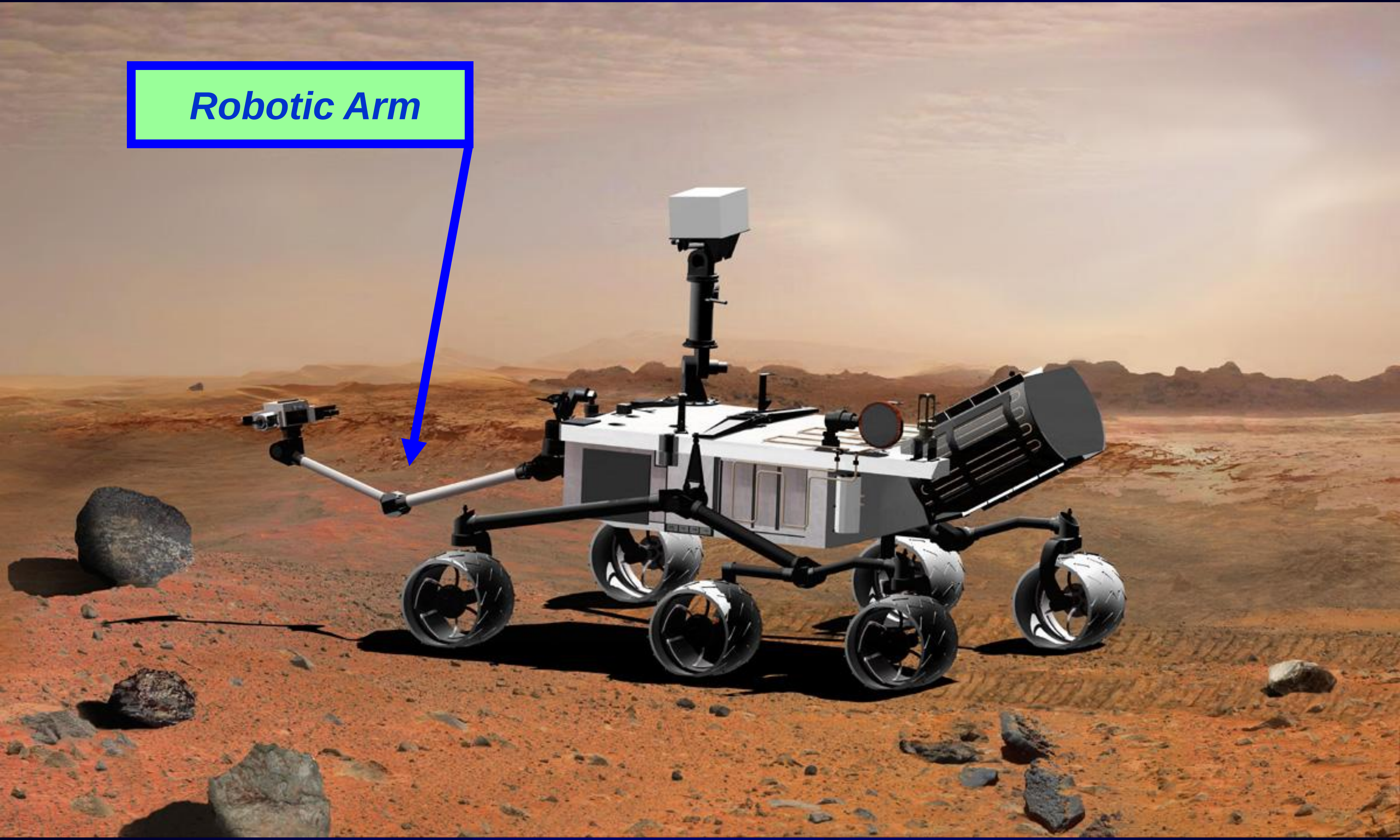

Image from: http://nssdc.gsfc.nasa.gov/planetary/mars_future.html

Mars Rovers

Robotic Arms

2000's and 2010's

ESA
"ExoMars"
Rover
Concept

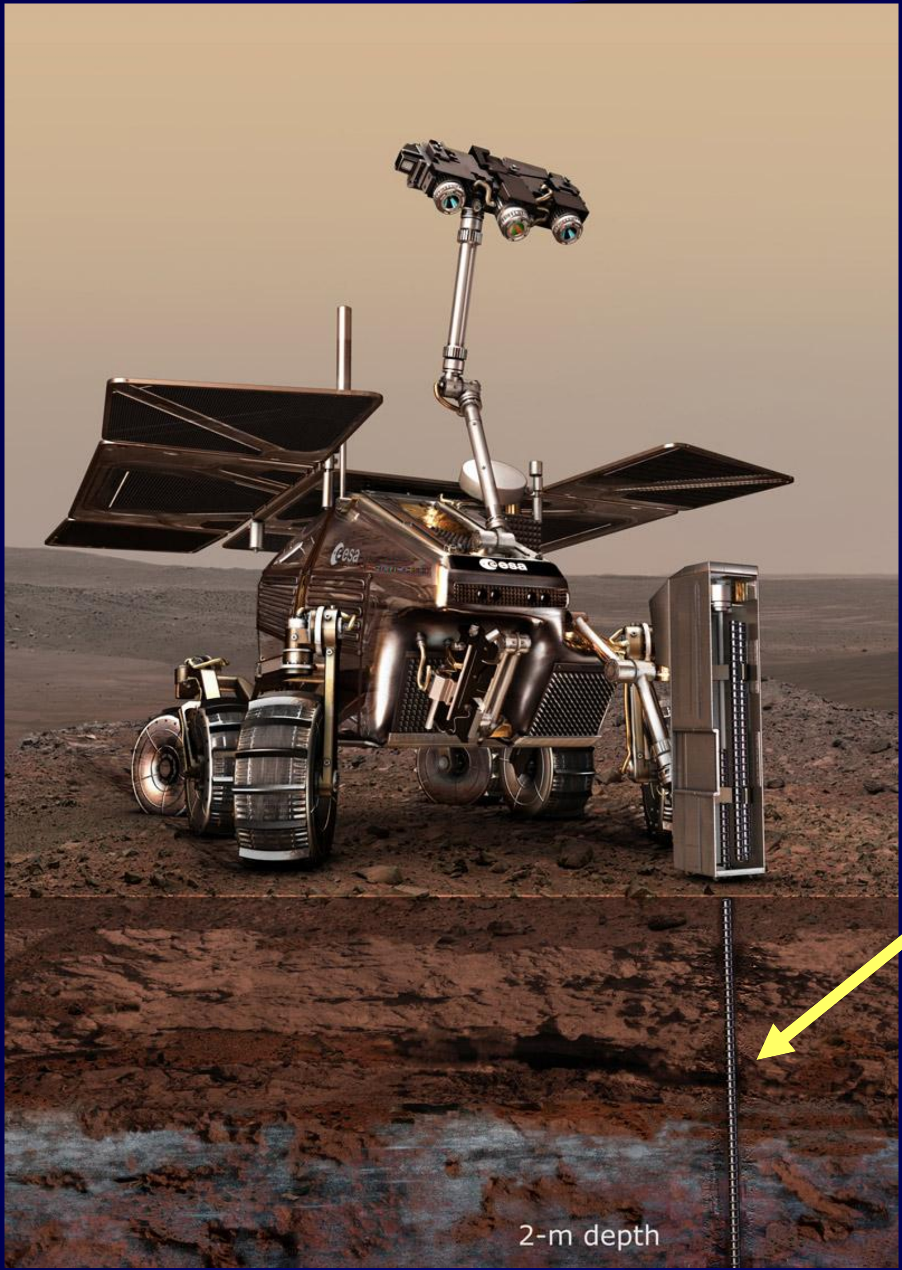

It has a drill

Image from: http://www.nasa.gov/centers/jpl/news/urey-20070209.html

Kinematics review

Before studying advanced robotic arm design we need to review basic manipulator kinematics. So let's look at pages 9 and 10 of:

Wunderlich, J.T. (2001). **Simulation vs. real-time control; with applications to robotics and neural networks**. In *Proceedings of 2001 ASEE Annual Conference & Exposition, Albuquerque, NM*: (session 2793), [CD-ROM]. ASEE Publications.

Kinematics review

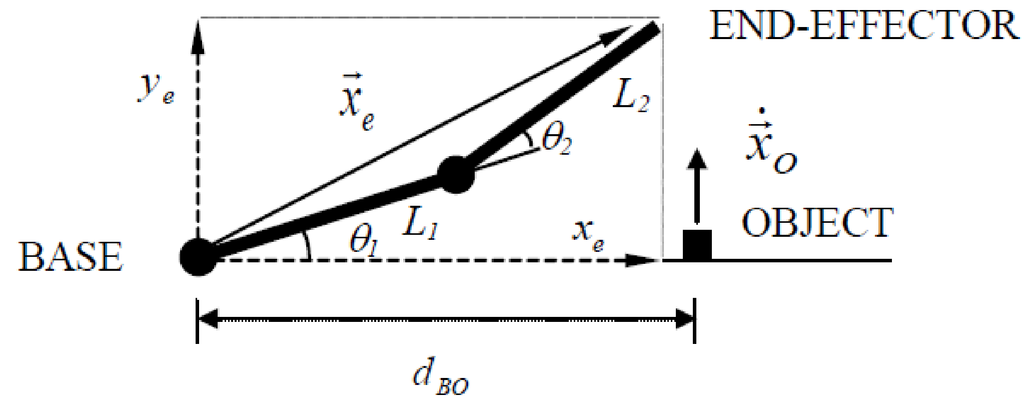

Figure 7. A two degree-of-freedom robotic-arm.

where $\vec{x}_e$ is the vector that locates the Cartesian position of the robotic-arm's end-effector with respect to the base. The end-effector position $\vec{x}_e$ is related to the joint angles by

$$\vec{x}_e = \begin{bmatrix} x_e \\ y_e \end{bmatrix} = \begin{bmatrix} L_1 \cos(\theta_1) + L_2 \cos(\theta_1 + \theta_2) \\ L_1 \sin(\theta_1) + L_2 \sin(\theta_1 + \theta_2) \end{bmatrix} \quad (2)$$

and the end-effector velocity (i.e., the derivative of $\vec{x}_e$ with respect to time) is

$$\dot{\vec{x}}_e = d\vec{x}_e / dt = \begin{bmatrix} \dot{x}_e \\ \dot{y}_e \end{bmatrix} = \begin{bmatrix} dx_e / dt \\ dy_e / dt \end{bmatrix} \quad (3)$$

FROM: Wunderlich, J.T. (2001). **Simulation vs. real-time control; with applications to robotics and neural networks**. In *Proceedings of 2001 ASEE Annual Conference & Exposition, Albuquerque, NM*: (session 2793), [CD-ROM]. ASEE Publications.

Kinematics review

FROM: Wunderlich, J.T. (2001). **Simulation vs. real-time control; with applications to robotics and neural networks**. In *Proceedings of 2001 ASEE Annual Conference & Exposition, Albuquerque, NM*: (session 2793), [CD-ROM]. ASEE Publications.

where, using the "chain-rule" of differentiation for multi-variable functions,

$$\frac{dx_e}{dt} = \frac{\partial x_e}{\partial \theta_1}\frac{d\theta_1}{dt} + \frac{\partial x_e}{\partial \theta_2}\frac{d\theta_2}{dt} \qquad (4)$$

$$\frac{dy_e}{dt} = \frac{\partial y_e}{\partial \theta_1}\frac{d\theta_1}{dt} + \frac{\partial y_e}{\partial \theta_2}\frac{d\theta_2}{dt} \qquad (5)$$

we obtain:

$$\begin{bmatrix} dx_e/dt \\ dy_e/dt \end{bmatrix} = \begin{bmatrix} \partial x_e/\partial\theta_1 & \partial x_e/\partial\theta_2 \\ \partial y_e/\partial\theta_1 & \partial y_e/\partial\theta_2 \end{bmatrix} \begin{bmatrix} d\theta_1/dt \\ d\theta_2/dt \end{bmatrix} \qquad (6)$$

or simply:

$$\dot{\vec{x}}_e = J_e \dot{\vec{\theta}} \qquad (7)$$

where J_e is the "Jacobian" matrix:

$$\mathbf{J_e} = \begin{bmatrix} -L_1\sin(\theta_1) - L_2\sin(\theta_1+\theta_2) & -L_2\sin(\theta_1+\theta_2) \\ L_1\cos(\theta_1) + L_2\cos(\theta_1+\theta_2) & L_2\cos(\theta_1+\theta_2) \end{bmatrix} \qquad (8)$$

which gives us our linear transformation between Cartesian end-effector velocities and robotic-arm joint-angle velocities. For simulating this system, we also need the Cartesian position of the robotic-arm's elbow with respect to it's base:

$$\vec{x}_{elbow} = \begin{bmatrix} x_{elbow} \\ y_{elbow} \end{bmatrix} = \begin{bmatrix} L_1\cos(\theta_1) \\ L_1\sin(\theta_1) \end{bmatrix} \qquad (9)$$

To command the end-effector to perform a task in Cartesian space, we need to command joint-angle velocities. This is accomplished by manipulating equation (7) to form:

$$\dot{\vec{\theta}} = J_e^{-1}\dot{\vec{x}}_e \qquad (10)$$

where J_e^{-1} is the inverse of J_e.

What kind of arm has OPTIMAL DEXTERITY?

A Redundant Manipulator?
(i.e., More **D**egrees **O**f **F**reedom than you *need*)

Human Arm is a 7 DOF Redundant Manipulator

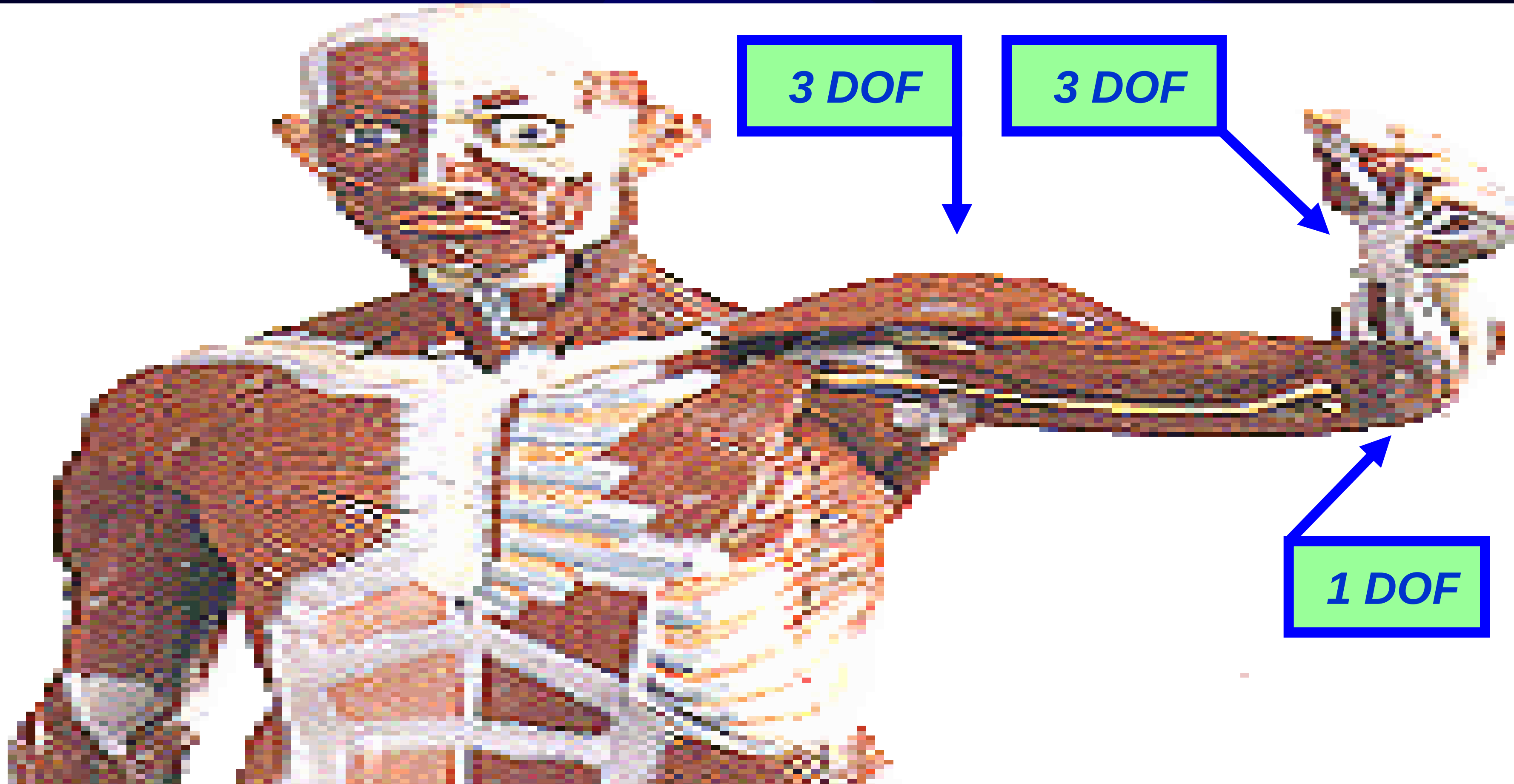

What kind of arm has OPTIMAL DEXTERITY?

A Hyper-Redundant Manipulator?
(i.e., Many more **D**egrees **O**f **F**reedom than "*needed*")

OPTIMAL DEXTERITY?

Would many Hyper-Redundant Manipulators be optimal?
(i.e., Each with many more **D**egrees **O**f **F**reedom than "*needed*")

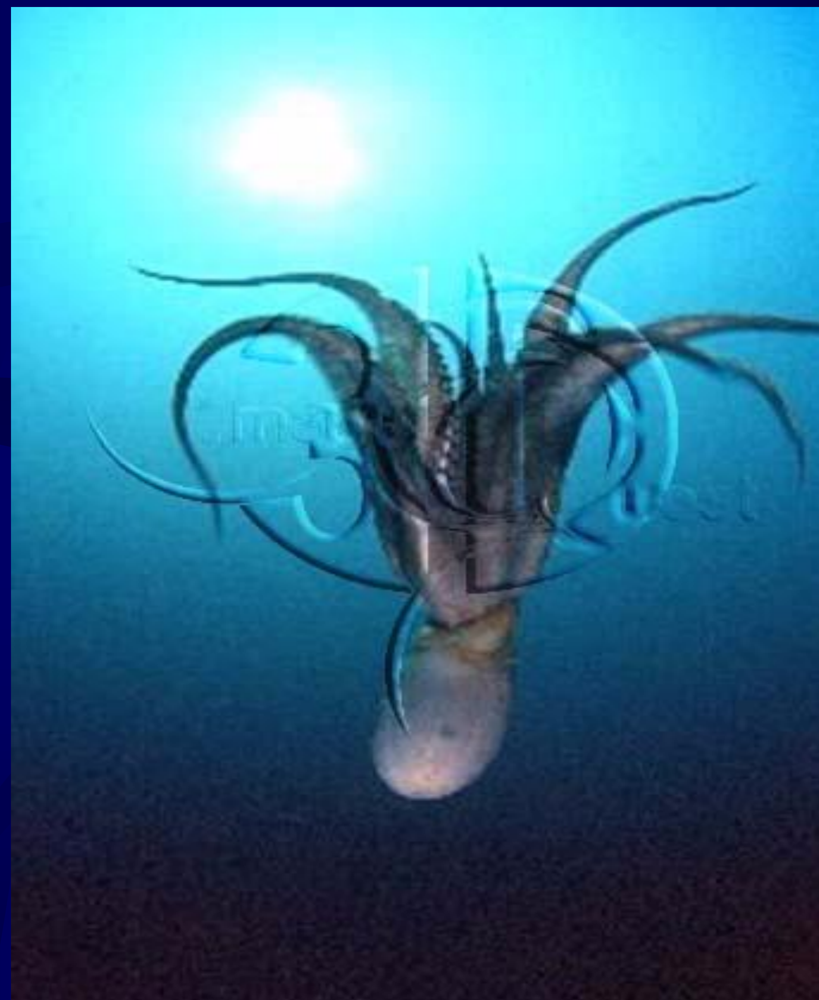

J. Wunderlich Related Publications

Wunderlich, J.T. (2004). **Simulating a robotic arm in a box: redundant kinematics, path planning, and rapid-prototyping for enclosed spaces.** In *Transactions of the Society for Modeling and Simulation International*: Vol. 80. (pp. 301-316). San Diego, CA: Sage Publications.

Wunderlich, J.T. (2004). **Design of a welding arm for unibody automobile assembly.** In *Proceedings of IMG04 Intelligent Manipulation and Grasping International Conference, Genova, Italy*, R. Molfino (Ed.): (pp. 117-122). Genova, Italy: Grafica KC s.n.c Press.

Automobile Unibody

Automobile Unibody

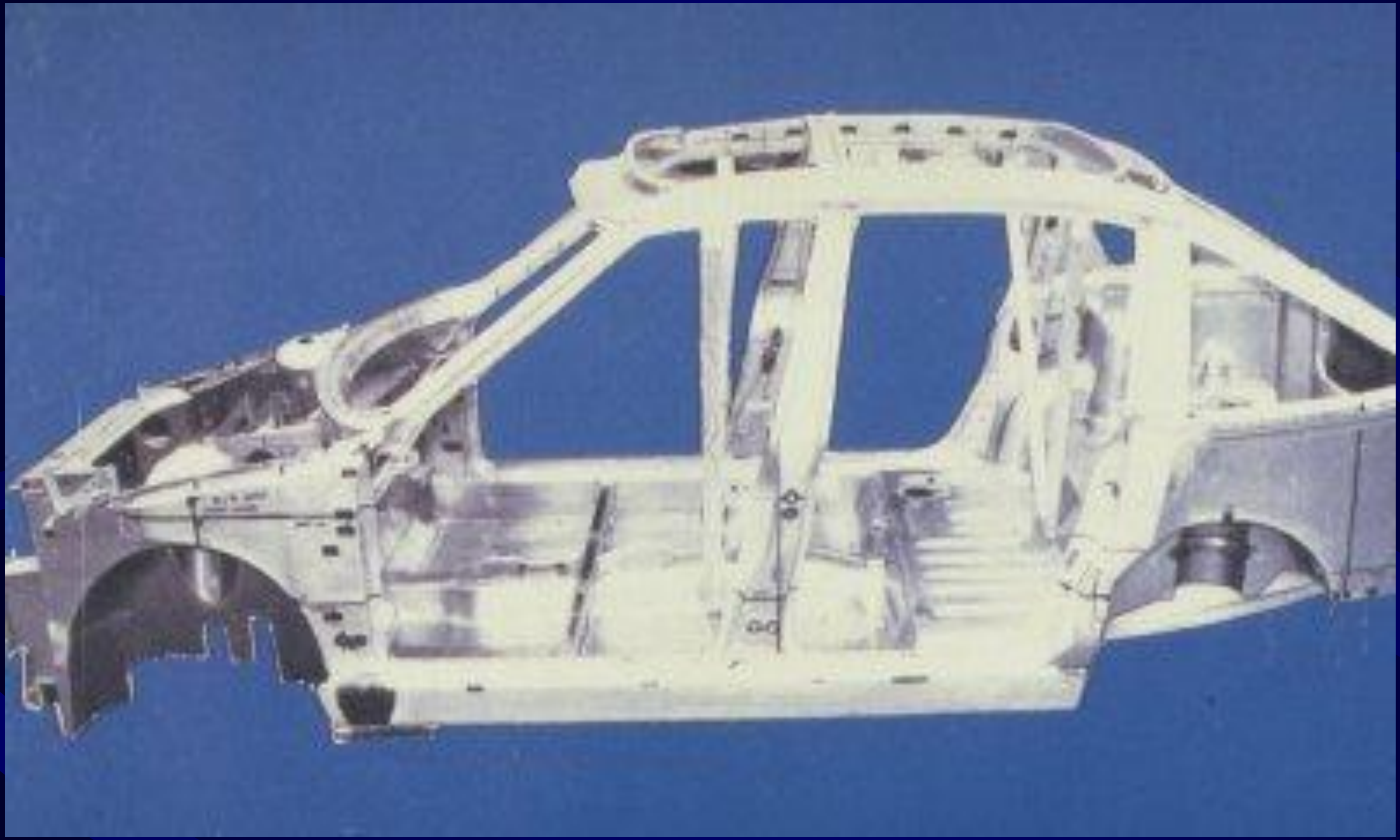

Automobile Unibody

Automobile Unibody

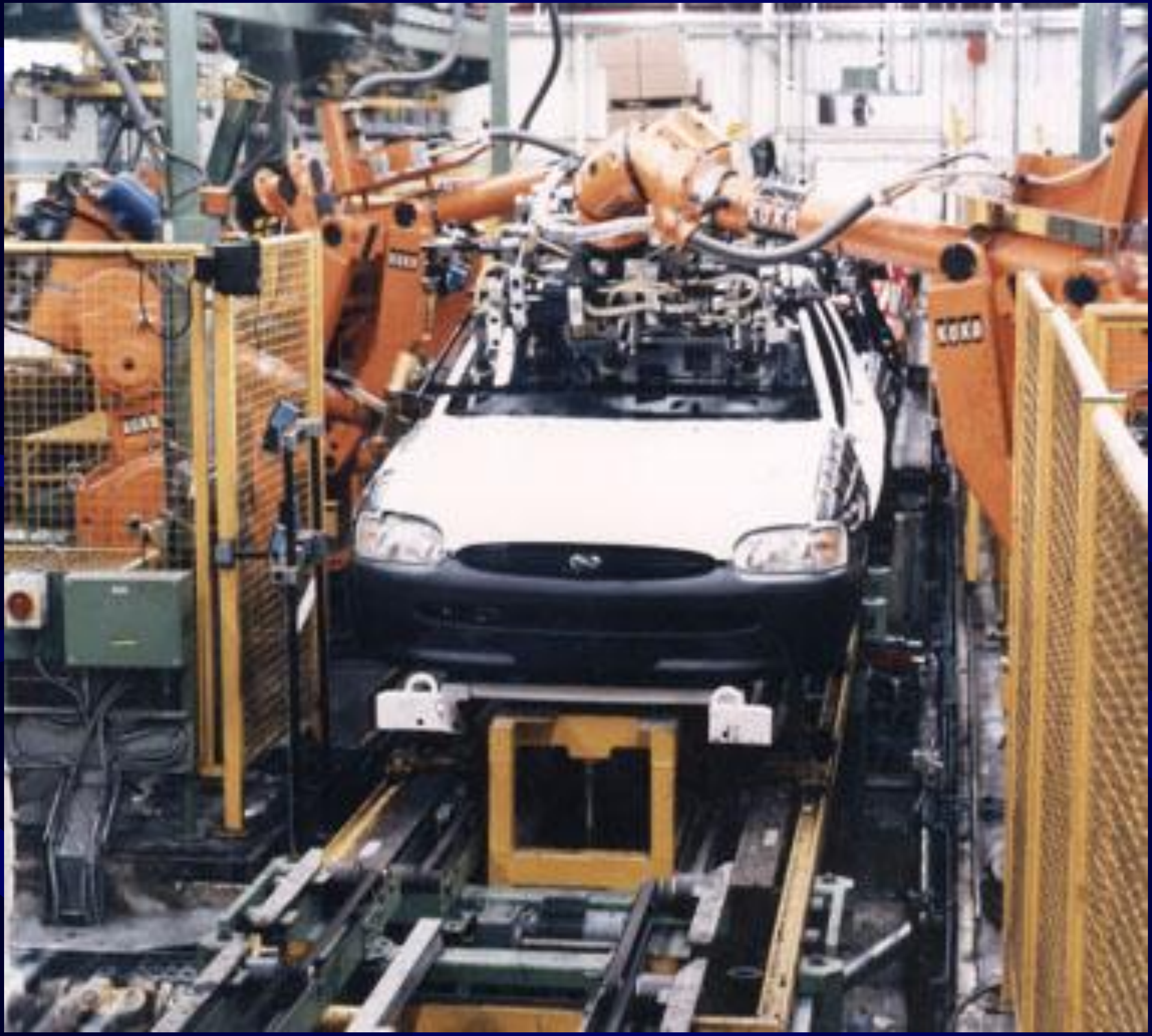

What Dr. Wunderlich saw in a US Chrysler automobile assembly plant in 1993
This inspired his PhD research

(this is a recent video of a Kia plant):

VIDEO: https://www.youtube.com/watch?v=sjAZGUcjrP8

Example for Welding Tasks

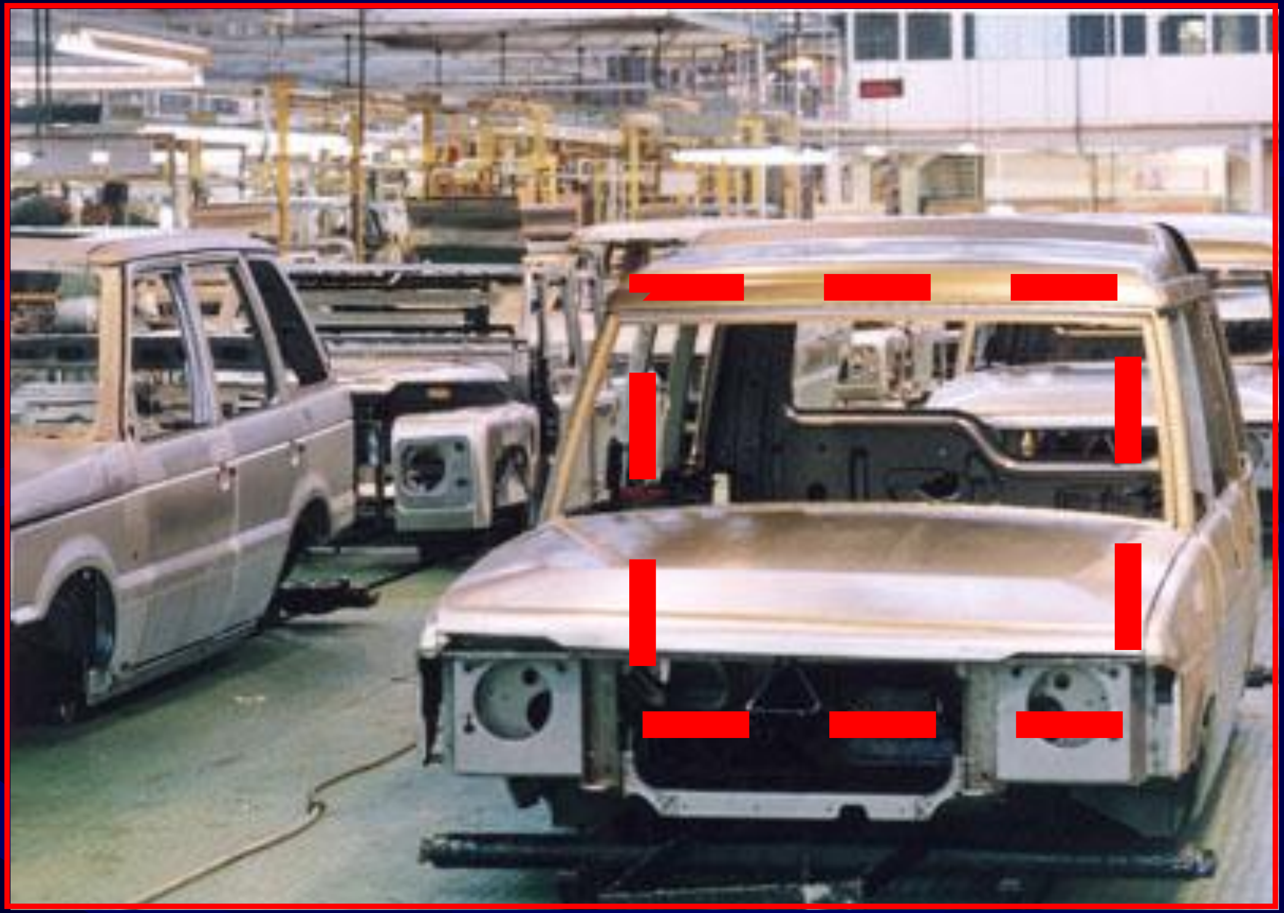

Example for Welding Tasks

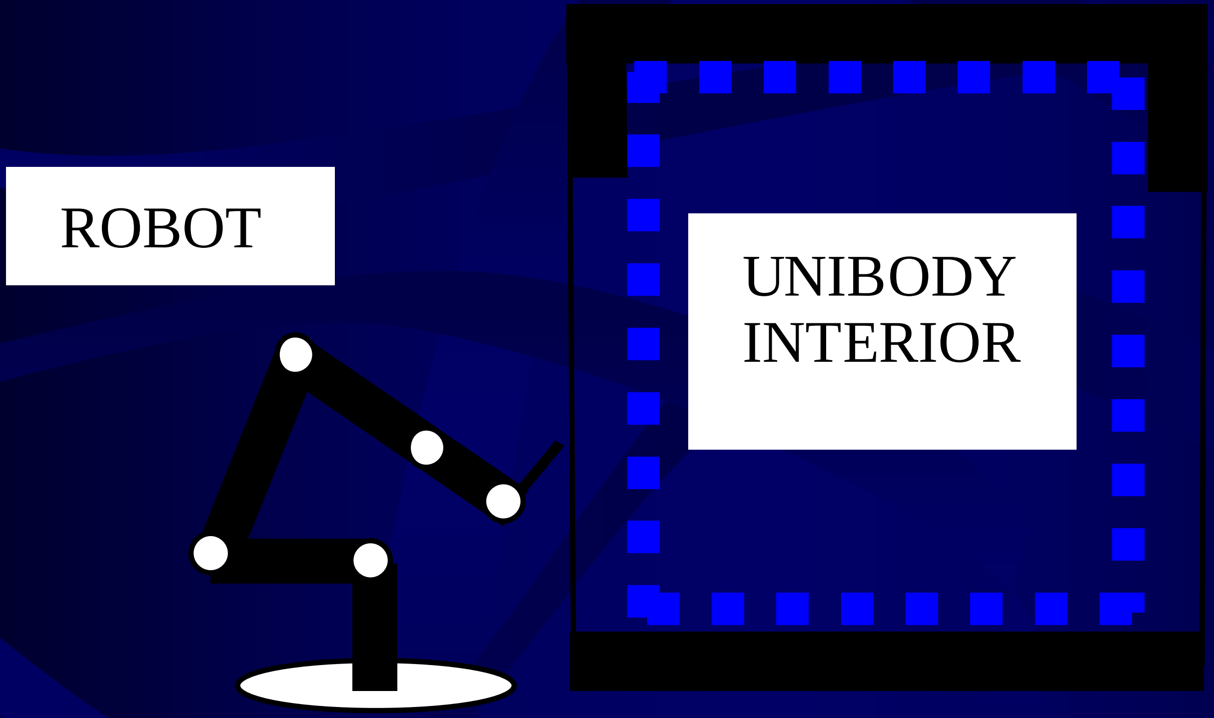

Simulation (initialization)

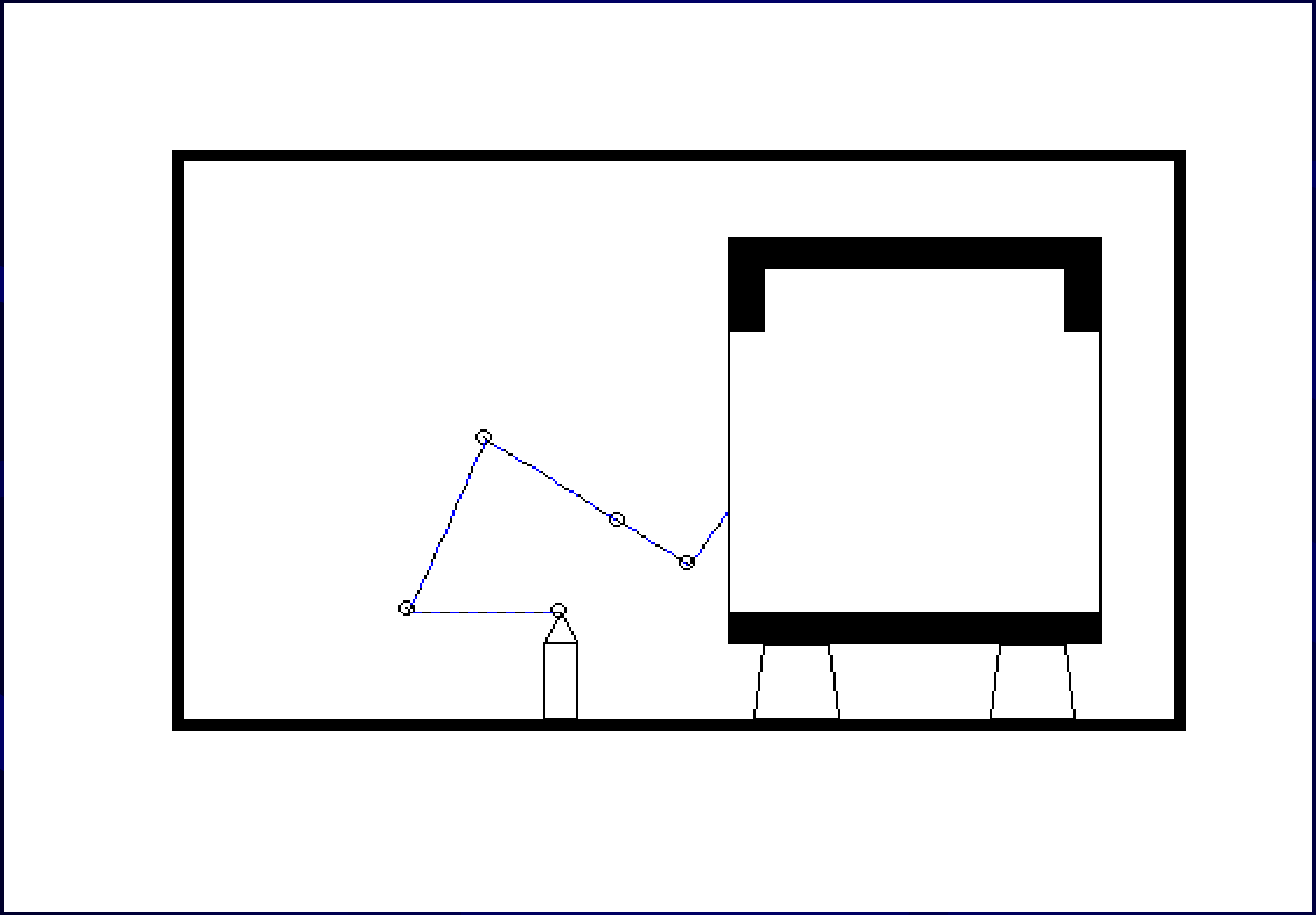

Simulation (go to task start point)

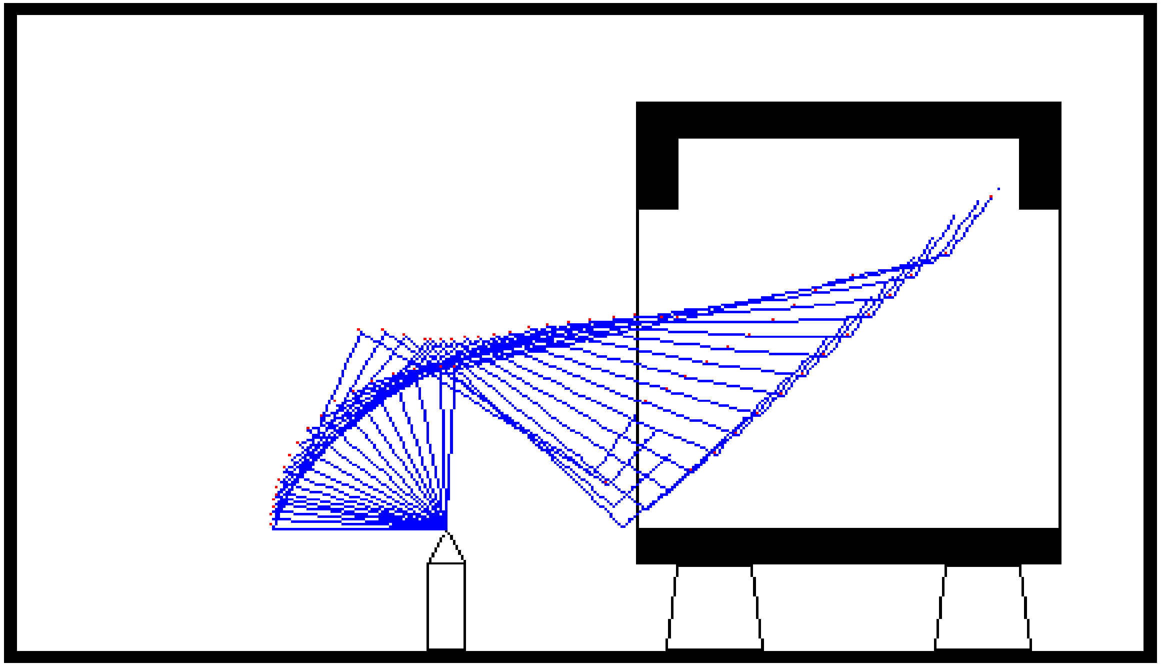

Simulation (perform welding task)

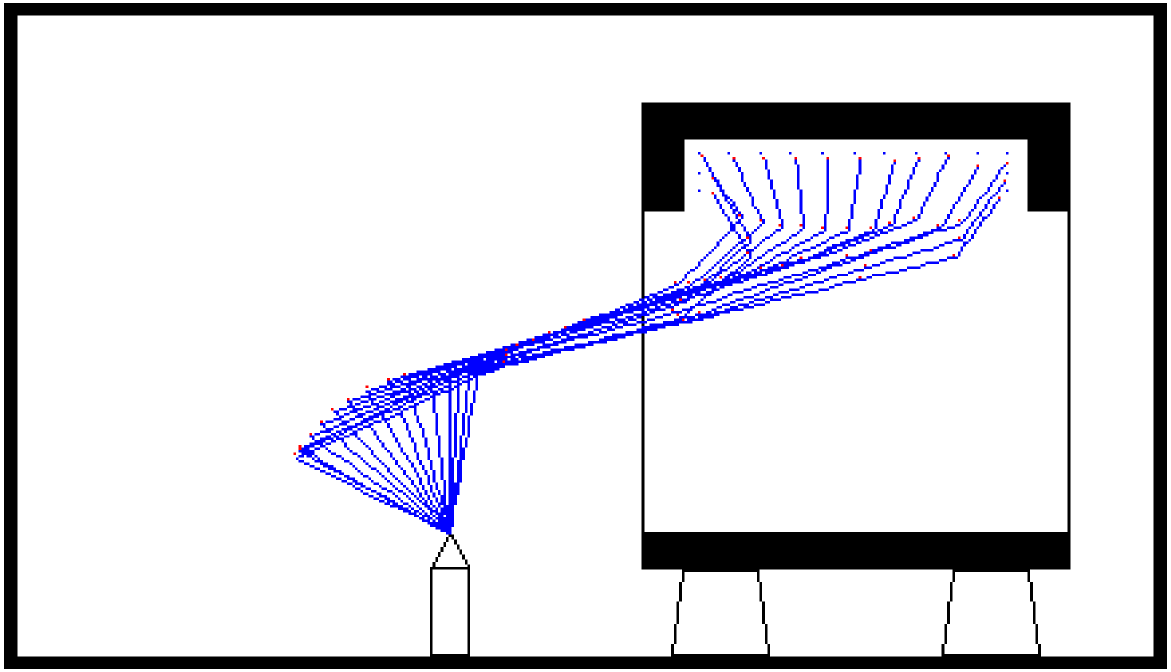

Path Planning

- Pseudo-inverse velocity control
- Attractive poles
- Repelling fields

Path Planning

- Pseudo-inverse velocity control

$$\dot{\mathbf{x}}_o = \mathbf{J}_o \dot{\theta}$$

$$\dot{\mathbf{x}}_o = \mathbf{J}_o \mathbf{J}_e{}^{\#} \dot{\mathbf{x}}_e + \mathbf{J}_o (\mathbf{I} - \mathbf{J}_e{}^{\#} \mathbf{J}_e) \dot{\Psi}$$

$$\dot{\theta} = \mathbf{J}_e{}^{\#} \dot{\mathbf{x}}_e + \left[\mathbf{J}_o (\mathbf{I} - \mathbf{J}_e{}^{\#} \mathbf{J}_e) \right]^{\#} (\dot{\mathbf{x}}_o - \mathbf{J}_o \mathbf{J}_e{}^{\#} \dot{\mathbf{x}}_e)$$

by specifying a desired end-effector velocity and a desired obstacle-avoidance-point velocity

For derivation of these equations, read pages 1 to 4 of:

Wunderlich, J.T. (2004). **Simulating a robotic arm in a box: redundant kinematics, path planning, and rapid-prototyping for enclosed spaces**. In *Transactions of the Society for Modeling and Simulation International*: Vol. 80. (pp. 301-316). San Diego, CA: Sage Publications.

Path Planning

- Pseudo-inverse velocity control
  - With new proposed methodology here:

$$\dot{\theta} = \mathbf{J}_{\mathrm{e}}^{\#}\dot{\mathbf{x}}_{\mathrm{e}} + \sum_{i=1}^{N}\left[[\mathbf{J}_{o_i}(\mathbf{I} - \mathbf{J}_{\mathrm{e}}^{\#}\mathbf{J}_{\mathrm{e}})]^{\#}\dot{\Lambda} \right]$$

by specifying a desired end-effector velocity and multiple desired obstacle-avoidance-point velocities:

$$\dot{\Lambda} = \dot{\mathbf{x}}_o - \mathbf{J}_o\mathbf{J}_{\mathrm{e}}{}^{\#}\dot{\mathbf{x}}_{\mathrm{e}}$$

For derivation of these equations, read pages 1 to 4 of:

Wunderlich, J.T. (2004). **Simulating a robotic arm in a box: redundant kinematics, path planning, and rapid-prototyping for enclosed spaces**. In *Transactions of the Society for Modeling and Simulation International*: Vol. 80. (pp. 301-316). San Diego, CA: Sage Publications……………………….

Path Planning

FROM: Wunderlich, J.T. (2004). **Simulating a robotic arm in a box: redundant kinematics, path planning, and rapid-prototyping for enclosed spaces**. In *Transactions of the Society for Modeling and Simulation nternational*: Vol. 80. (pp. 301-316). San Diego, CA: Sage Publications

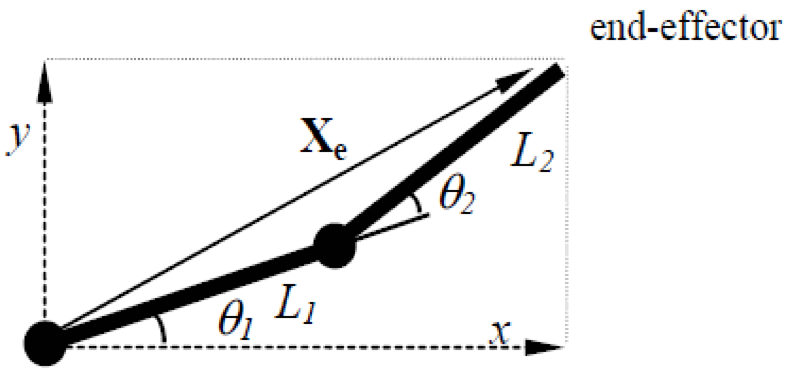

In general, for an n-DOF planar arm, the end-effector position is given by

$$\mathbf{x}_e = \begin{bmatrix} x \\ y \end{bmatrix} = \begin{bmatrix} \sum_{i=1}^{n} L_i * \left(\cos \left(\sum_{j=1}^{i} \theta_j \right) \right) \\ \sum_{i=1}^{n} L_i * \left(\sin \left(\sum_{j=1}^{i} \theta_j \right) \right) \end{bmatrix}, \qquad (1)$$

and the end-effector velocity is

$$\dot{\mathbf{x}}_e = \begin{bmatrix} \dot{x} \\ \dot{y} \end{bmatrix} = \begin{bmatrix} \partial x/\partial\theta_1 & \partial x/\partial\theta_2 \cdots & \partial x/\partial\theta_n \\ \partial y/\partial\theta_1 & \partial y/\partial\theta_2 \cdots & \partial y/\partial\theta_n \end{bmatrix} \begin{bmatrix} \dot{\theta}_1 \\ \dot{\theta}_2 \\ \vdots \\ \dot{\theta}_n \end{bmatrix}, \qquad (2)$$

or simply

$$\dot{\mathbf{x}}_e = \mathbf{J}_e \dot{\theta}, \qquad (3)$$

where $\mathbf{J}_e$ is the Jacobian matrix. Assuming $n > m$, where m is the dimension of the workspace, we have a redundant manipulator, and the general form of the least squares approximate solution to this underdetermined set of linear equations is

$$\dot{\theta} = \mathbf{J}_e^{\#} \dot{\mathbf{x}}_e + (\mathbf{I} - \mathbf{J}_e^{\#} \mathbf{J}_e) \dot{\mathbf{\Psi}}, \qquad (4)$$

Path Planning

FROM: Wunderlich, J.T. (2004). **Simulating a robotic arm in a box: redundant kinematics, path planning, and rapid-prototyping for enclosed spaces**. In *Transactions of the Society for Modeling and Simulation nternational*: Vol. 80. (pp. 301-316). San Diego, CA: Sage Publications

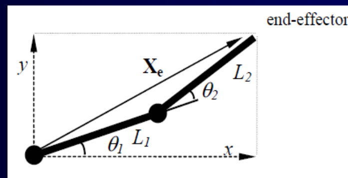

where $\mathbf{J}_e^\#$ is the pseudo-inverse, $\mathbf{I}$ is an identity matrix, $\dot{\boldsymbol{\Psi}}$ is an arbitrary joint-velocity vector that can be used for a variety of optimization and path-planning tasks, and $(\mathbf{I} - \mathbf{J}_e^\#\mathbf{J}_e)\dot{\boldsymbol{\Psi}}$ is the projection of $\dot{\Psi}$ onto the null space of $\mathbf{J}_e$ [4]. The pseudo-inverse $\mathbf{J}_e^\#$ is

$$\mathbf{J}_e^\# = \mathbf{J}_e^T(\mathbf{J}_e\mathbf{J}_e^T)^{-1} \tag{5}$$

here since $(m < n)$, and $\mathbf{J}_e$ is assumed to be of rank m. Equation (4) represents the least squares solution that minimizes the error norm,

$$\min \left\| \dot{\mathbf{x}}_e - \mathbf{J}_e\dot{\theta} \right\| , \tag{6}$$

and focuses on the *exactness* of the solution [5]. The first term of (4) represents the minimum norm solution among all solutions provided by (4) by also satisfying

$$\min \left\| \dot{\theta} \right\| , \tag{7}$$

which relates to the *feasibility* of implementing a solution since excessively large joint-angle velocities are not realizable [5].

The pseudo-inverse velocity-control part of the proposed path-planning technique is a variation of that used in Maciejewski and Klein [8], where $\dot{\Psi}$ in (4) is used to repel a point X_o on an arm away from obstacles by commanding a Cartesian velocity:

$$\dot{\mathbf{x}}_o = \mathbf{J}_o\dot{\theta}, \tag{8}$$

where (o) designates the point on the arm closest to an obstacle (*obstacle-avoidance point*). In Maciejewski and Klein [8], (4) is substituted into (8) to yield

$$\dot{\mathbf{x}}_o = \mathbf{J}_o\mathbf{J}_e^\#\dot{\mathbf{x}}_e + \mathbf{J}_o(\mathbf{I} - \mathbf{J}_e^\#\mathbf{J}_e)\dot{\Psi}, \tag{9}$$

where $\mathbf{J}_o\mathbf{J}_e^\#\dot{\mathbf{x}}_e$ is the Cartesian motion at the obstacle-avoidance point to satisfy the end-effector velocity constraint. The second term of (9) represents the mapping of the $(\mathbf{I} - \mathbf{J}_e^\#\mathbf{J}_e)\dot{\boldsymbol{\Psi}}$ null-space joint-velocity vector to a Cartesian vector at the obstacle-avoidance point. The vector $\dot{\boldsymbol{\Psi}}$ is found by rewriting (9) as

$$\dot{\mathbf{x}}_o - \mathbf{J}_o\mathbf{J}_e^\#\dot{\mathbf{x}}_e = \mathbf{J}_o(\mathbf{I} - \mathbf{J}_e^\#\mathbf{J}_e)\dot{\Psi}, \tag{10}$$

where $\dot{\mathbf{x}}_o - \mathbf{J}_o\mathbf{J}_e^\#\dot{\mathbf{x}}_e$ is the desired obstacle-avoidance point Cartesian velocity:

$$\dot{\Lambda} = \dot{\mathbf{x}}_o - \mathbf{J}_o\mathbf{J}_e^\#\dot{\mathbf{x}}_e, \tag{11}$$

and $\mathbf{J}_o(\mathbf{I} - \mathbf{J}_e^\#\mathbf{J}_e)$ is the transformation of the orthogonal projection operator from the end effector to the obstacle-avoidance point:

$$\Gamma = \mathbf{J}_o(\mathbf{I} - \mathbf{J}_e^\#\mathbf{J}_e. \tag{12}$$

Using (11) and (12), we can rewrite (10) as

$$\dot{\Lambda} = \Gamma \dot{\Psi}, \tag{13}$$

where the general form of the least squares $\dot{\boldsymbol{\Psi}}$ solution is

$$\dot{\Psi} = \Gamma^{\#} \dot{\Lambda} + (\mathbf{I} - \Gamma^{\#} \Gamma) \dot{\beta}, \tag{14}$$

where $\mathbf{I}$ is an identity matrix, $\dot{\boldsymbol{\beta}}$ is an arbitrary vector, and $(\mathbf{I} - \boldsymbol{\Gamma}^{\#}\boldsymbol{\Gamma})\dot{\boldsymbol{\beta}}$ is the projection of $\dot{\boldsymbol{\beta}}$ into the null space of Γ.

This equation represents the least squares solution that minimizes the error norm:

$$\min \left\| \dot{\Lambda} - \Gamma \dot{\Psi} \right\| . \tag{15}$$

The first term of (14) represents the minimum-norm solution among all of the solutions provided by (14) by also satisfying

$$\min \left\| \dot{\Psi} \right\| , \tag{16}$$

which has the effect of increasing the minimum obstacle distance [8].

Substituting (14) into (4) yields

$$\begin{aligned} \dot{\theta} = {} & \mathbf{J}_e^{\#} \dot{\mathbf{x}}_e + (\mathbf{I} - \mathbf{J}_e^{\#} \mathbf{J}_e) \Gamma^{\#} \dot{\Lambda} \\ & + (\mathbf{I} - \mathbf{J}_e^{\#} \mathbf{J}_e) \left[(\mathbf{I} - \Gamma^{\#} \Gamma) \dot{\beta} \right] . \end{aligned} \tag{17}$$

In Nakamura, Hanafusa, and Yoshikawa [7], the third term of (17) is used for a tertiary-priority task if *enough* available redundancy remains after the higher priority tasks are satisfied. In Maciejewski and Klein [8], this term is dropped, and (17) is expanded to yield

$$\begin{aligned} \dot{\theta} = {} & \mathbf{J}_e^{\#} \dot{\mathbf{x}}_e + (\mathbf{I} - \mathbf{J}_e^{\#} \mathbf{J}_e) \\ & \left[\mathbf{J}_o (\mathbf{I} - \mathbf{J}_e^{\#} \mathbf{J}_e) \right]^{\#} (\dot{\mathbf{x}}_o - \mathbf{J}_o \mathbf{J}_e^{\#} \dot{\mathbf{x}}_e). \end{aligned} \tag{18}$$

In Maciejewski and Klein [8], it is shown that the second term of (18) can be reduced to $[\mathbf{J}_o(\mathbf{I} - \mathbf{J}_e^{\#}\mathbf{J}_e)]^{\#}(\dot{\mathbf{x}}_o - \mathbf{J}_o\mathbf{J}_e^{\#}\dot{\mathbf{x}}_e)$ since the projection operator $(\mathbf{I} - \mathbf{J}_e^{\#}\mathbf{J}_e)$ is both hermetian and idempotent, and therefore joint-angle velocities are governed by

$$\begin{aligned} \dot{\theta} = {} & \mathbf{J}_e^{\#} \dot{\mathbf{x}}_e + \left[\mathbf{J}_o (\mathbf{I} - \mathbf{J}_e^{\#} \mathbf{J}_e) \right]^{\#} \\ & (\dot{\mathbf{x}}_o - \mathbf{J}_o \mathbf{J}_e^{\#} \dot{\mathbf{x}}_e), \end{aligned} \tag{19}$$

by specifying a desired end-effector velocity $\dot{\mathbf{x}}_e$ and a desired obstacle-avoidance point velocity $\dot{\boldsymbol{\Lambda}} = \dot{\mathbf{x}}_o - \mathbf{J}_o\mathbf{J}_e^{\#}\dot{\mathbf{x}}_e$ through the selection of $\dot{\mathbf{x}}_o$.

The proposed technique for avoiding many obstacles within a complex enclosure is a variation of (19) and is given by

$$\dot{\theta} = \mathbf{J}_e^{\#} \dot{\mathbf{x}}_e + \sum_{i=1}^{N} \left[[\mathbf{J}_{o_i} (\mathbf{I} - \mathbf{J}_e^{\#} \mathbf{J}_e)]^{\#} \dot{\Lambda} \right] , \tag{20}$$

where $\dot{\boldsymbol{\Lambda}}$ is commanded directly, and where N is the number of obstacle-avoidance points, one fixed at each of the arm's joints (with the exception of the first two since they remain outside the enclosure). Up to eight obstacle-avoidance points have been simulated (i.e., on a 10-DOF arm). Here, unlike in (19), there is no need to locate these points on the arm since they are fixed; however mid-link collisions with obstacles become possible and are avoided by setting minimum allowable distances from obstacles.

Path Planning

- Pseudo-inverse velocity control
  - Technique made feasible by:
    - Attractive Poles
    - Repelling Fields
      - Proportional to obstacle proximity
      - Direction related to poles (or goal)
      - Limited range

Search for Feasible Designs

1) Guess initial kinematics
   - Link-lengths and DOF to reach furthest point in unibody
2) Find repelling-velocity magnitudes
3) Use heuristic(s) to change link-lengths
   - Test new designs
   - Can minimize DOF directly

Example Search

- Using heuristic that changes link lengths by 10cm, two at a time, results in 3489 new designs from an original (90,120,95,50,40,)cm 5-DOF design
  - This includes 104 4-DOF designs
- Another search; one designed specifically to minimize DOF, quickly yields 15 4-DOF designs (and 41 5-DOF designs)

New 4-DOF Design
(Generated from original 5-DOF design)

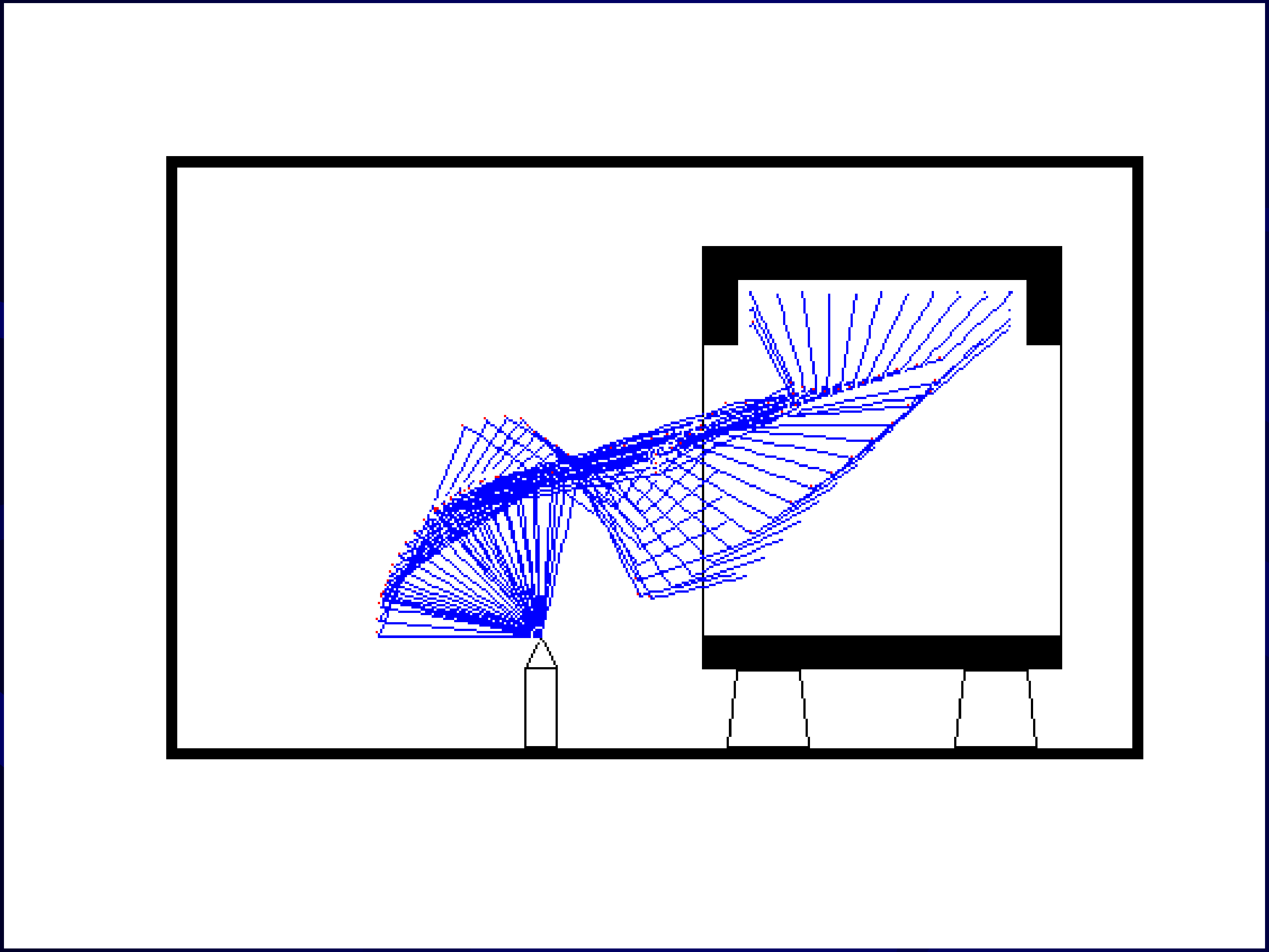

New 4-DOF Design
(Generated from original 5-DOF design)

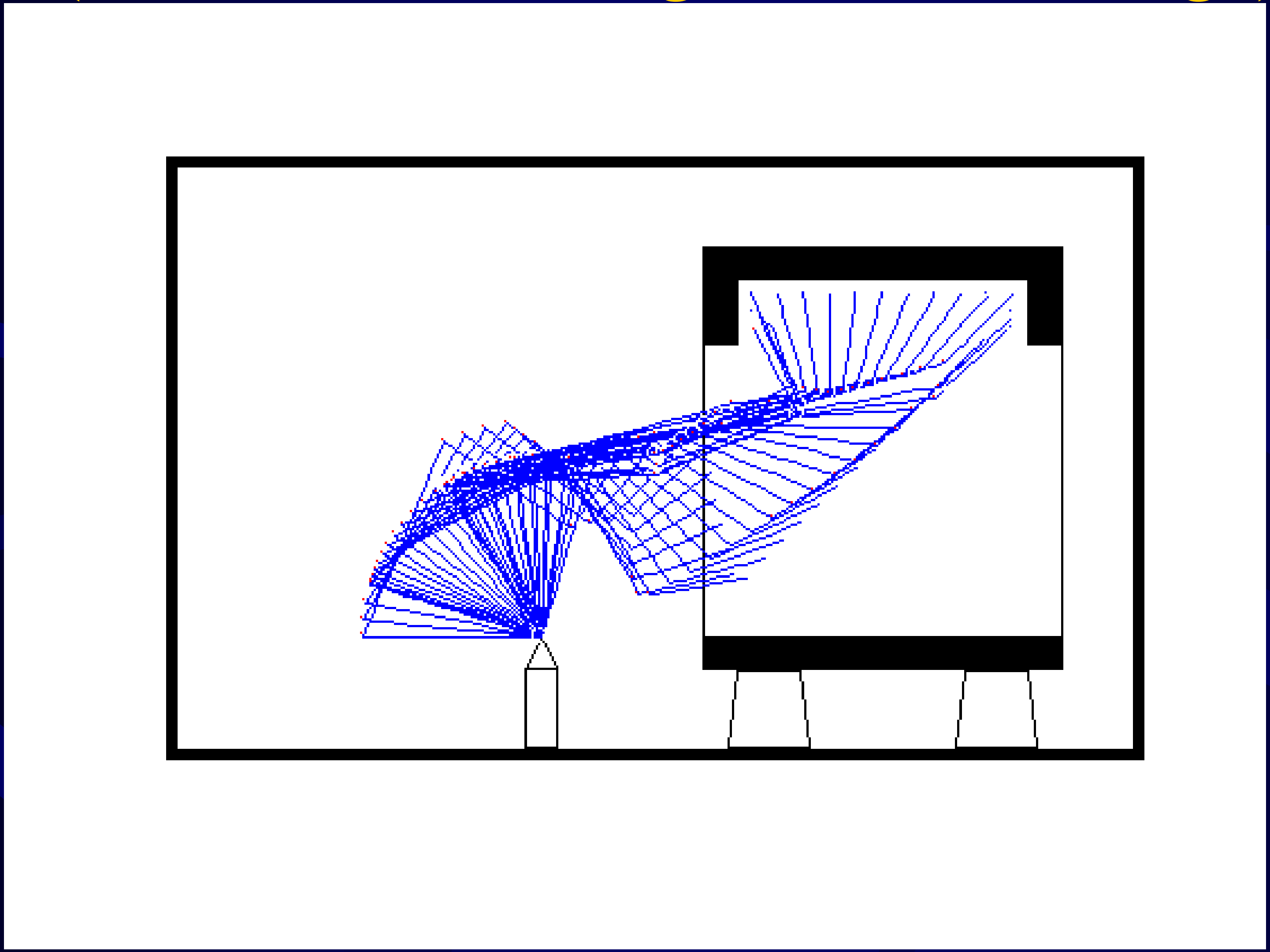

New 4-DOF Design
(Generated from original 5-DOF design)

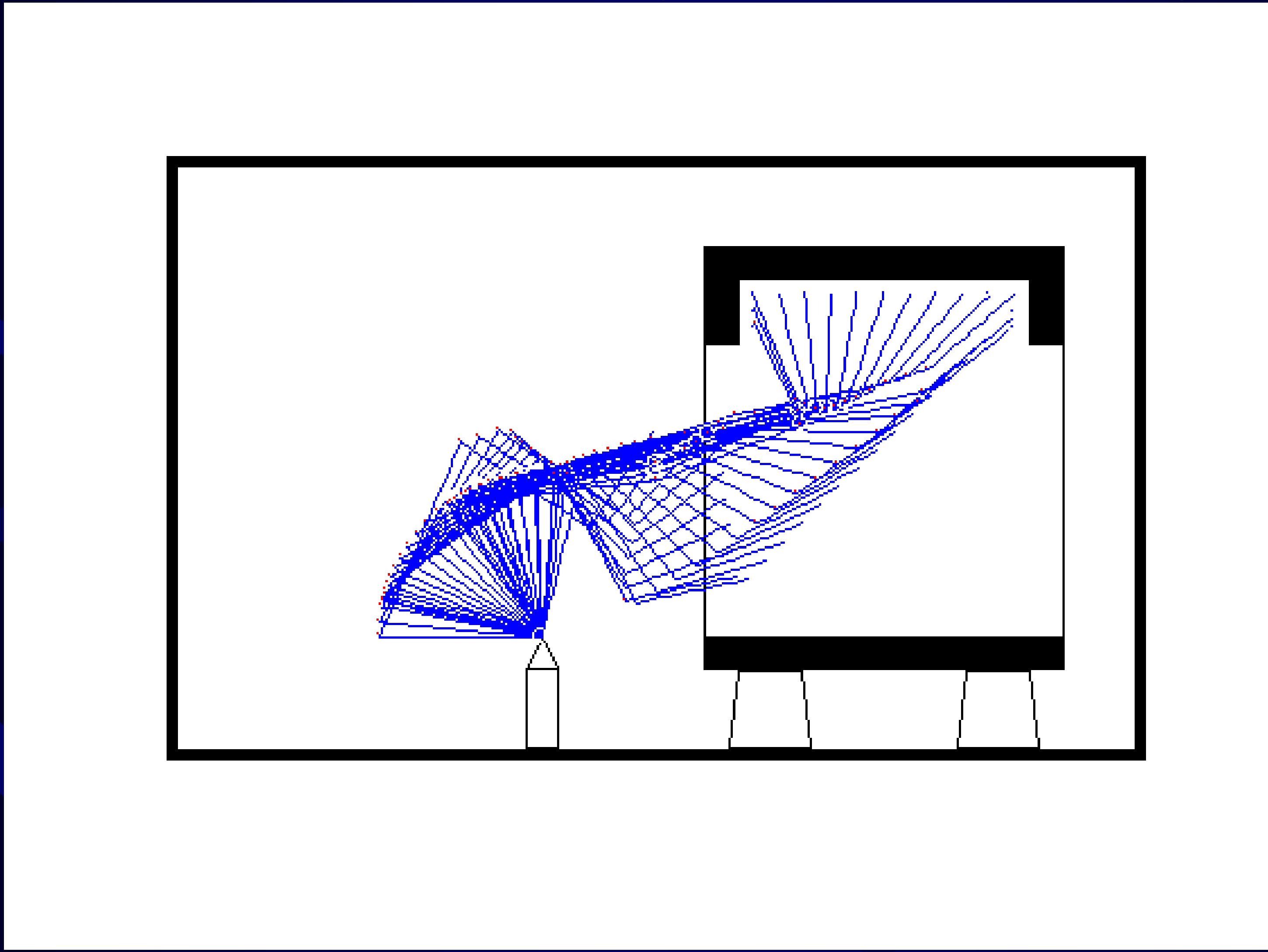

New 4-DOF Design
(Generated from original 5-DOF design)

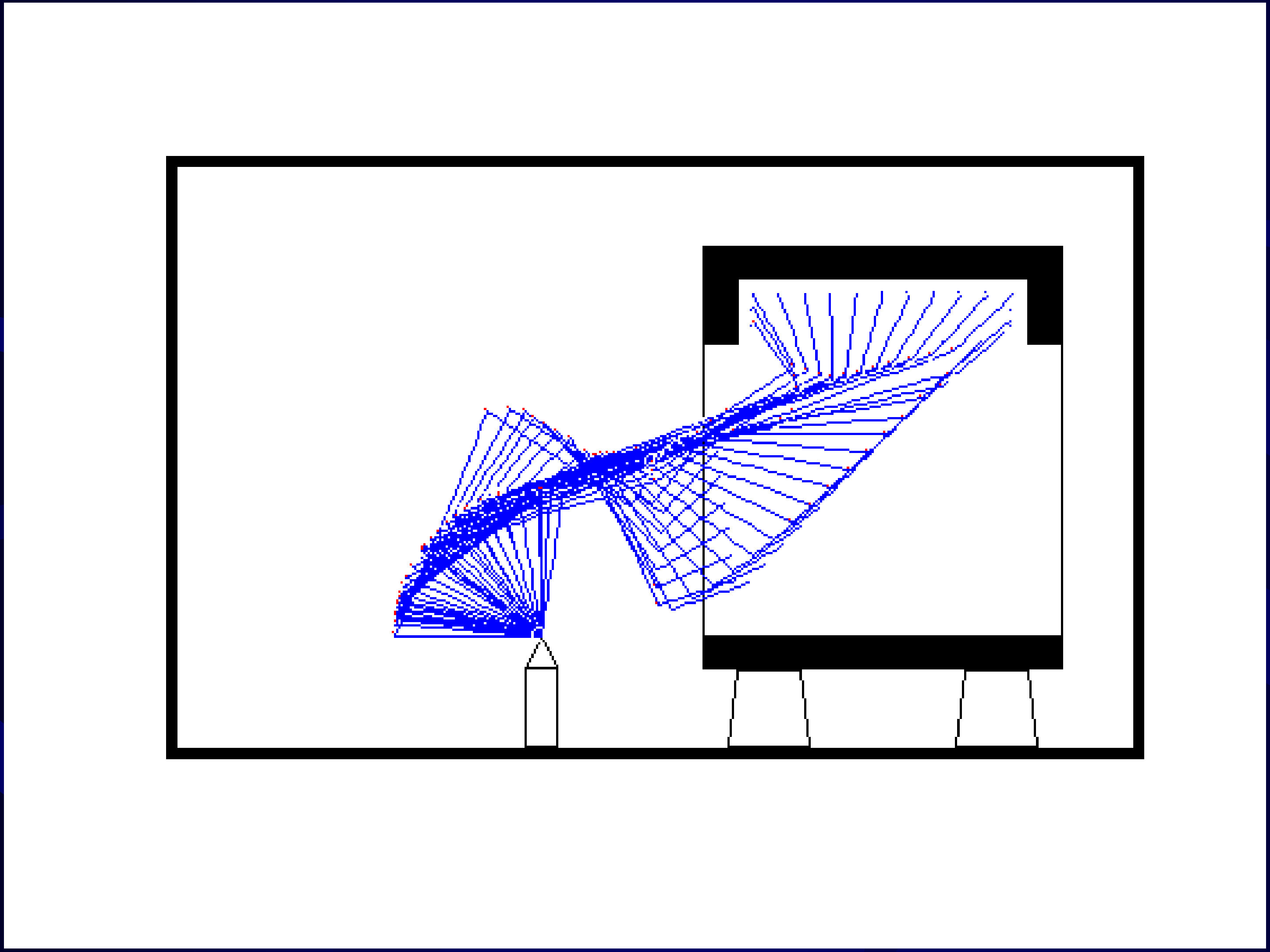

New 4-DOF Design
(Generated from original 5-DOF design)

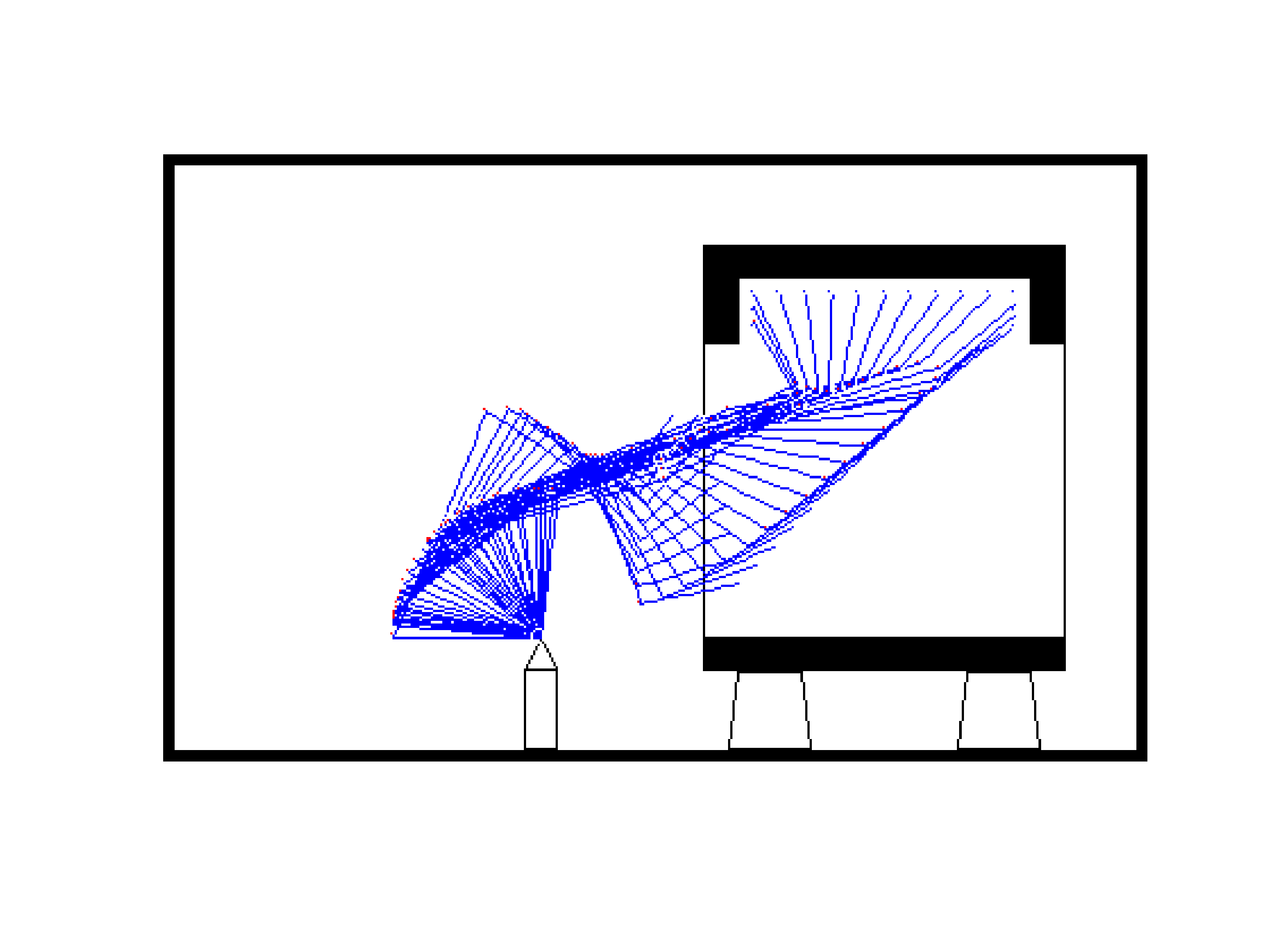

New 4-DOF Design
(Generated from original 5-DOF design)

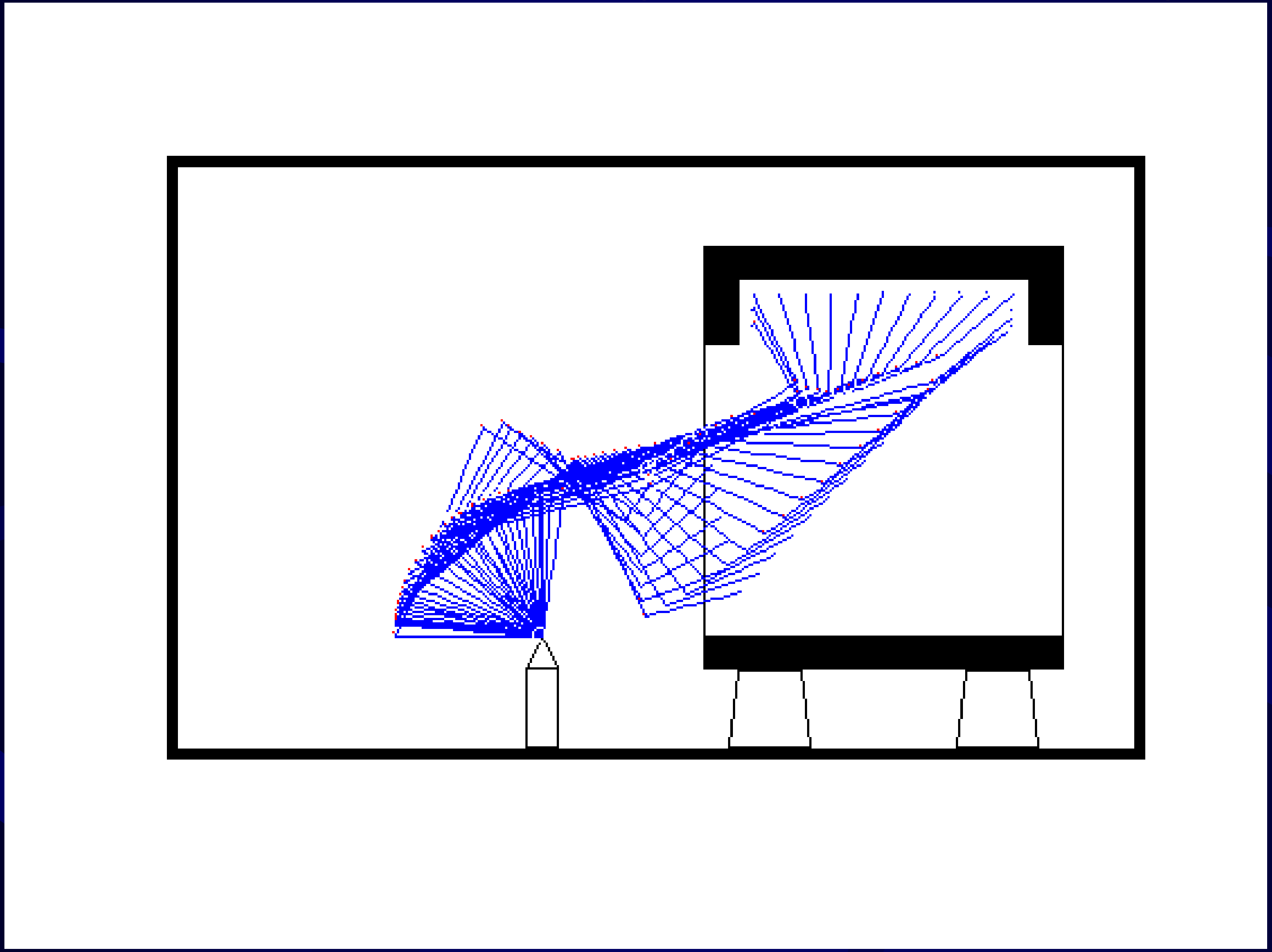

New 4-DOF Design
(Generated from original 5-DOF design)

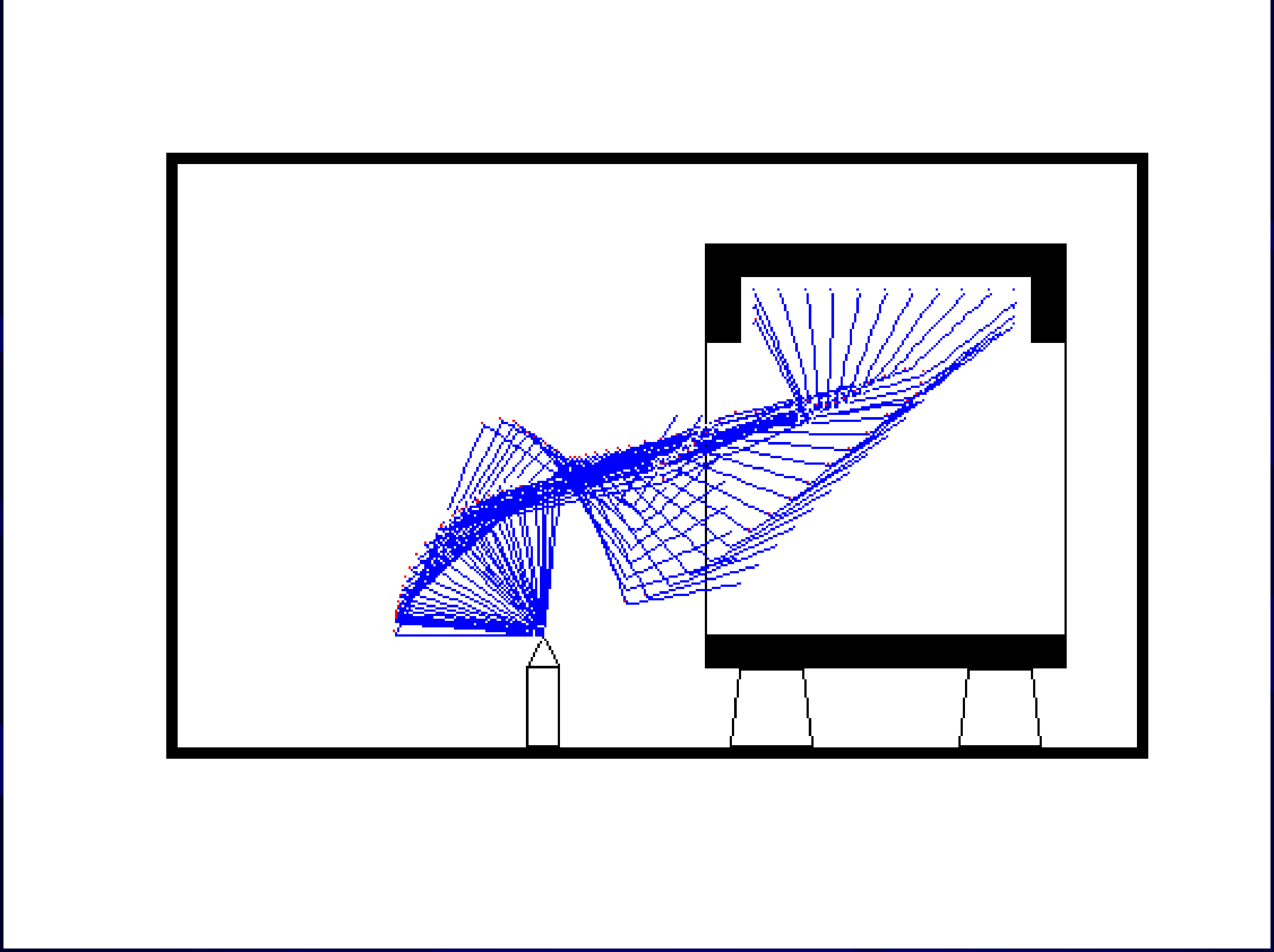

New 4-DOF Design
(Generated from original 5-DOF design)

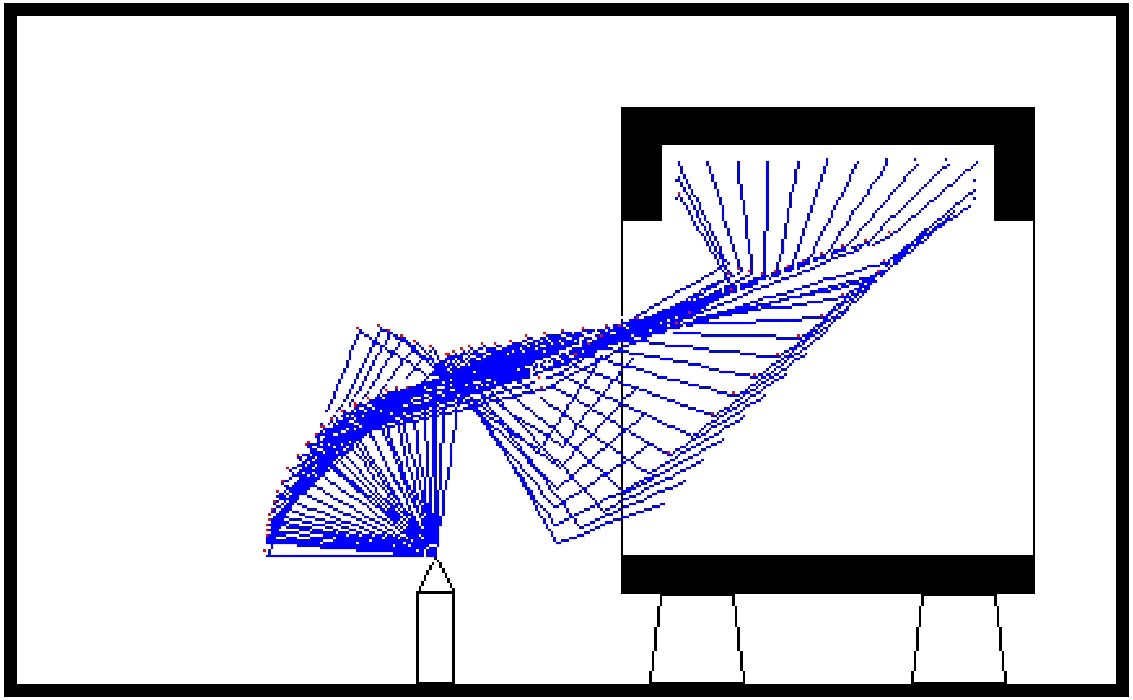

New 4-DOF Design
(Generated from original 5-DOF design)

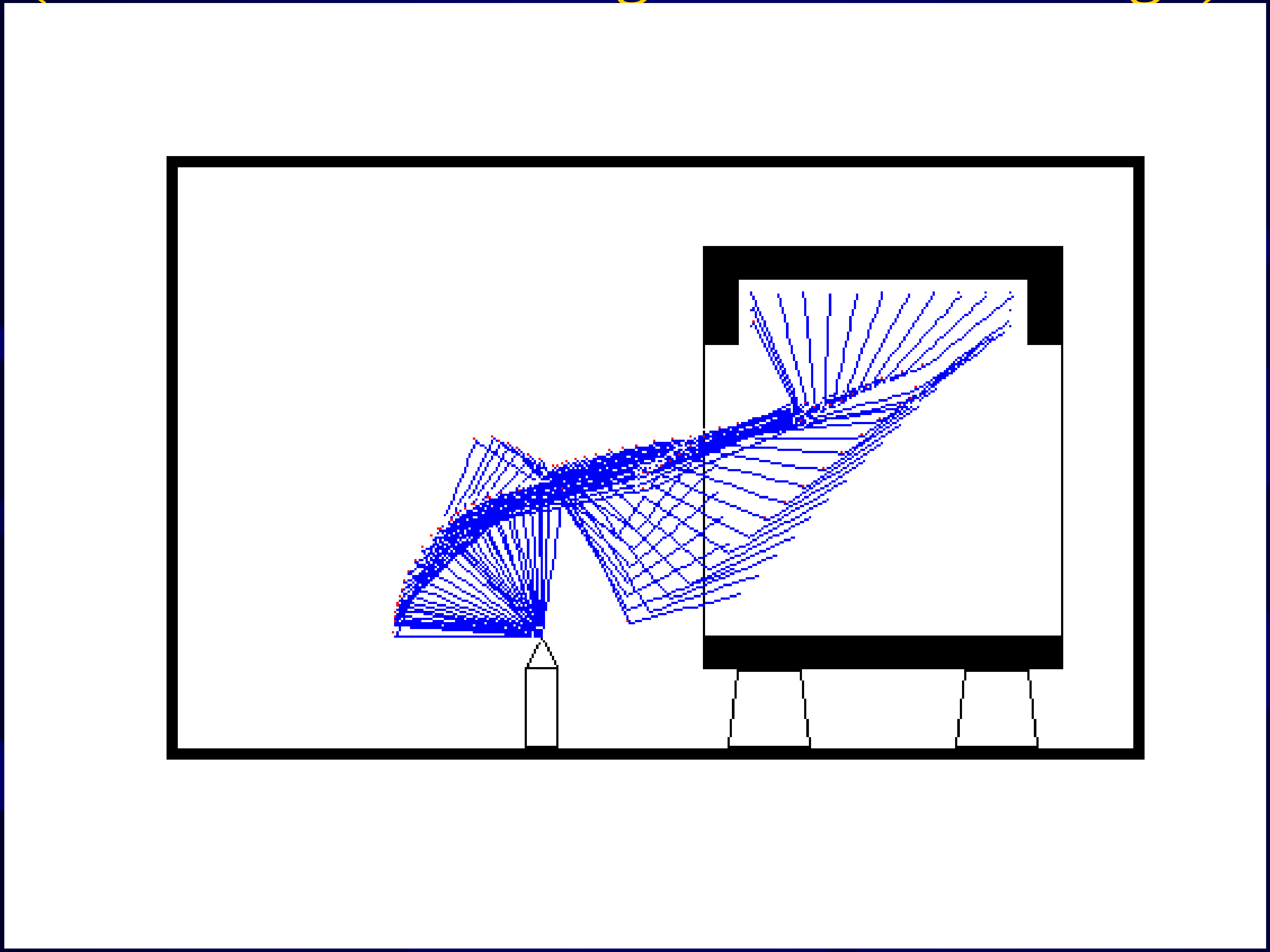

New 4-DOF Design
(Generated from original 5-DOF design)

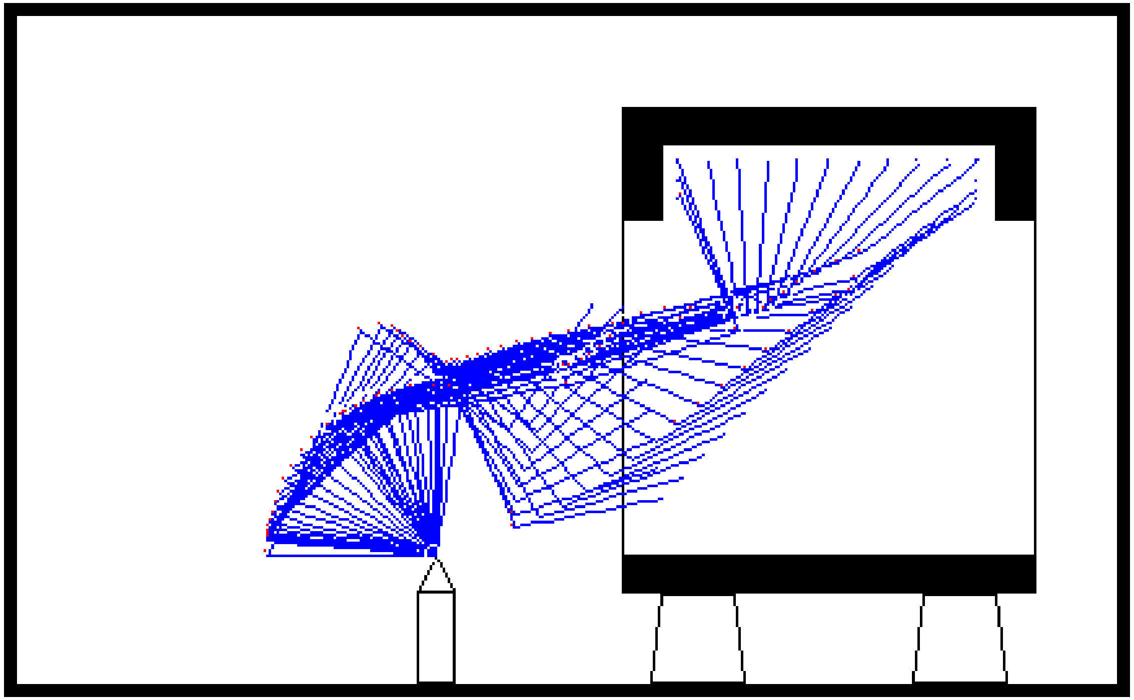

New 4-DOF Design
(Generated from original 5-DOF design)

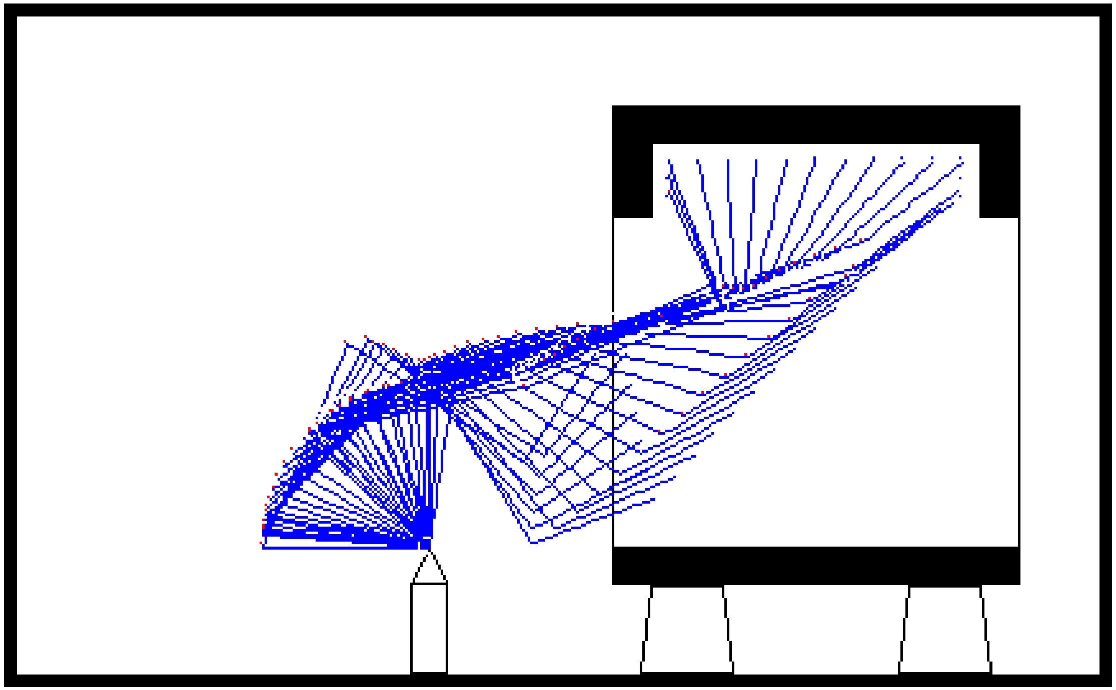

New 4-DOF Design
(Generated from original 5-DOF design)

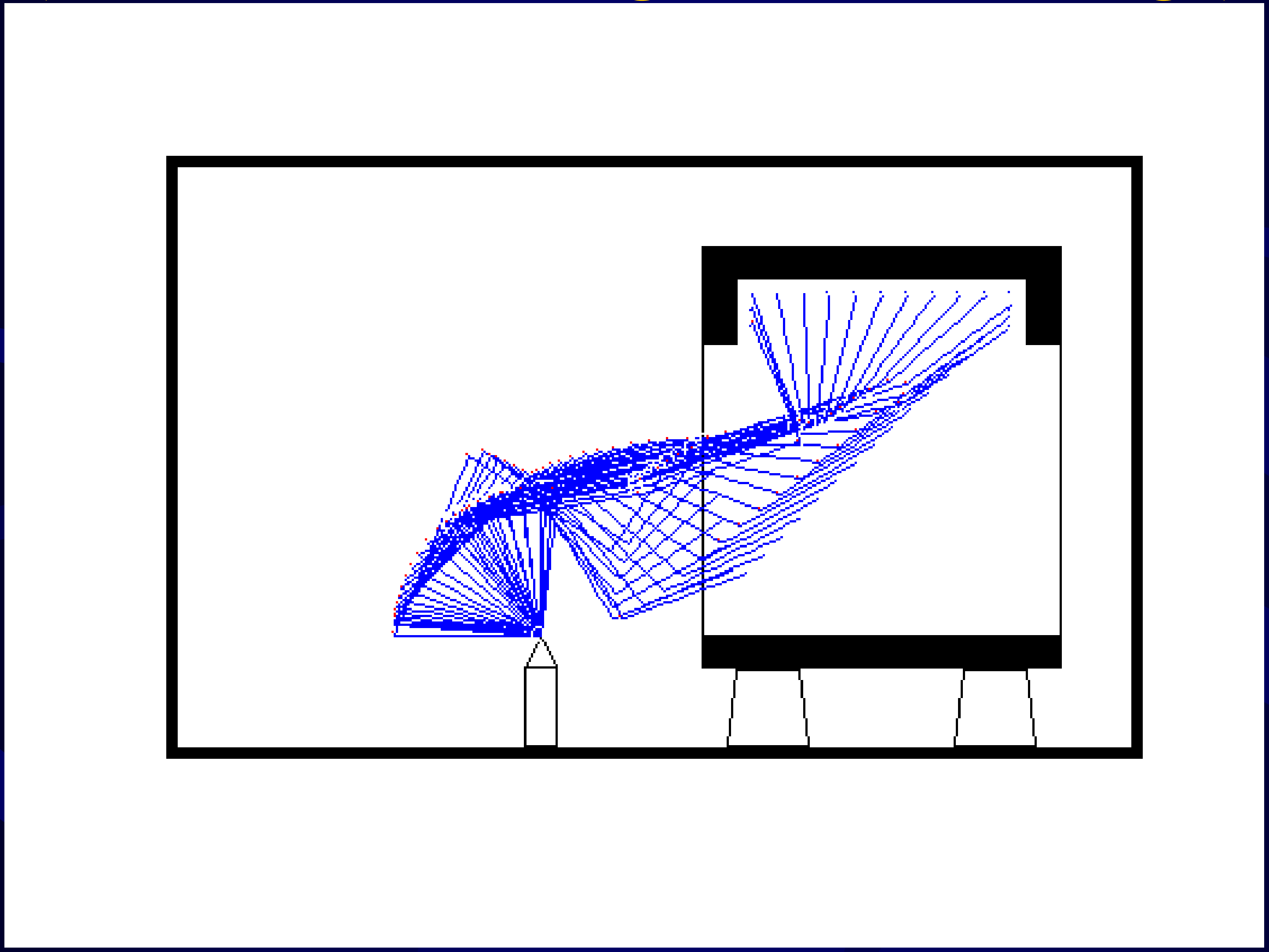

Selecting a Design

- Compare measures taken during search
  - DOF
  - Joint-angle displacement
  - Manipulability
  - Simulated speed
  - Consumption of available redundancy

DOF (minimize)

- Decrease initial financial cost
- Decrease financial operating costs

Joint-angle displacement (minimize)

- Related to the mechanical work required to maneuver
  - Increase usable life of equipment
  - Decrease financial operating costs

$$R_{02} = \int_{t0}^{t_2} \left(\sum_{i=1}^{DOF} \left| \Delta\theta_i(t) \right| \right) dt$$

Manipulability (maximize)

- Indication of how far arm configuration is from singularities over trajectory

$$w = \sqrt{\det(\mathbf{J}\mathbf{J}^T)}$$

$$\overline{w}_{12} = \left[\frac{\int_{t1}^{t_2} (\sqrt{\det(\mathbf{J}\mathbf{J}^T)})dt}{t_2 - t_1} \right]$$

$$\hat{\overline{w}}_{12} = \left[\frac{\overline{w}_{12}}{\hat{w}_{\max}} \right]$$

New proposed measure here:

Consumption Of Available Redundancy (COAR)
(minimize it)

- Indication how redundancy used over trajectory
- COAR varies significantly over trajectory when joint angle changes vary significantly due to obstacle avoidance

$$COAR = \left[\frac{\left\| (\mathbf{I} - \mathbf{J}_{\mathrm{e}}{}^{\#}\mathbf{J}_{\mathrm{e}})\dot{\Psi} \right\|}{\left\| \mathbf{J}_{\mathrm{e}}{}^{\#}\dot{\mathbf{x}}_{\mathrm{e}} \right\|} \right] = \left[\frac{\left\| \sum_{i=1}^{N} \left[[\mathbf{J}_{o_i}(\mathbf{I} - \mathbf{J}_{\mathrm{e}}^{\#}\mathbf{J}_{\mathrm{e}})]^{\#}(\dot{\mathbf{x}}_{o_i} - \mathbf{J}_{o_i}\mathbf{J}_{\mathrm{e}}^{\#}\dot{\mathbf{x}}_{\mathrm{e}}) \right] \right\|}{\left\| \mathbf{J}_{\mathrm{e}}{}^{\#}\dot{\mathbf{x}}_{\mathrm{e}} \right\|} \right]$$

COAR

(Example highly-constricted workspace)

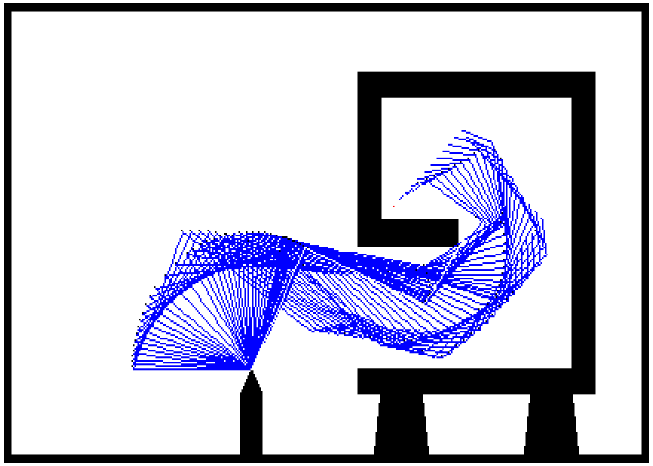

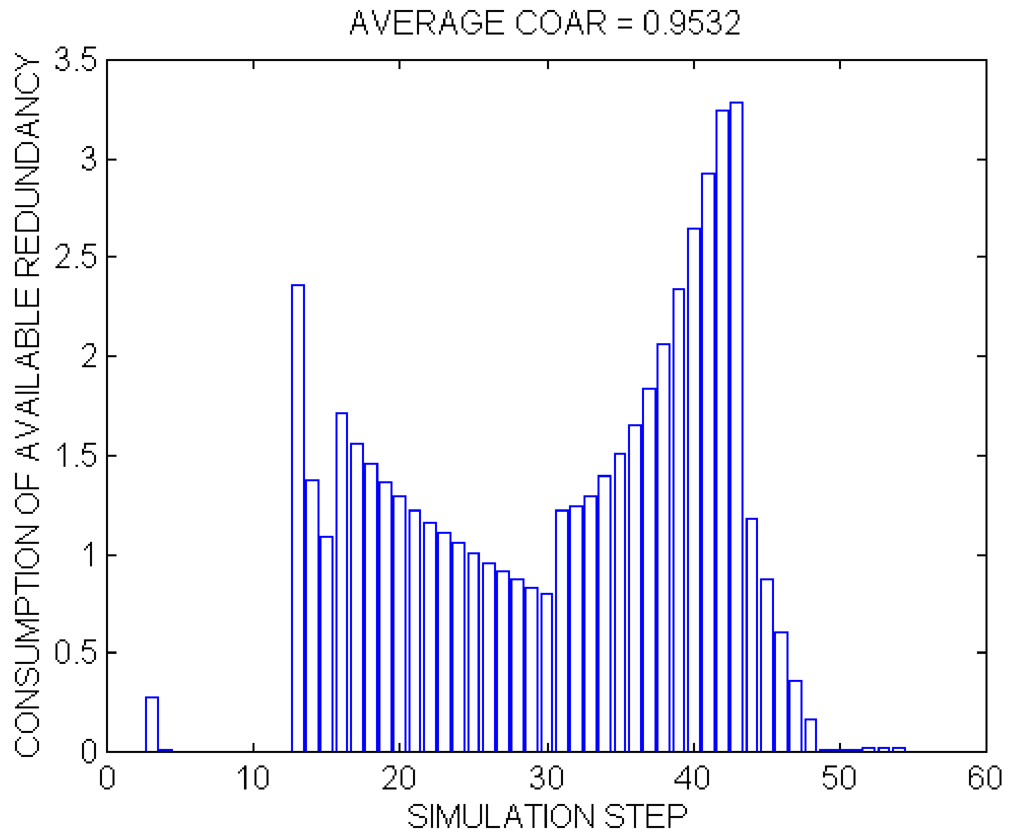

Simulated speed (maximize)

- Simply number of simulation steps in a trajectory
  - Indication of how trajectory compromised
    - Local minima
    - High COAR

“High-Quality” Final Design

(selected from all feasible designs from search)

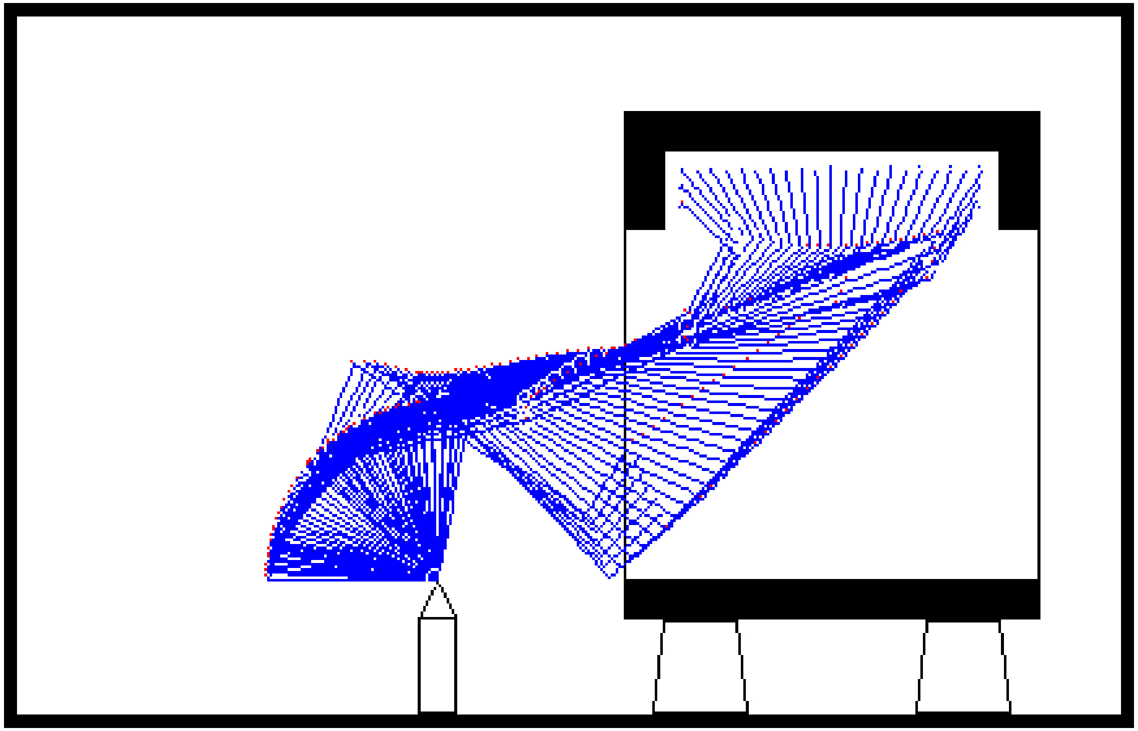

How Robust is Methodology?

- Dependent on initial configuration?
- Can escape local minima?
- Can deal with singularities?
- Can be extended to more complex workspaces?

Dependent on initial configuration?

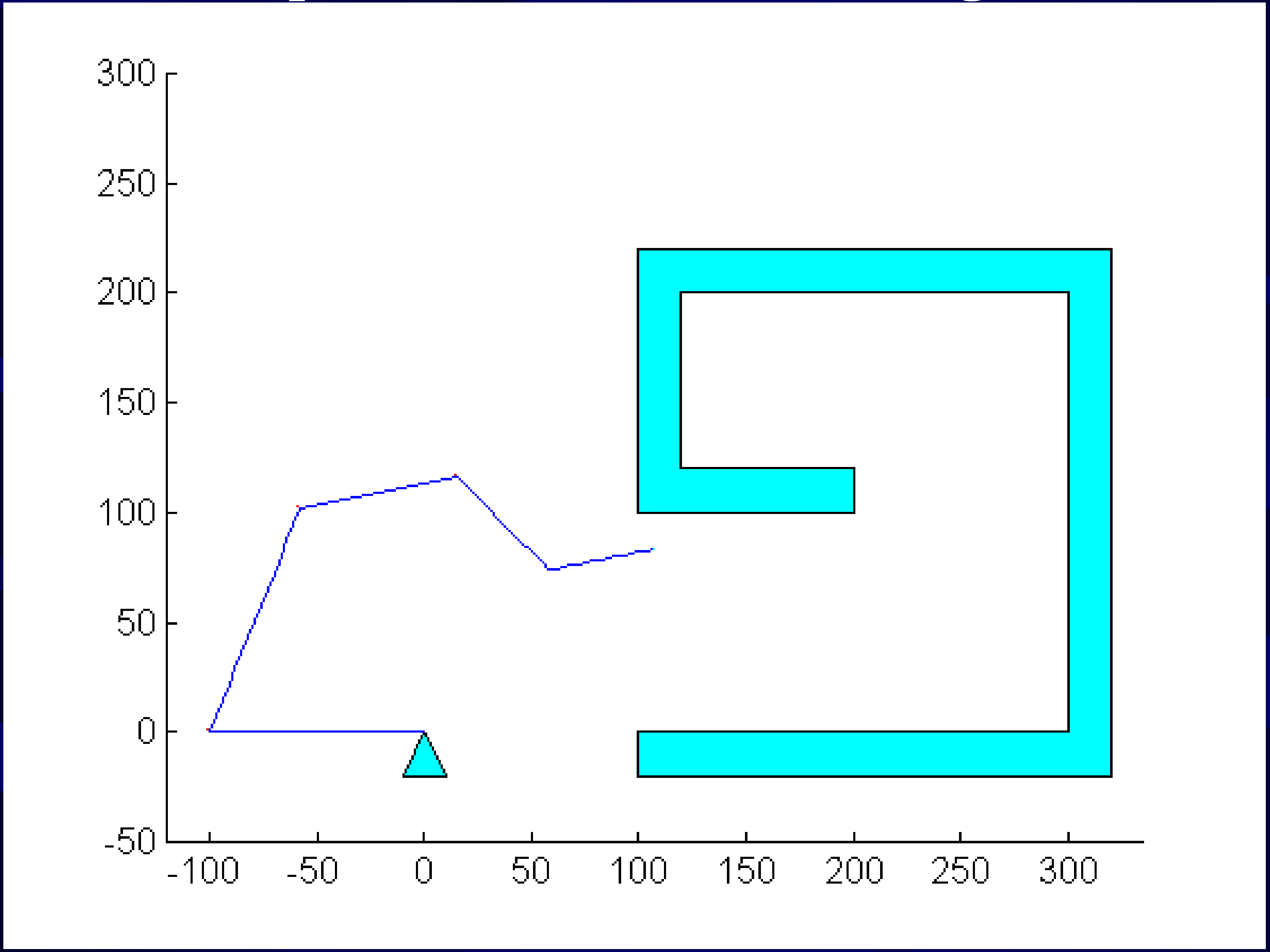

Dependent on initial configuration?

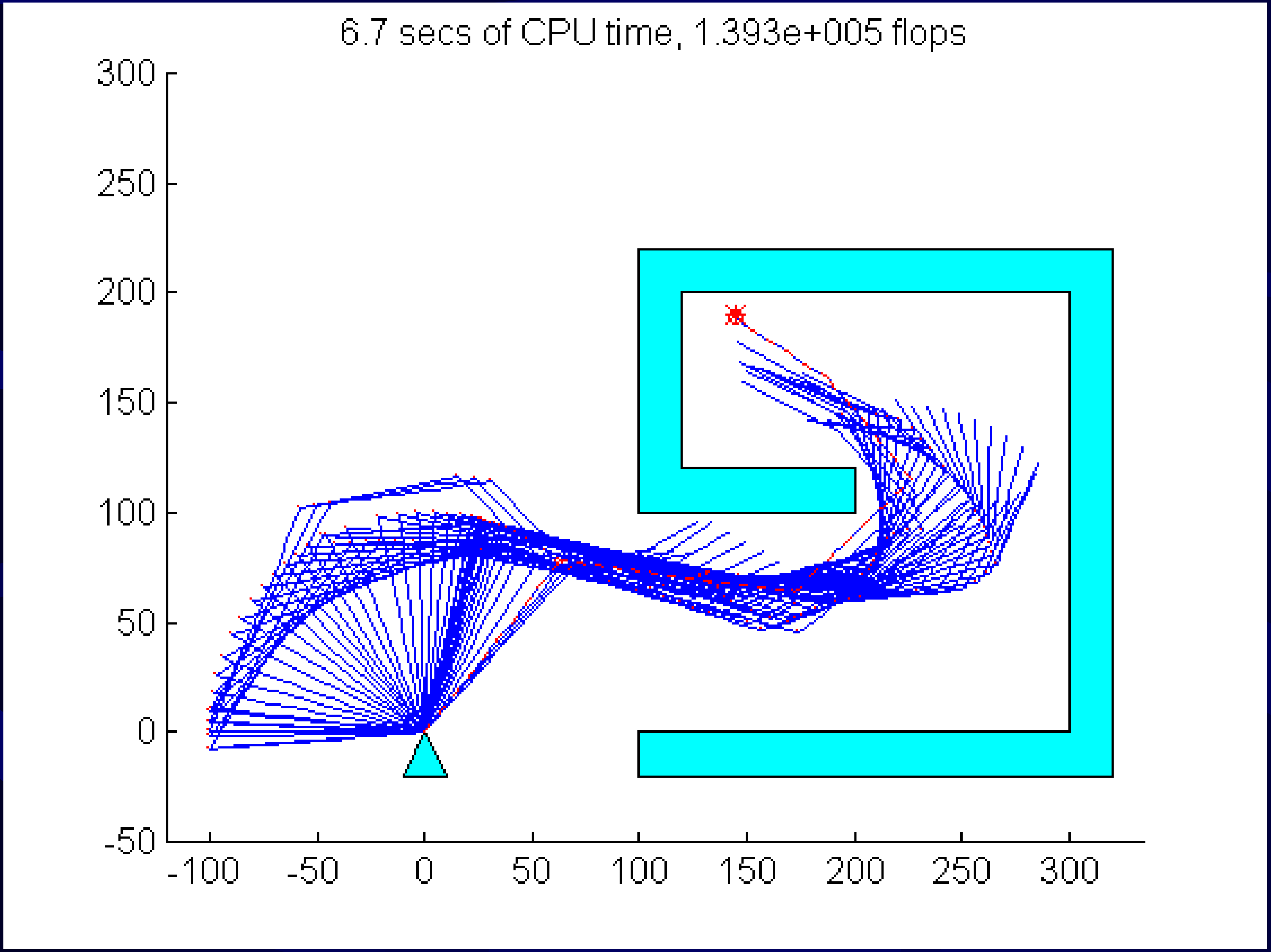

Dependent on initial configuration?

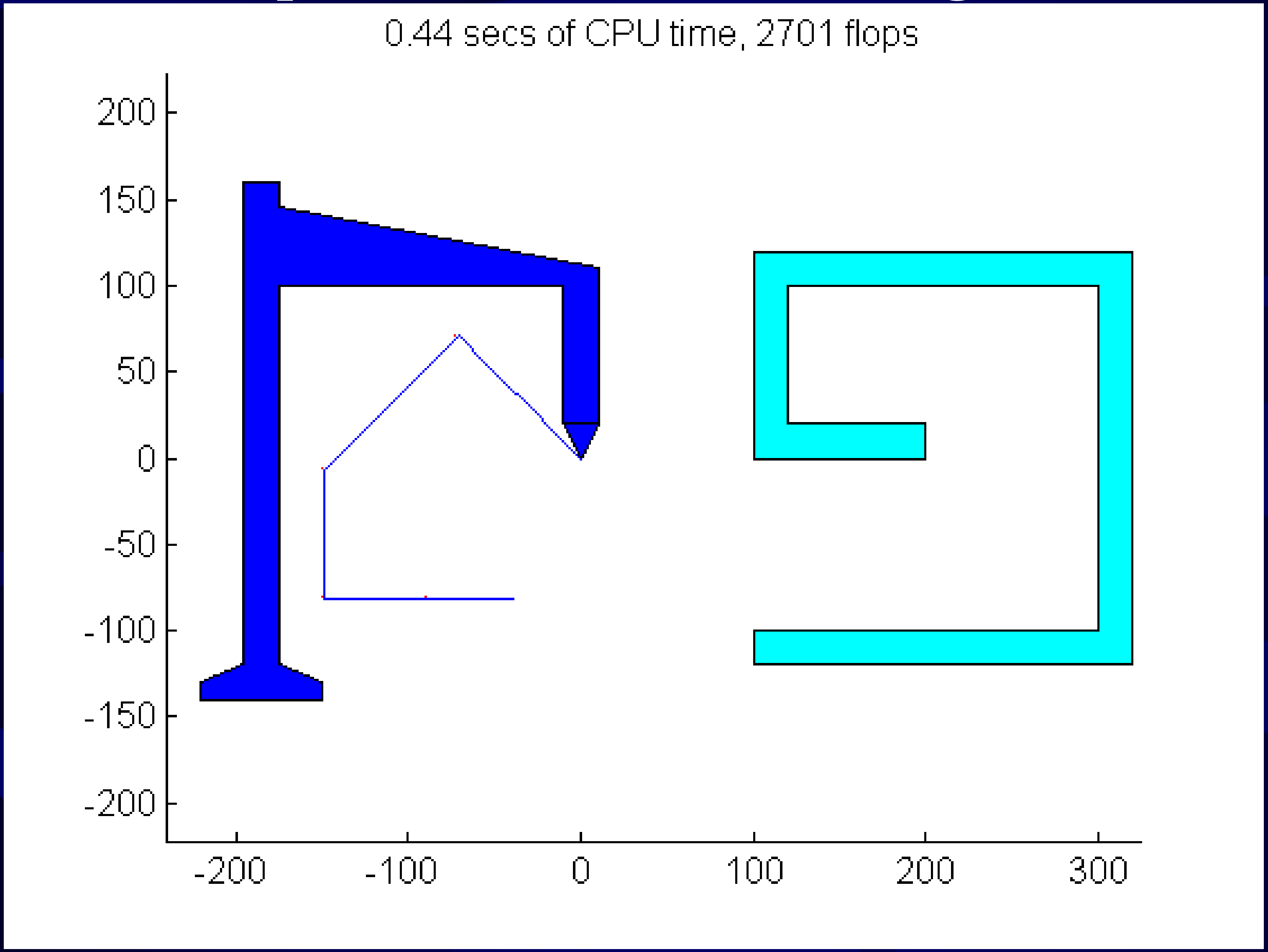

Dependent on initial configuration?

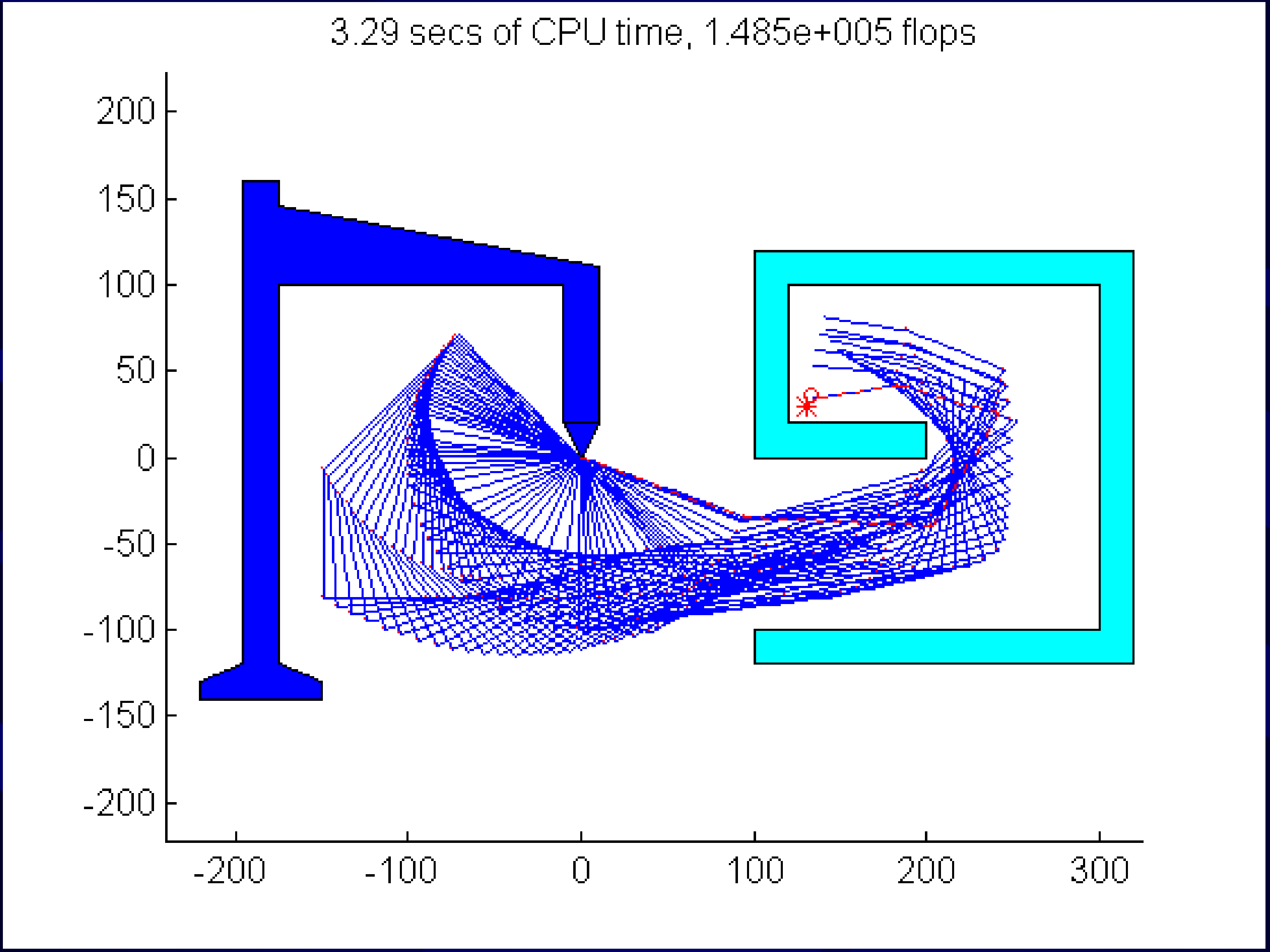

Dependent on initial configuration?

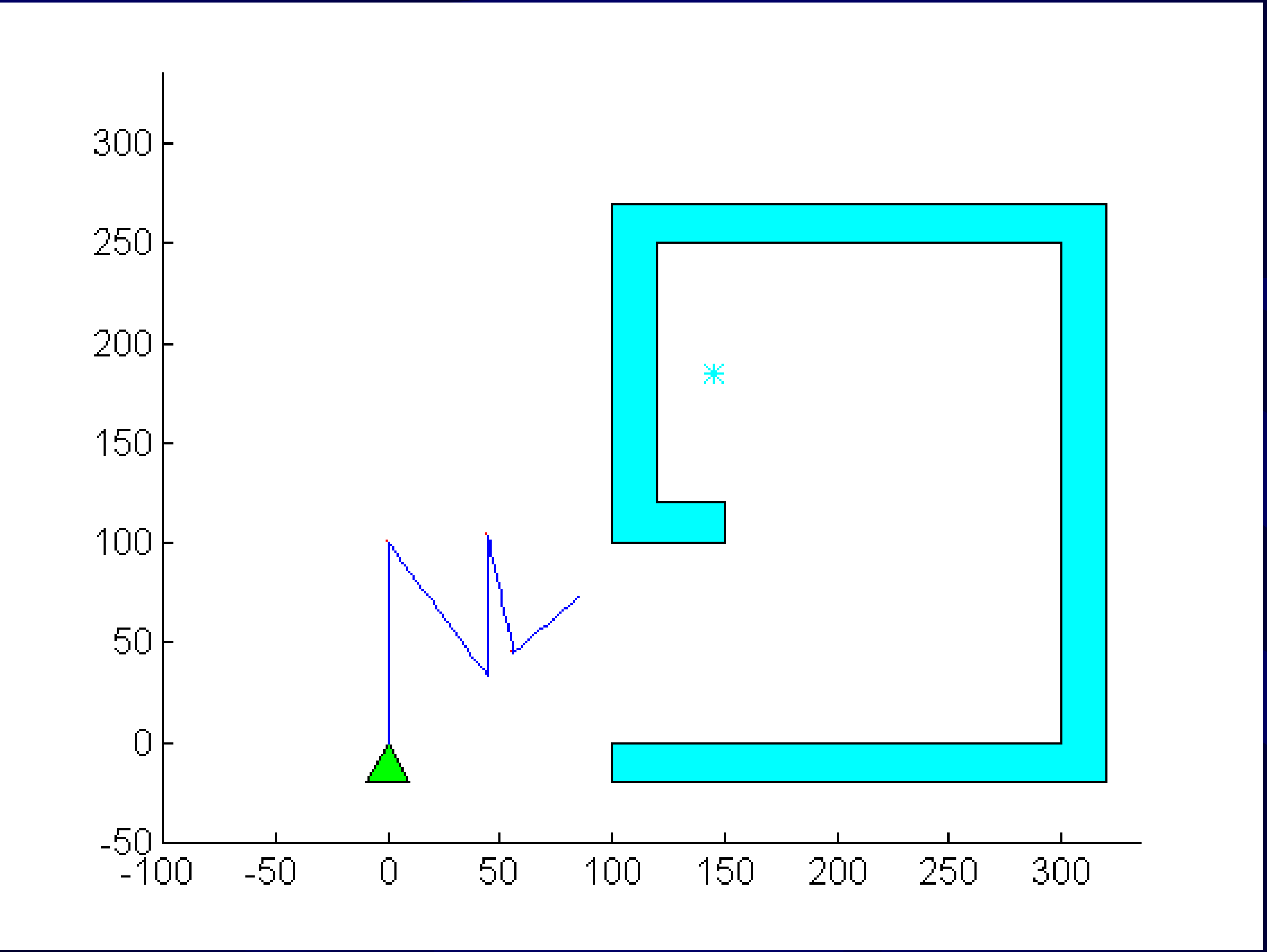

Dependent on initial configuration?

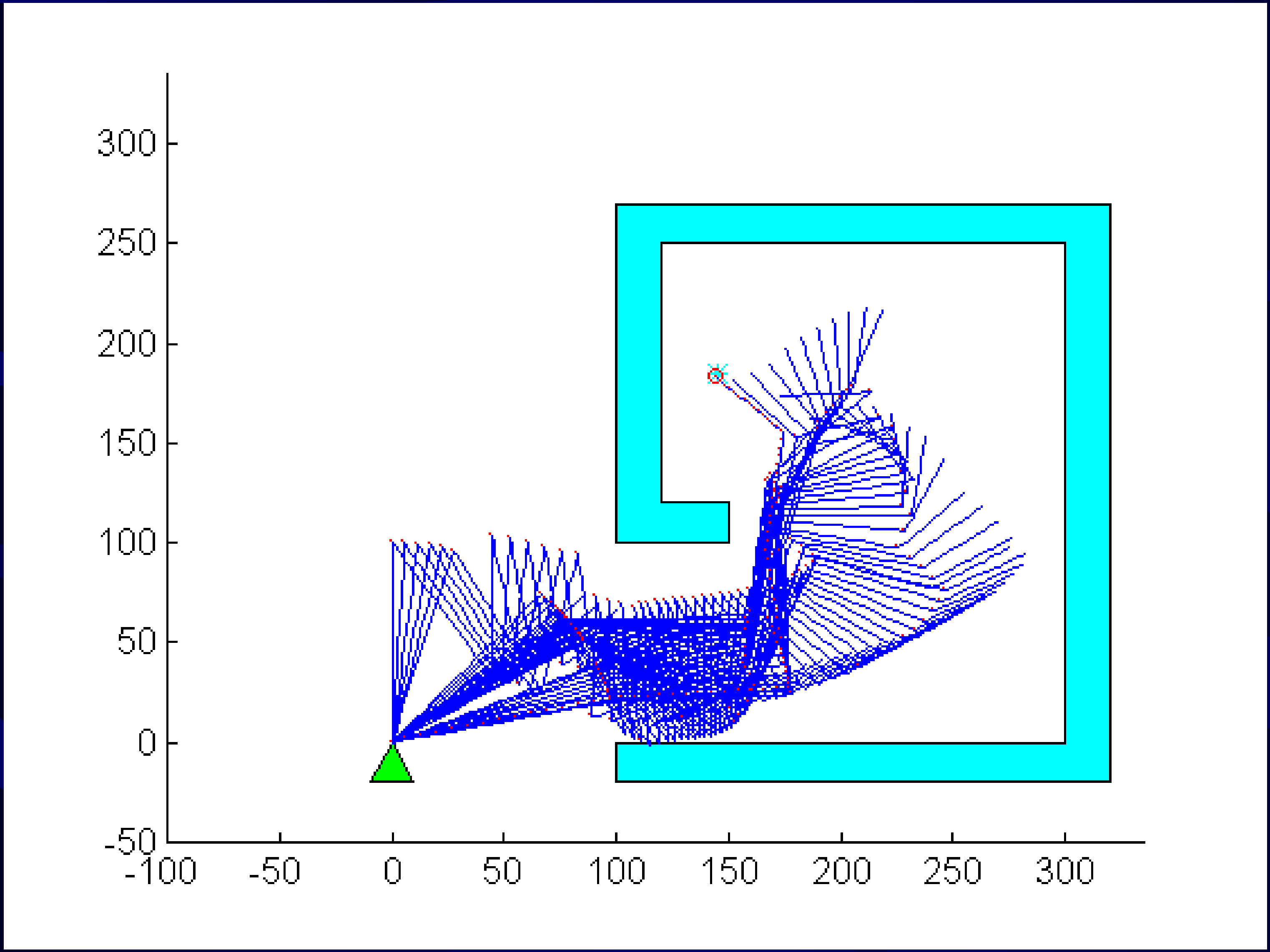

Can escape local minima?

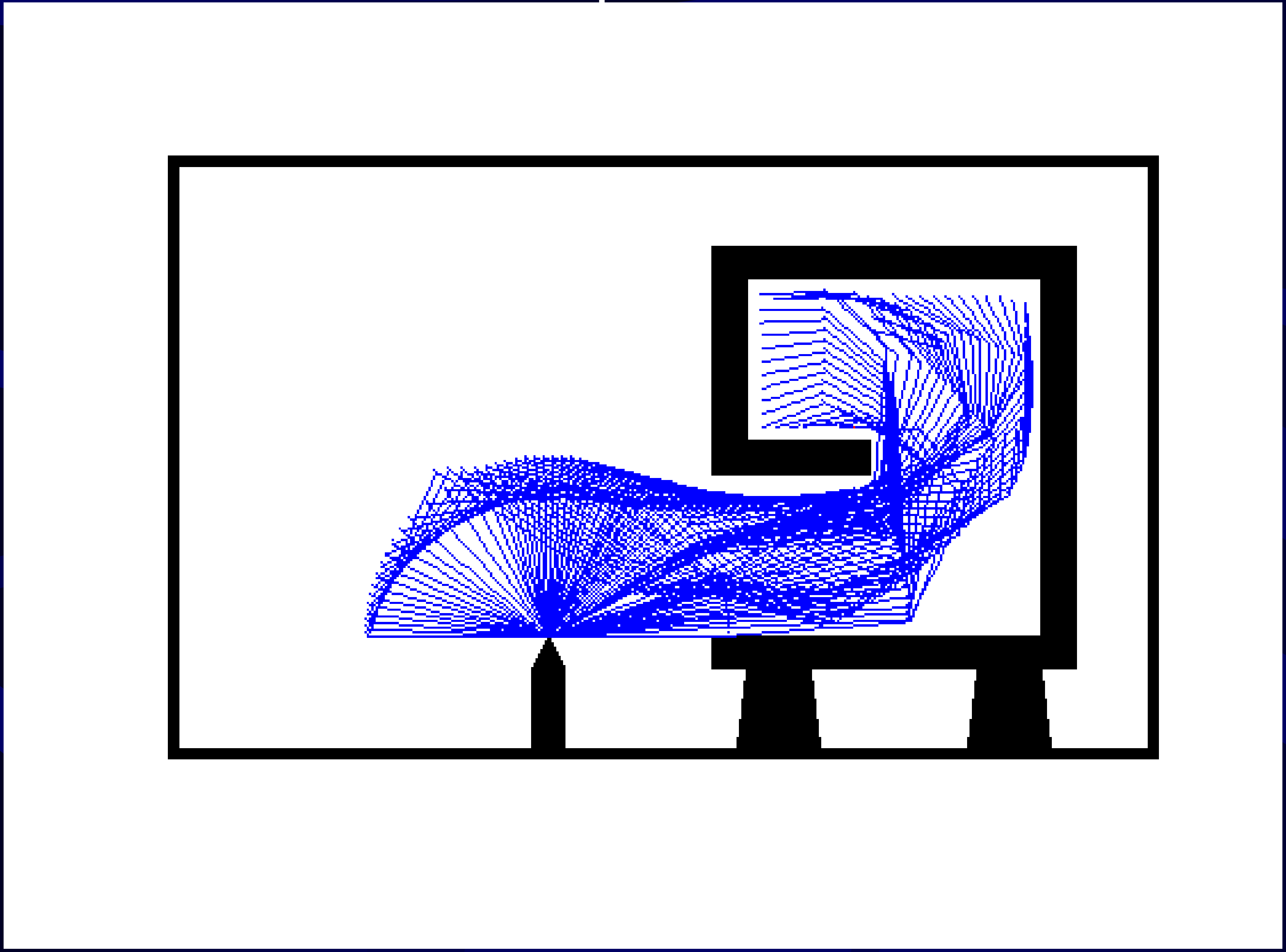

Can deal with singularities?

- Considered "damped least squares" and "weighting matrix"
- Considered treating singularity configurations as obstacles
  - but could push arm into repelling fields
- Using "manipulability measure" to compare all candidate designs
  - "*natural selection*"

Extend methodology to more complex workspaces

Create enclosure from simulation Primitives

	TUNNEL	LEFT ELBOW	RIGHT ELBOW	TERMINATOR
ATTRACTIVE POLE (●) REPELLING ANGLES (u_j) ↗	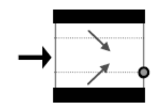	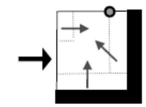	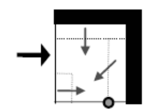	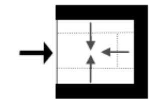
REPELLING FIELD WIDTH (t_j)	OUTER-BANK: 30% OF ENCLOSURE WIDTH INNER-BANK: 40% OF ENCLOSURE WIDTH	OUTER-BANK: 20% OF ENCLOSURE WIDTH INNER-BANK: 40% OF ENCLOSURE WIDTH		30% OF ENCLOSURE WIDTH
(E)	OUTER-BANK: E = 0.1 INNER-BANK: E = 1.0	OUTER-BANK: E = 0.1 INNER-BANK: E = 0.0		E = 0.1

EXAMPLE K_j's for $t_j = 20$, $d_{ABORT} = 0$, $V_j = V_e = 1$

$$K_j = V_j V_e \left[1 - \left(\frac{d_j - d_{ABORT}}{t_j} \right)^E \right]$$

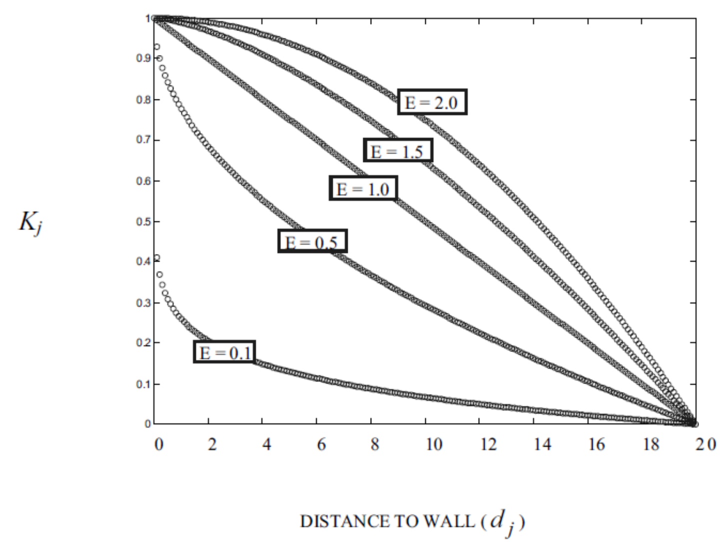

Note: If a goal or *fixed*-trajectory task is specified within primitive, the attractive pole is disabled and repelling-angles are set to 90 degrees.

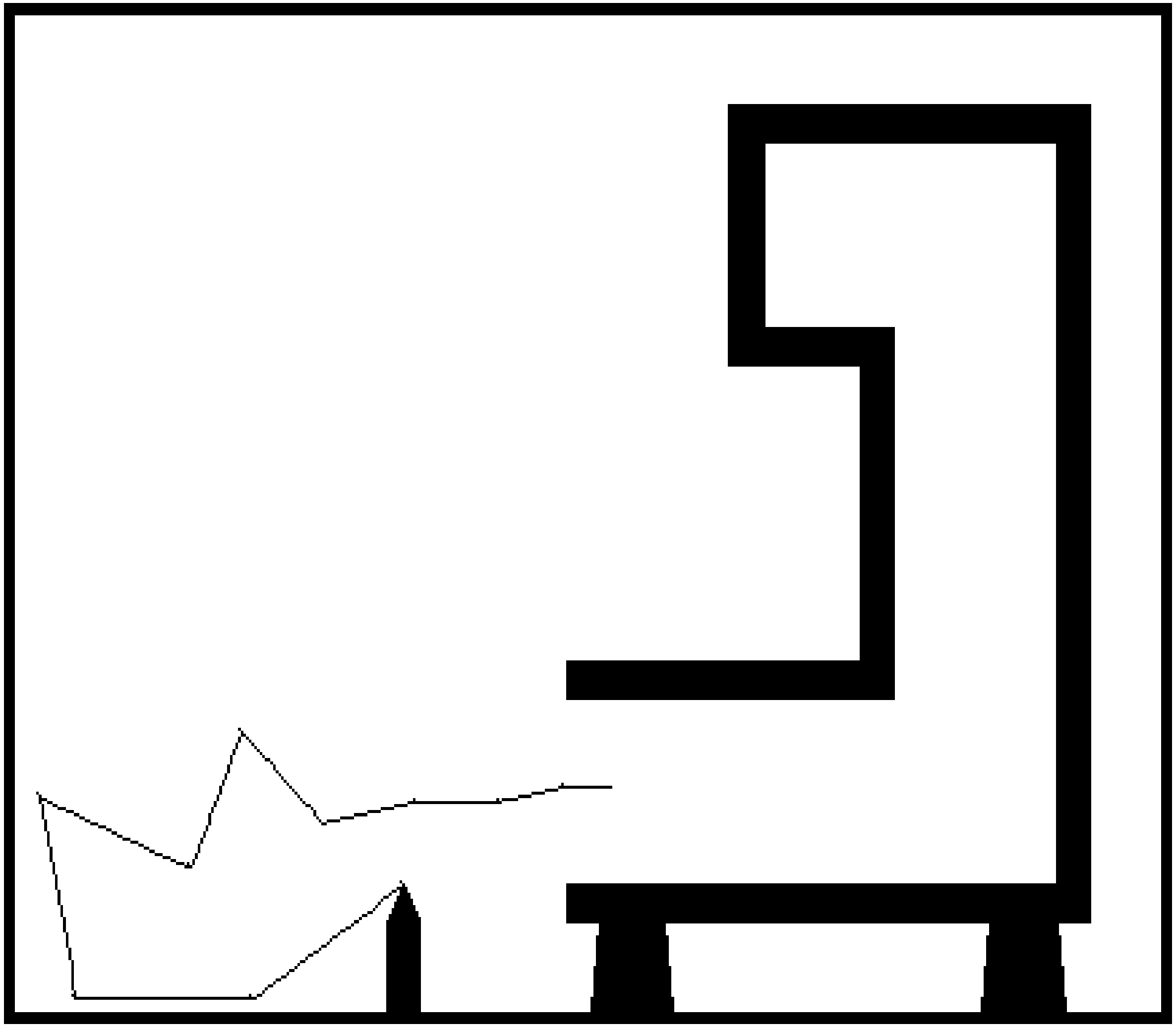

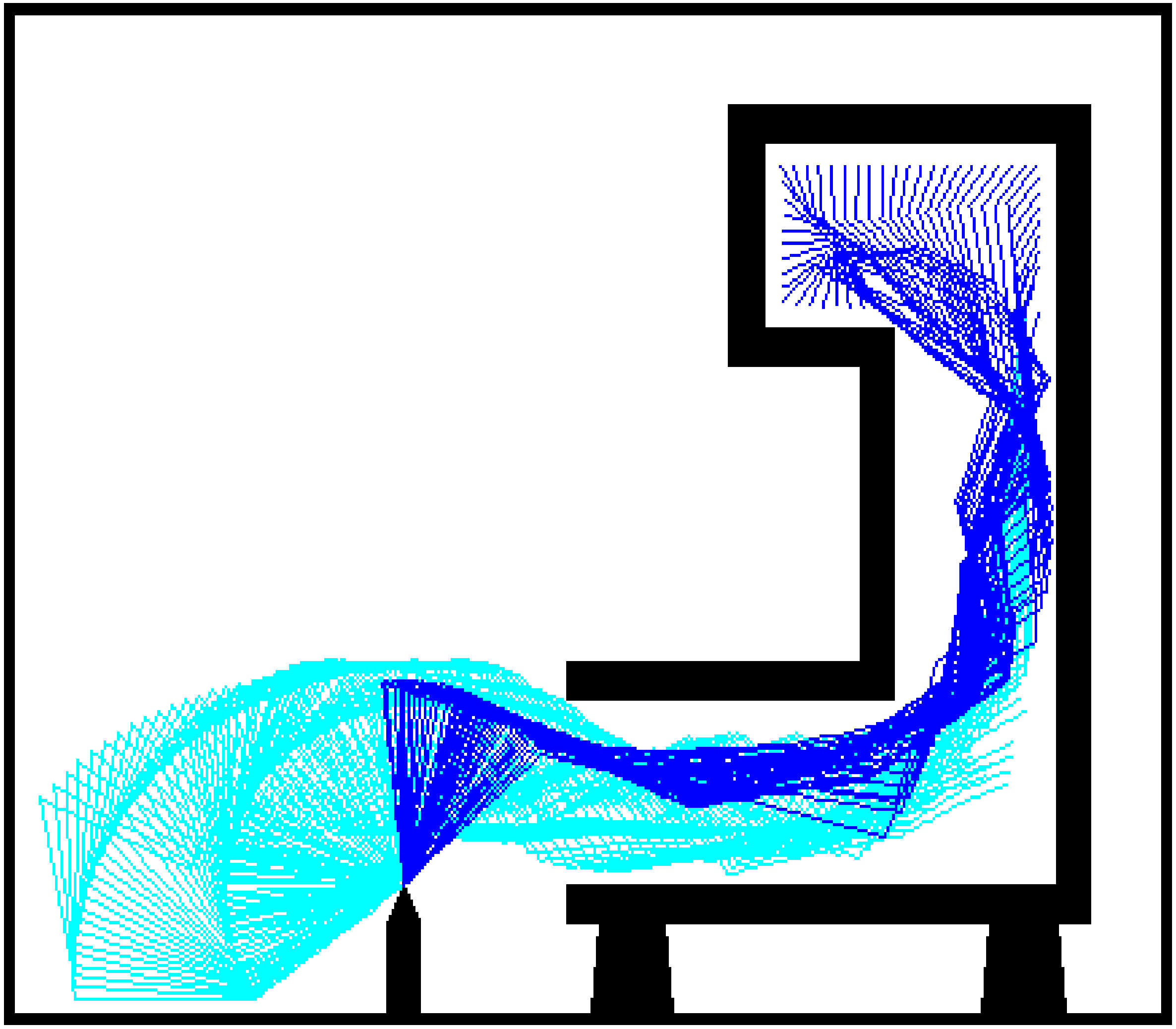

How Robust is Methodology?

- Dependent on initial configuration?
  - Only somewhat
- Can escape local minima?
  - Yes
- Can deal with singularities?
  - Considered less desirable designs
- Can be extended to more complex workspaces?
  - Yes

Extended methodology to finding a set of designs for a more complex enclosure

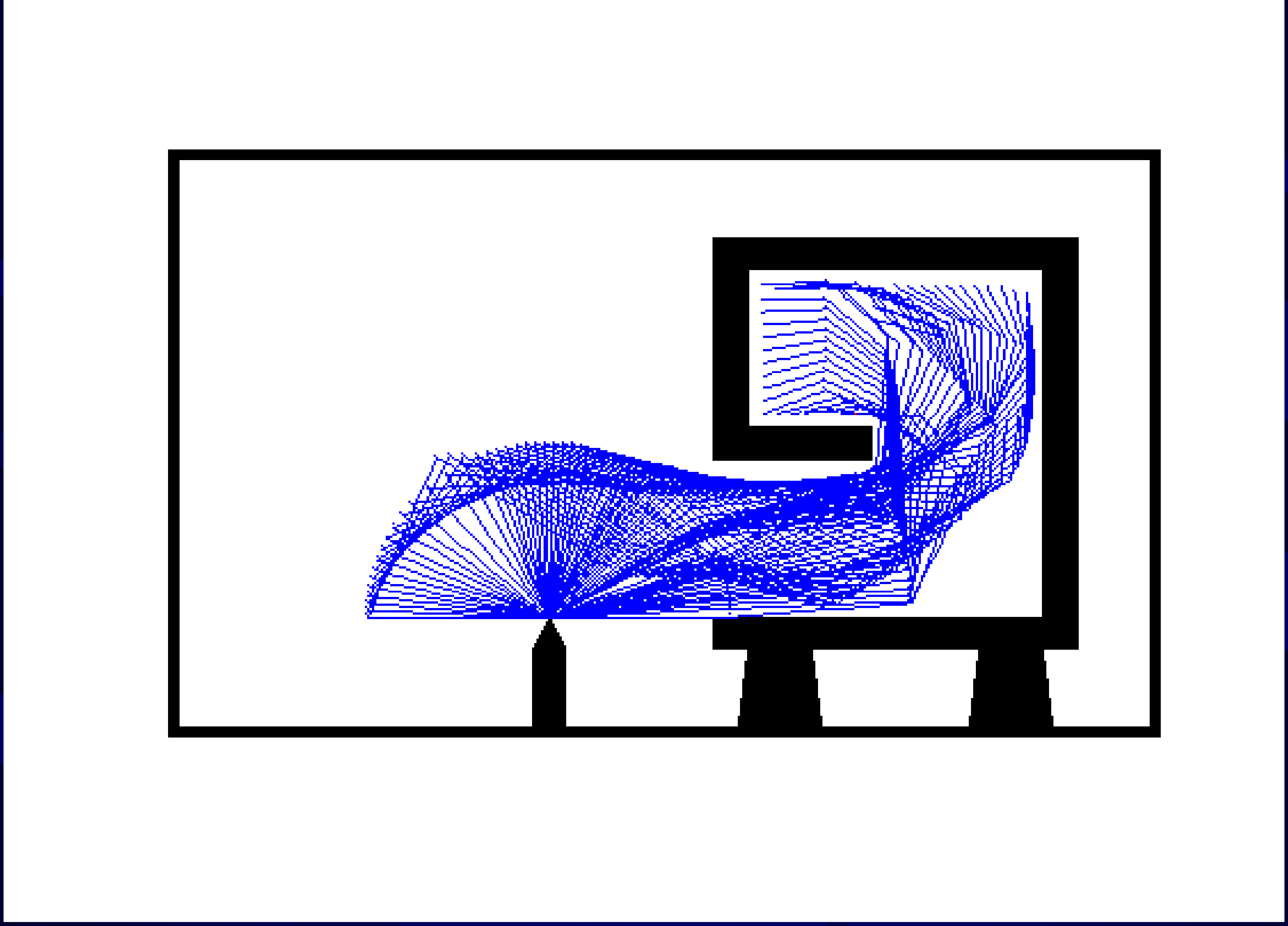

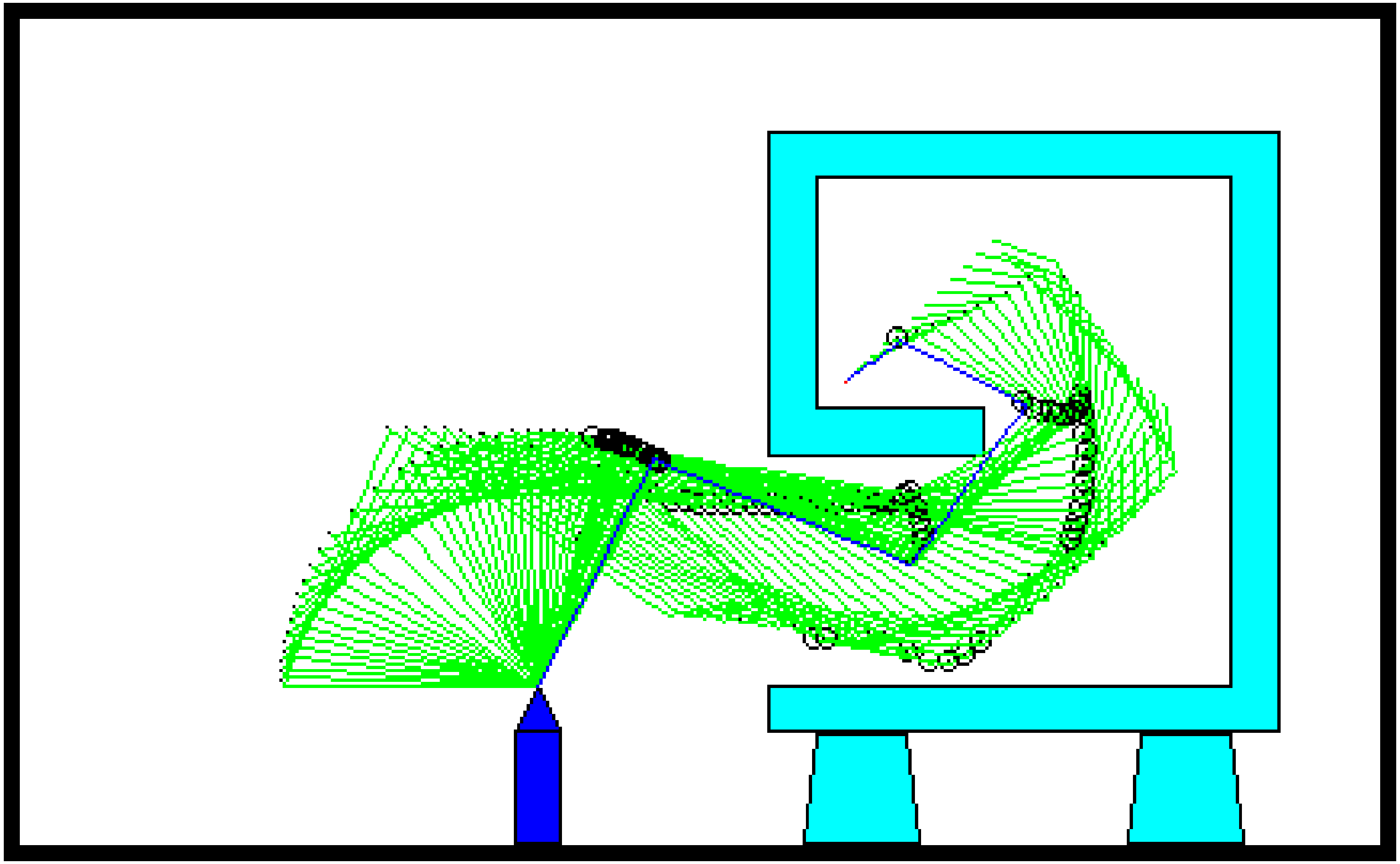

Circles show elbows being repelled from surfaces

Results of a test design run where red arms are successful at reaching goal (red X) and blue arms are not.

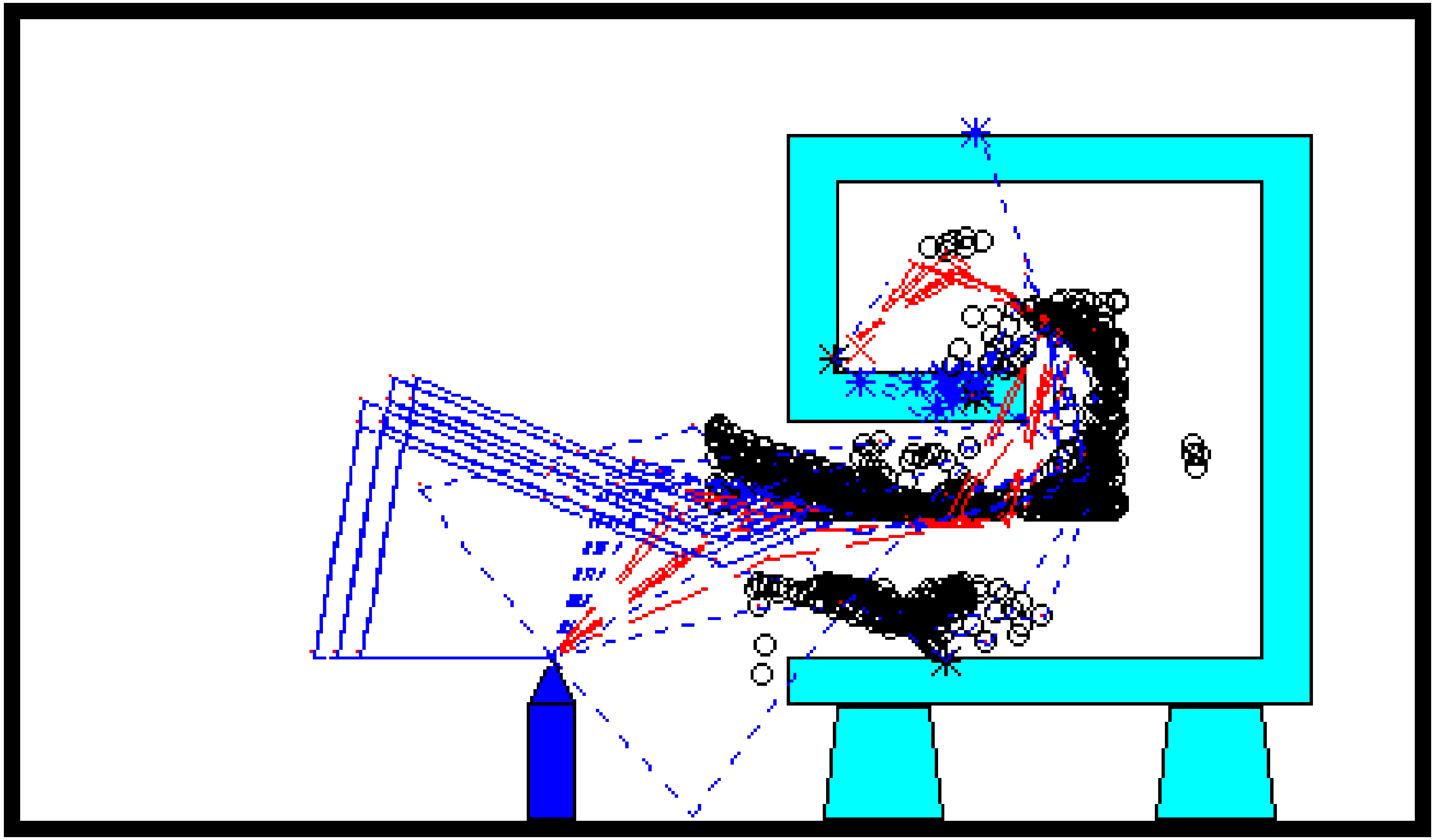

Circles show elbows being repelled from surfaces

Robotic Arm Design

Using complex path-planning and obstacle avoidance

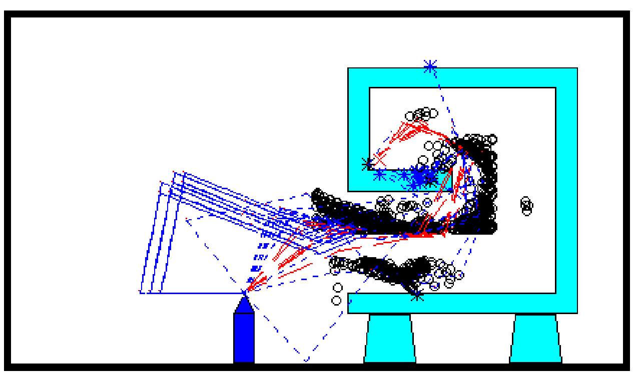

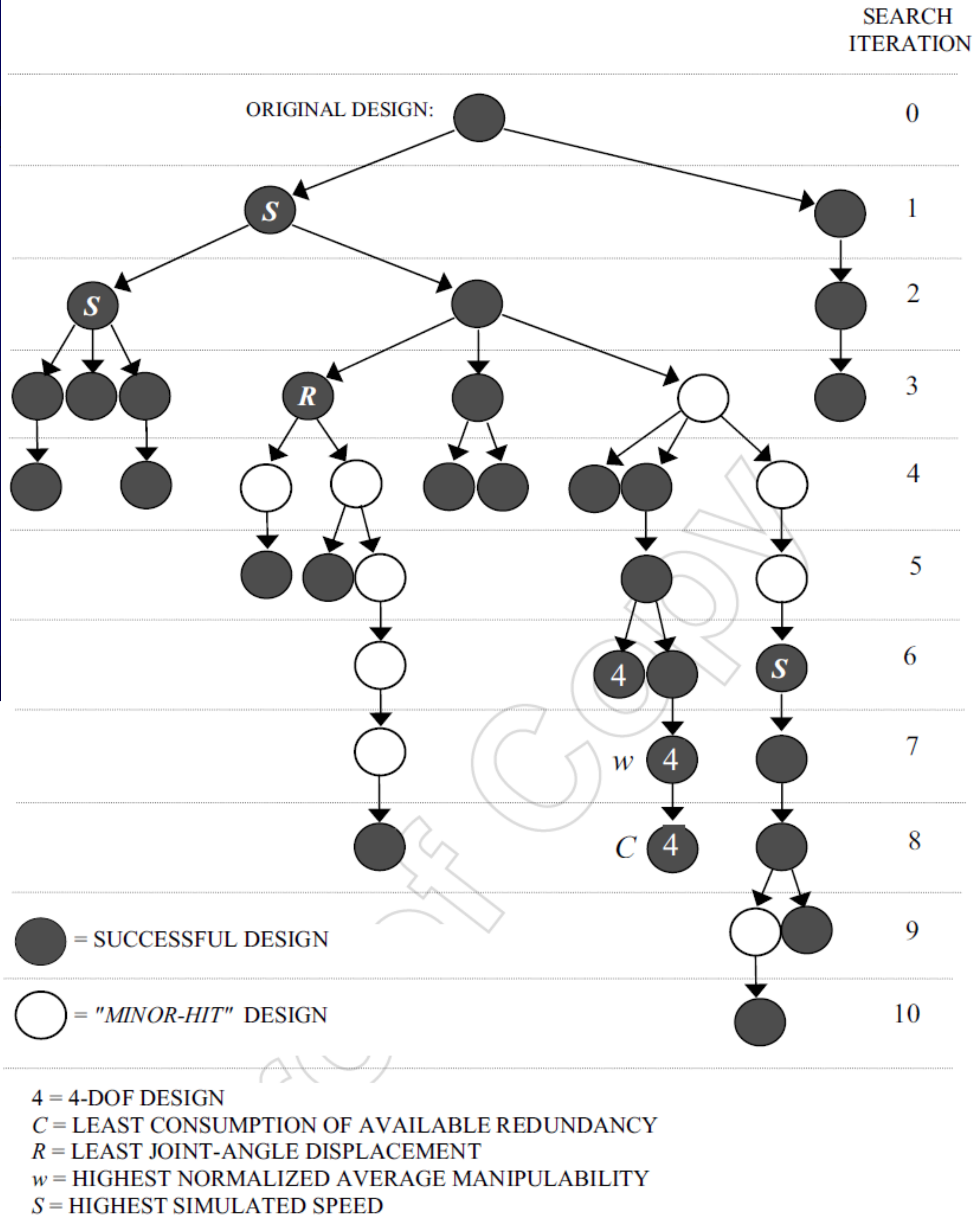

Robotic Arm Design

Selected Design from Search

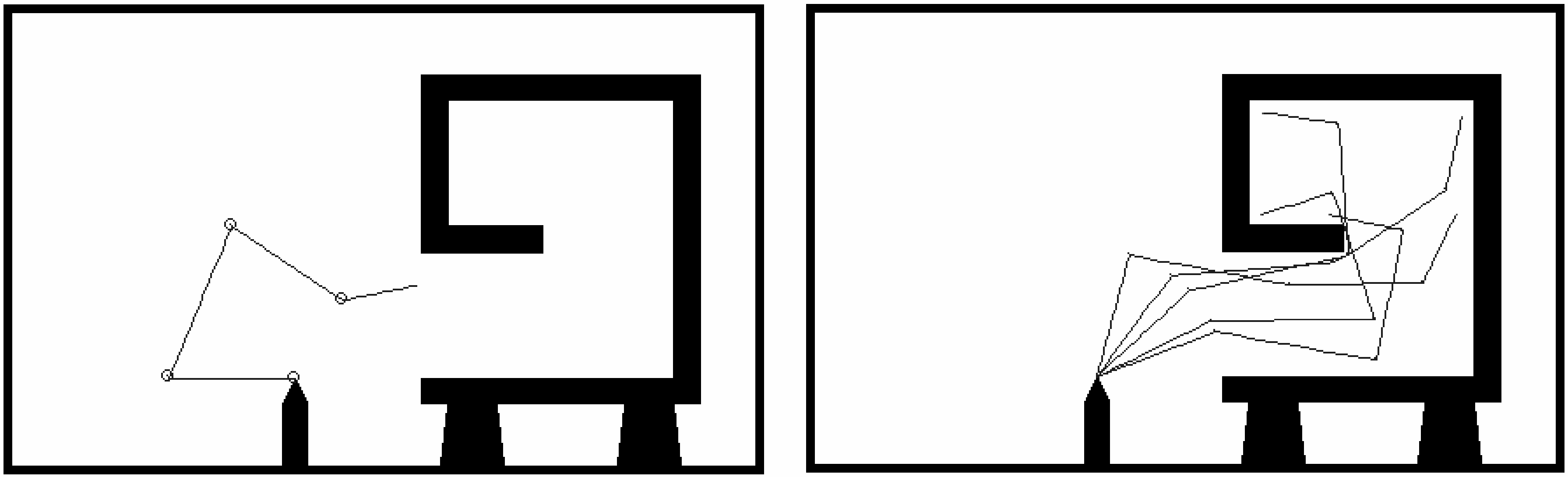

Wunderlich, J.T. (2004). **Simulating a robotic arm in a box: redundant kinematics, path planning, and rapid-prototyping for enclosed spaces**. In *Transactions of the Society for Modeling and Simulation International*: Vol. 80. (pp. 301-316). San Diego, CA: Sage Publications.

Robotic Arm Design

- This modified psuedoinverse path-planning works fine for rapidly prototyping designs
  - And can easily use simpler control scheme for real-time control if concerned about psuedoinverse velocity control implementation difficulties
- Rapid prototyping of *quality designs*
  - Dexterous
  - Minimal DOF
  - Low energy
  - Good geometric *fit*
  - Semi task-specific

Future Possibilities

- 3-D
  - Tubular primitives
  - Cube primitives
- Dynamic Model to optimize forces for cutting, drilling, material handling, etc.
- Learn environment (anticipate walls)
- Adaptive repelling fields
- Use COAR to drive design process
- Probabilistically complete search

Would many Hyper-Redundant Manipulators be optimal?

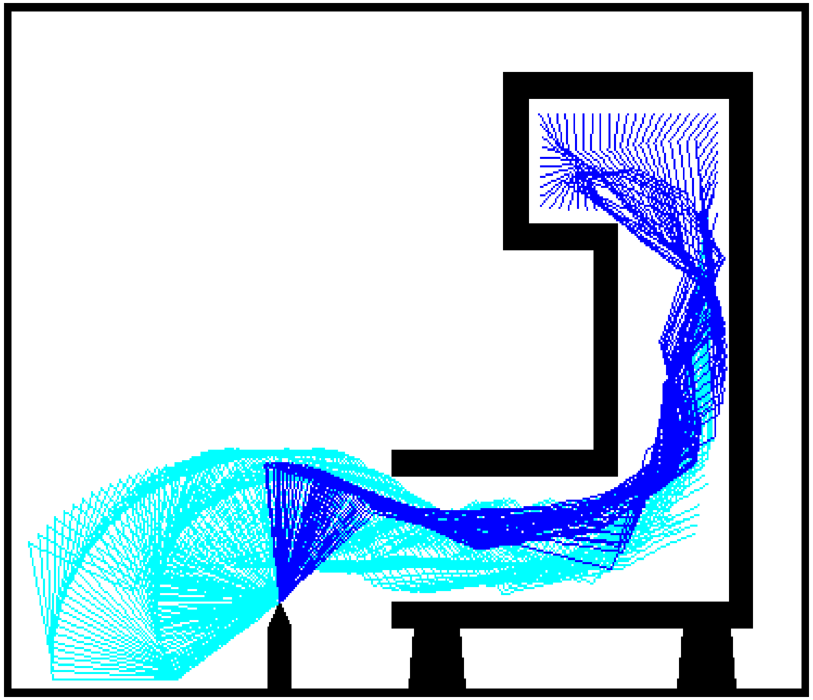

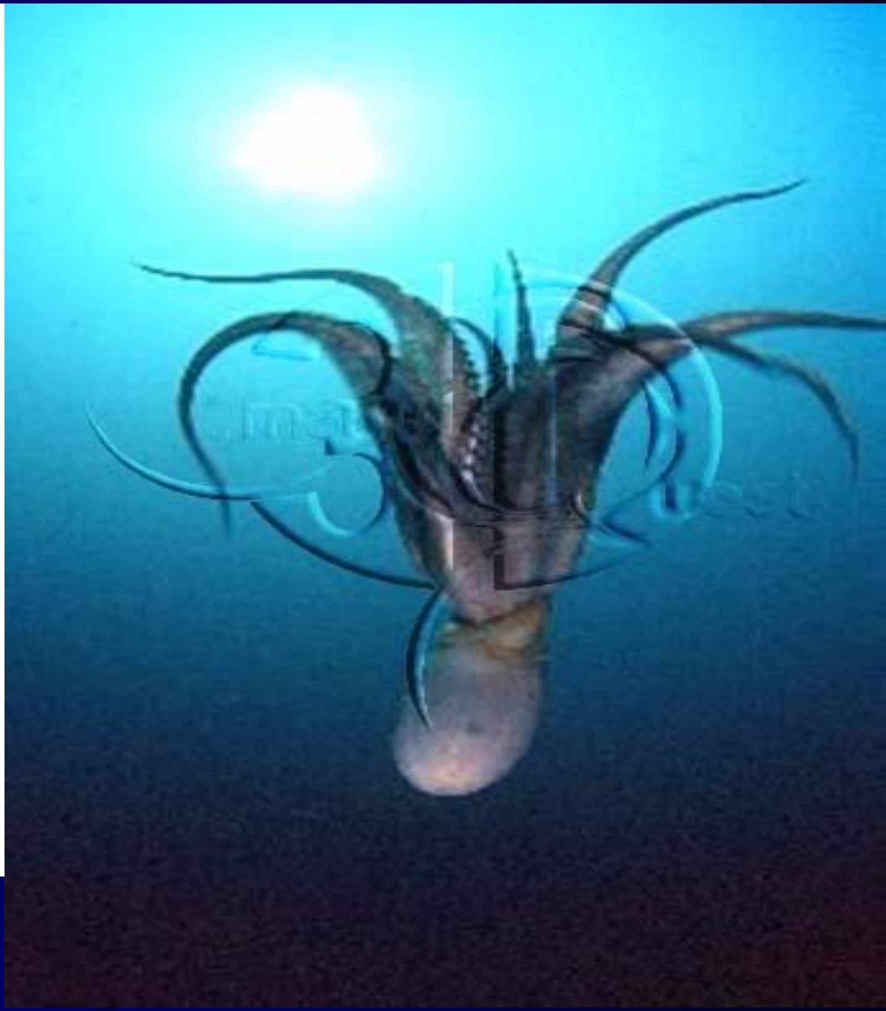

Other Dr. Wunderlich PhD Research in early 1990's

Telerobotics & Force-Feedback for assisting Quadriplegic Children

AI Dupont Children's Hospital, Applies Science & Engineering Lab

Wunderlich, J.T., S. Chen, D. Pino, and T. Rahman (1993). **Software architecture for a kinematically dissimilar master-slave telerobot**. In *Proceedings of SPIE Int'l Conference on Telemanipulator Technology and Space Telerobotics*, Boston, MA: Vol. (2057). (pp. 187-198). SPIE Press.

FIGURE 1. Test-Bed Control Scheme.

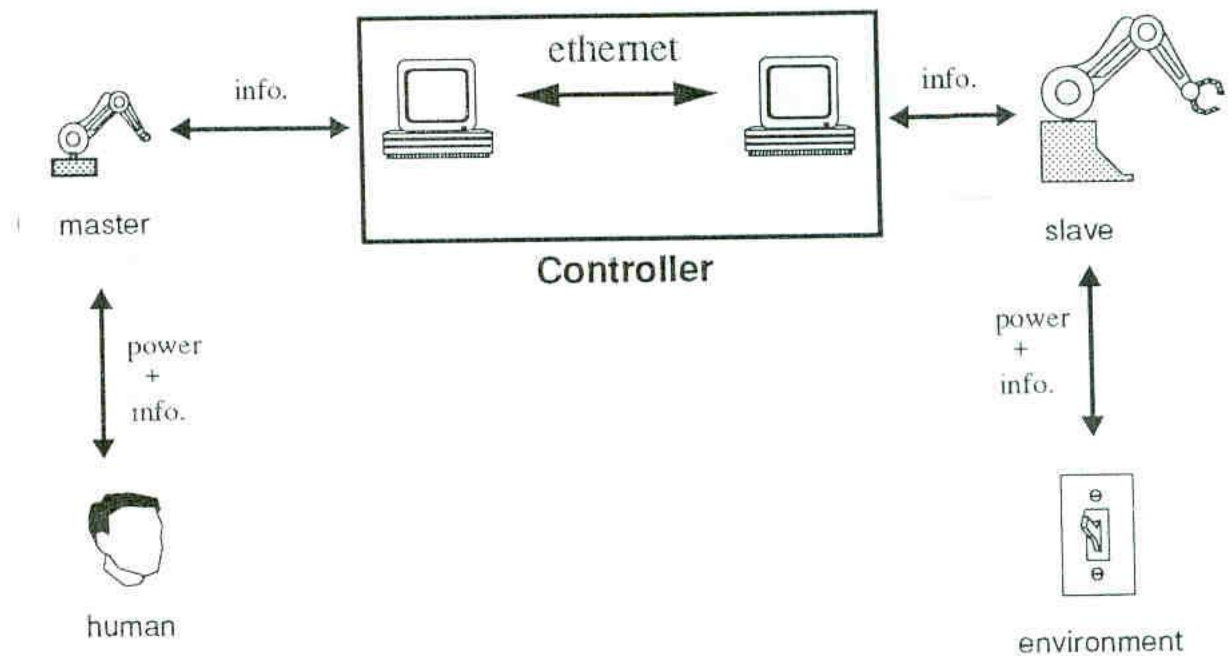

Other Dr. Wunderlich PhD Research in early 1990's

Telerobotics & Force-Feedback for assisting Quadriplegic Children

AI Dupont Children's Hospital, Applies Science & Engineering Lab

FIGURE 1. Test-Bed Control Scheme.

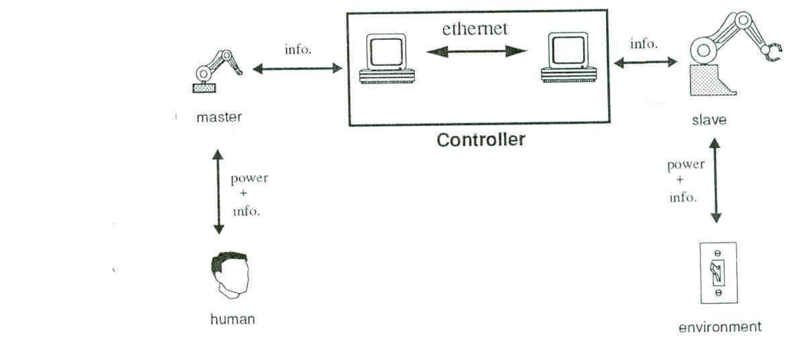

FIGURE 3. Force Reflection Scheme

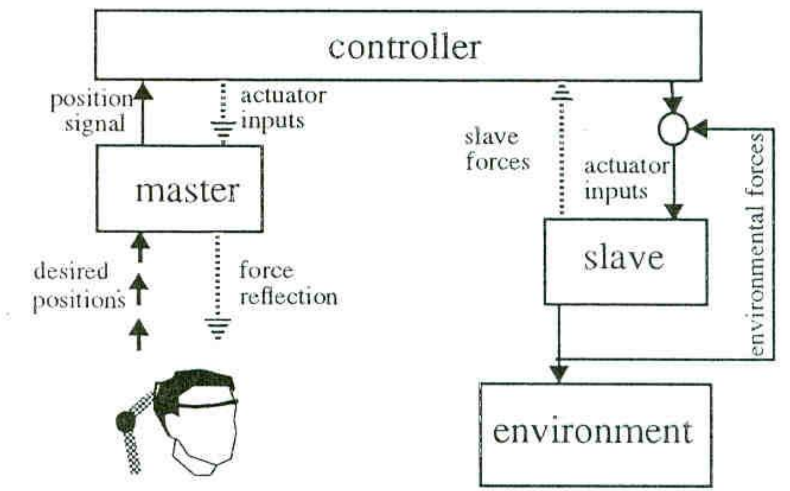

Wunderlich, J.T., S. Chen, D. Pino, and T. Rahman (1993). **Software architecture for a kinematically dissimilar master-slave telerobot**. In *Proceedings of SPIE Int'l Conference on Telemanipulator Technology and Space Telerobotics*, Boston, MA: Vol. (2057). (pp. 187-198). SPIE Press

Robotic Arms

STATICS

Endpoint Compliance Analysis

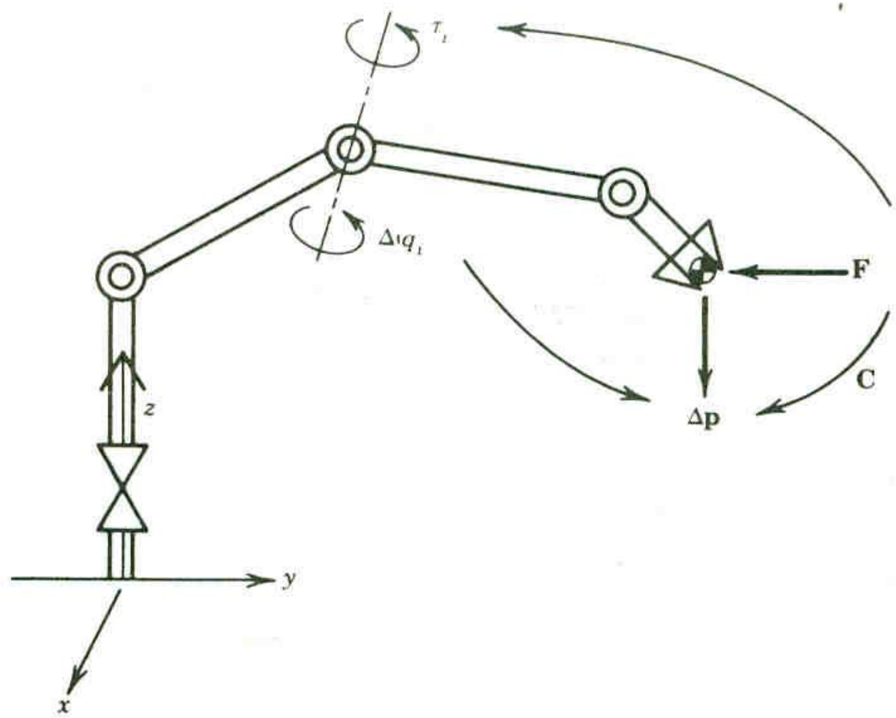

Endpoint compliance and joint servo stiffness.

$$\tilde{\tau} = \mathbf{J}^T \tilde{\mathbf{F}}$$

$$\mathbf{J} = \begin{bmatrix} -l_1 \sin\theta_1 - l_2 \sin(\theta_1+\theta_2) & -l_2 \sin(\theta_1+\theta_2) \\ l_1 \cos\theta_1 + l_2 \cos(\theta_1+\theta_2) & l_2 \cos(\theta_1+\theta_2) \end{bmatrix}$$

From 1992 J. Wunderlich talk at A.I. Dupont Research Institute including excerpts from several advanced robotics texts

Coordinate frames

Robotic Arms

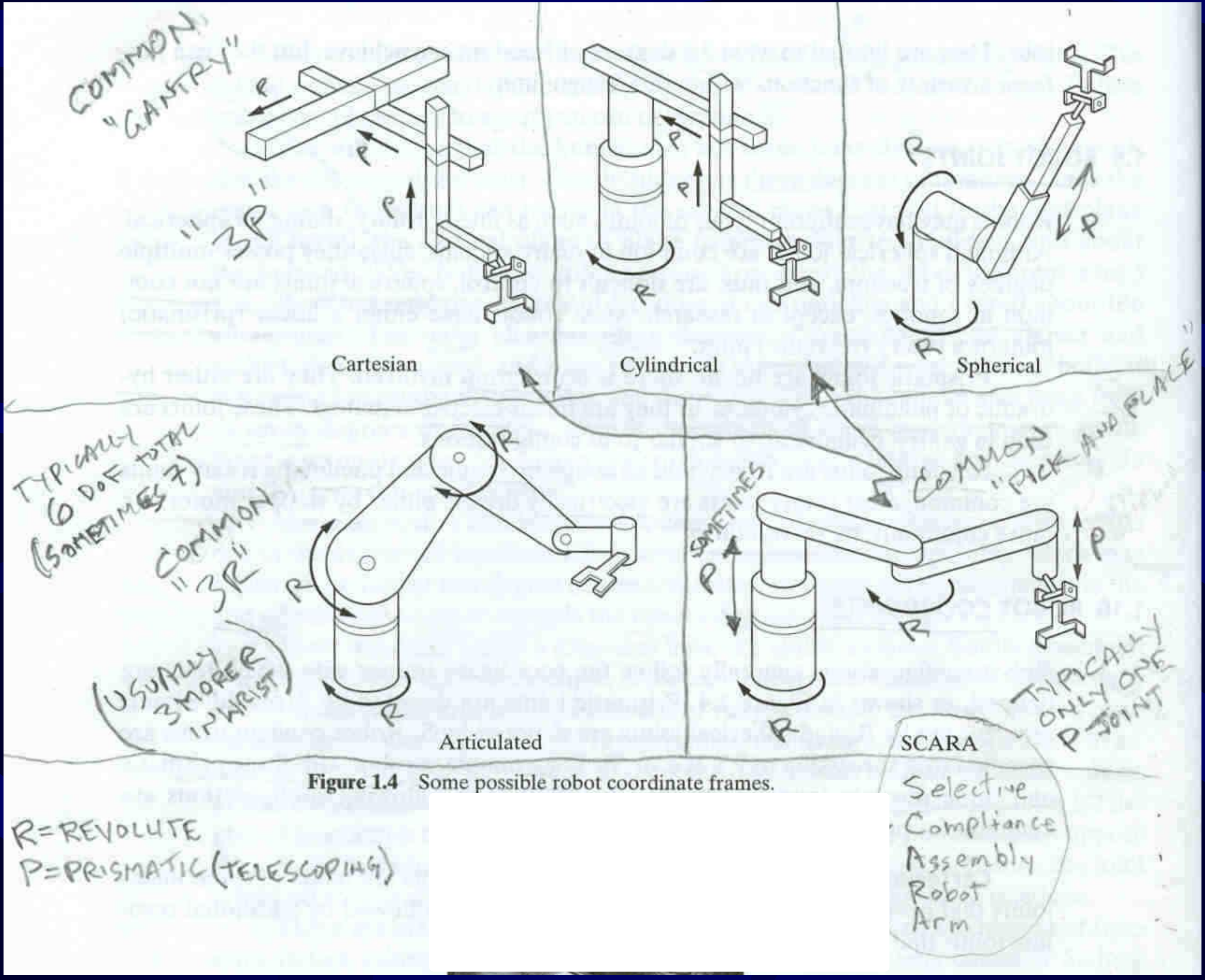

Figure 1.4 Some possible robot coordinate frames.

Source: **S. .B. Niku, *Introduction to Robotics: Analysis, Systems, Applications*, Prentice Hall, July 30, 2001.**

Tool reference-frames

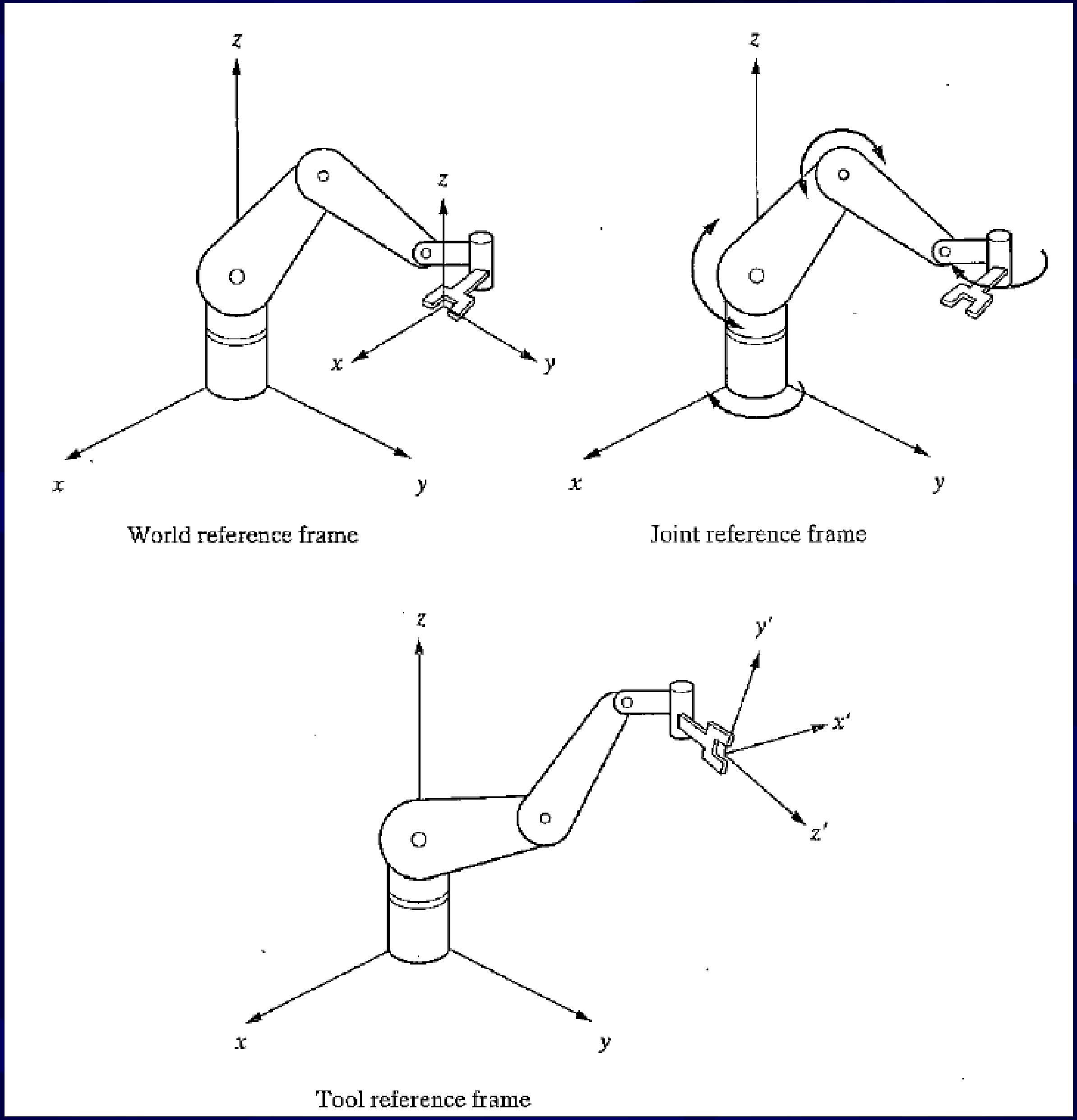

Source: **S. .B. Niku, *Introduction to Robotics: Analysis, Systems, Applications*, Prentice Hall, July 30, 2001.**

Robot Workspace Envelope
Defines reach of end-effector

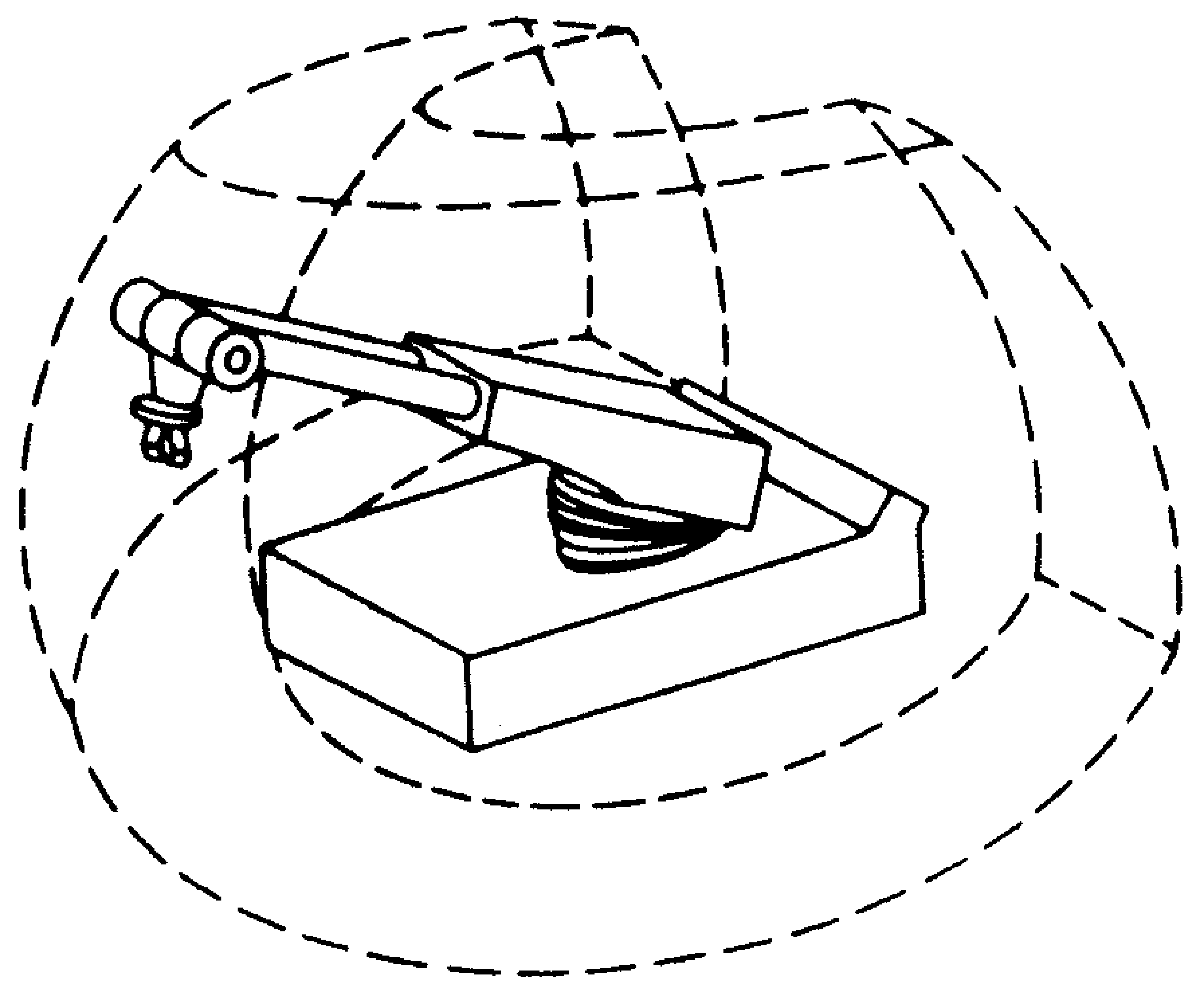

Source: http://faculty.petra.ac.id/dwahjudi/private/robot1.htm

Robot Workspace Envelope

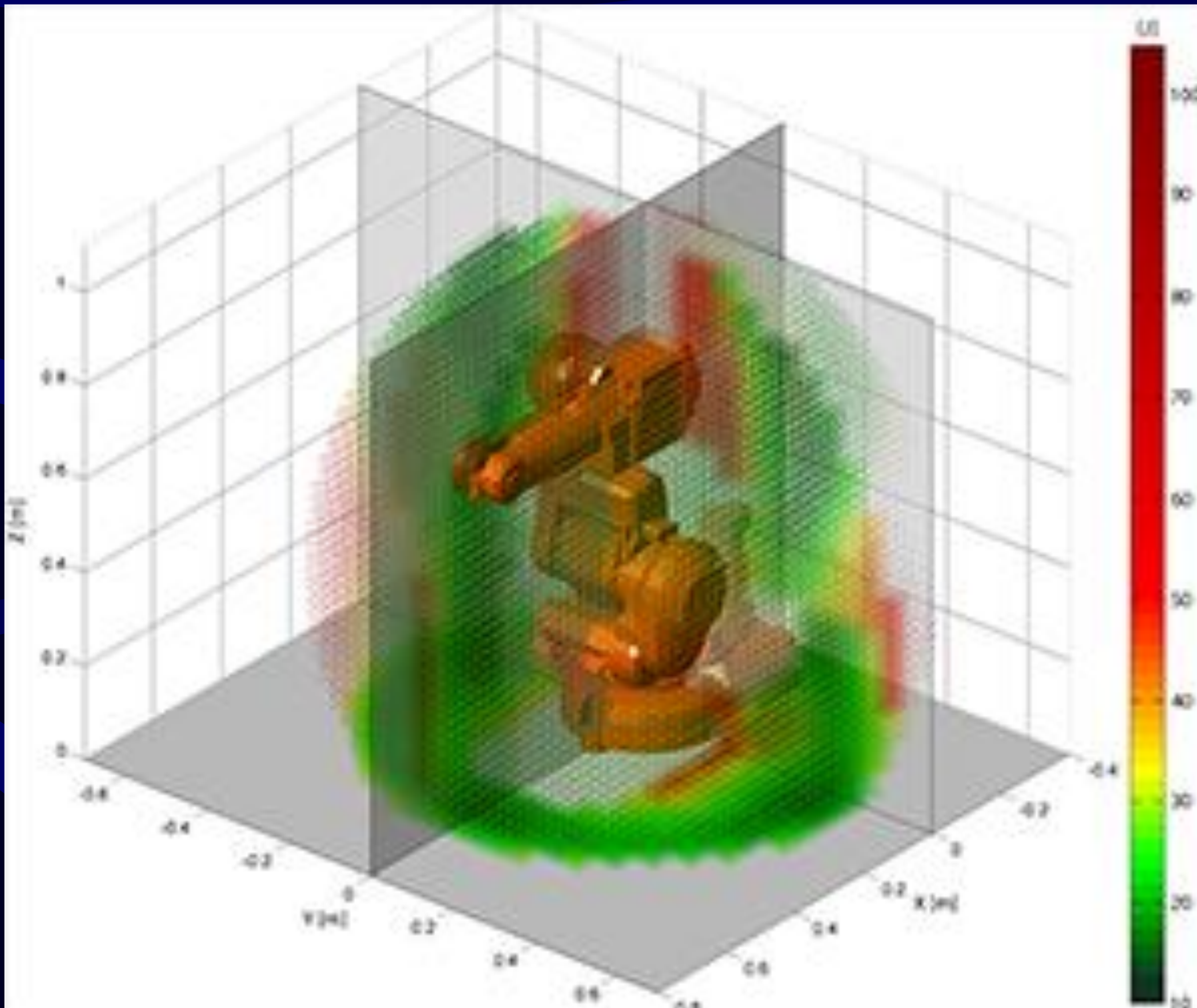

“robot’s energy map envelope in colours, an operator can keep the workpiece in the green zone and avoid the orange zone to save energy”

Source: http://faculty.petra.ac.id/dwahjudi/private/robot1.htm

Industrial Robot Manufacturers MOTOMAN (Japanese)

Robotic Arms

Source: http://doosanrobot.com/apply/arc.php

Industrial Robot Manufacturers MOTOMAN (Japanese)

Source: https://www.used-robots.com/blog/viewing/robotics-industry-growing-with-used-robots

Industrial Robot Manufacturers MOTOMAN (Japanese)

Robotic Arms

Source: http://robotpalletizing.co.uk/tag/motoman/page/2/

Industrial Robot Manufacturers
MOTOMAN (Japanese)

Robotic Arms

Source: http://robotpalletizing.co.uk/2013/01/

Industrial Robot Manufacturers
MOTOMAN (Japanese)

Robotic Arms

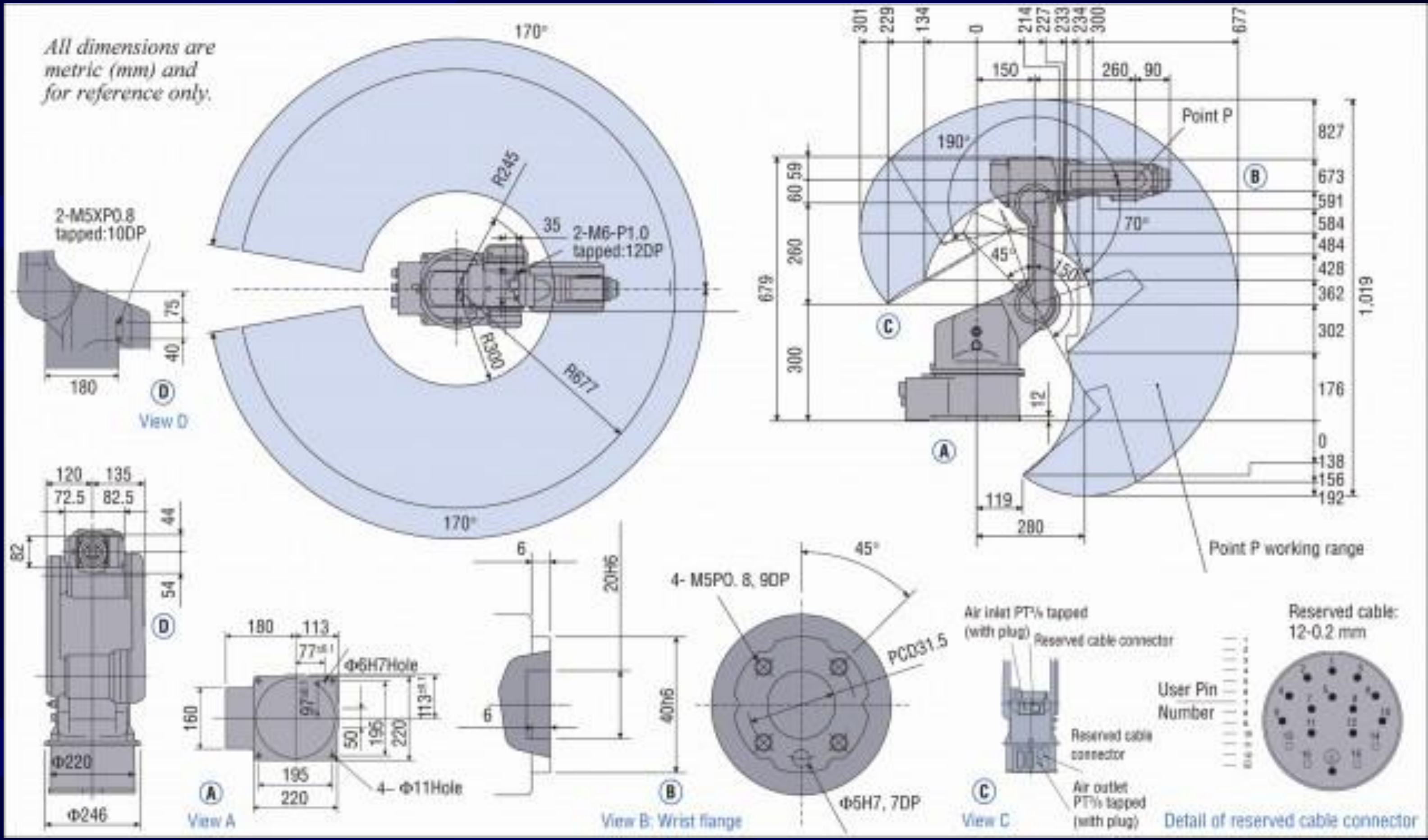

Source: http://research.fit.edu/rassl/motoman-sv3.php

Industrial Robot Manufacturers MOTOMAN (Japanese)

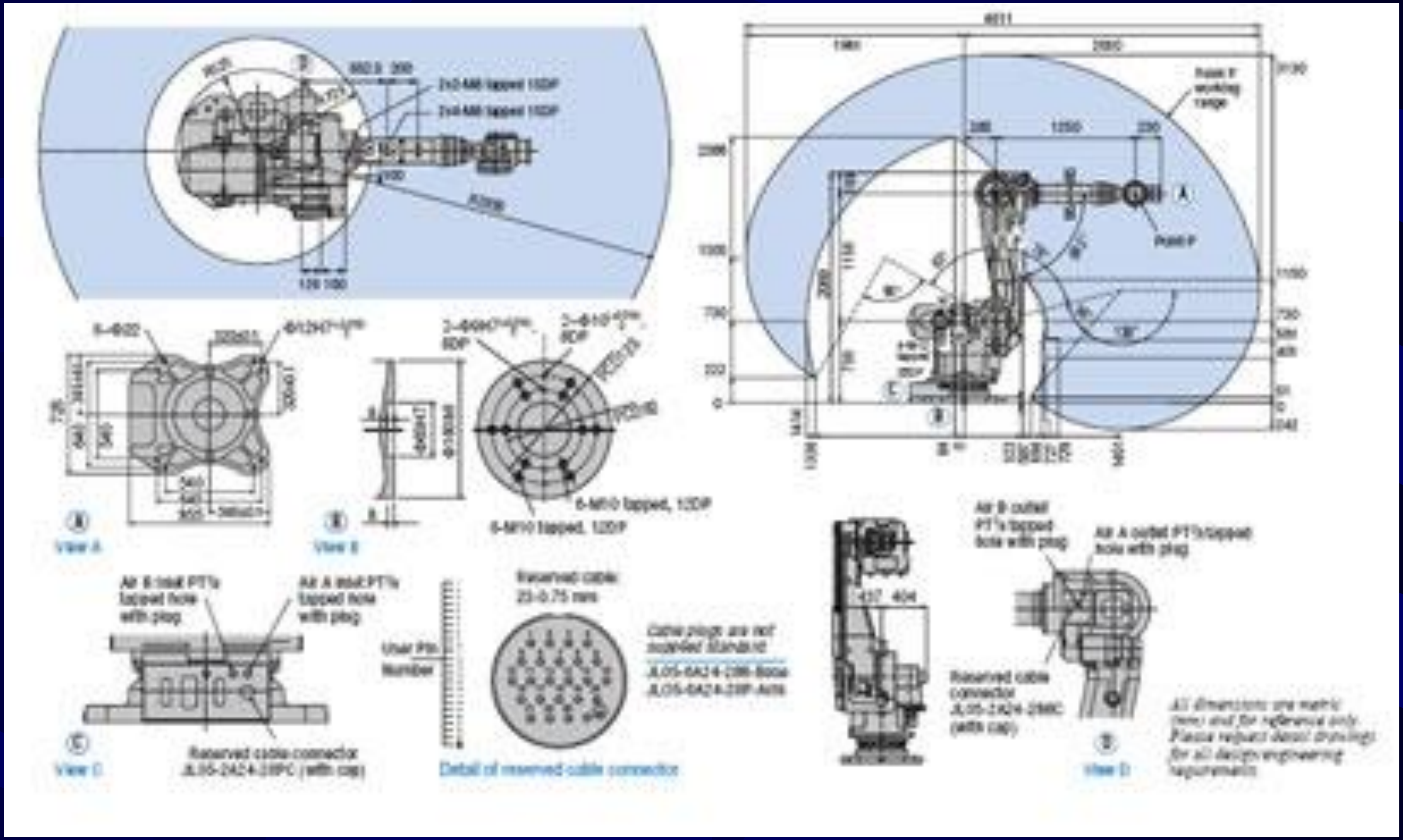

Source: http://research.fit.edu/rassl/motoman-sv3.php

Industrial Robot Manufacturers
MOTOMAN (Japanese)

Robotic Arms

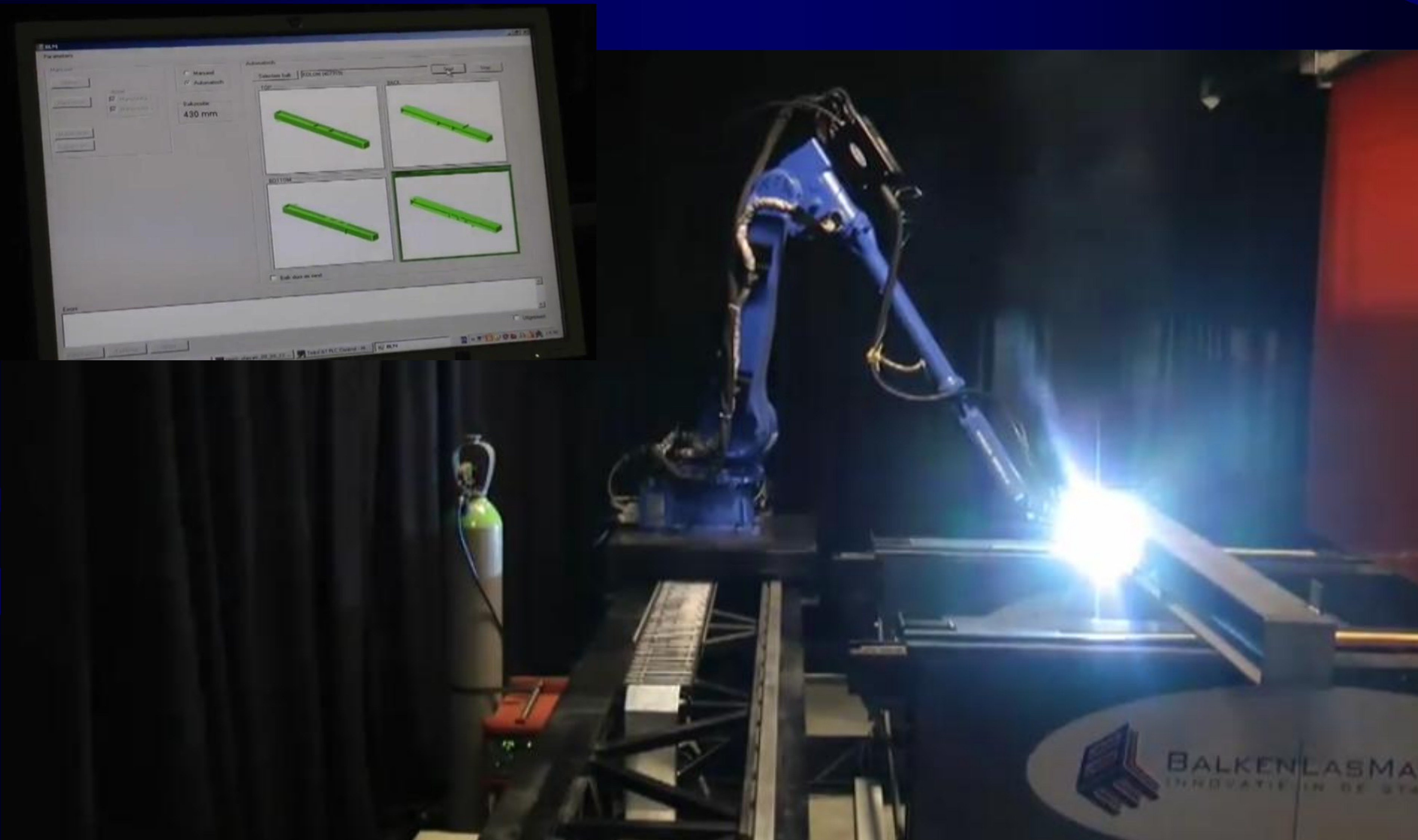

VIDEO: https://www.youtube.com/watch?v=361jCrhLSrA

Industrial Robot Manufacturers
KUKA (German)

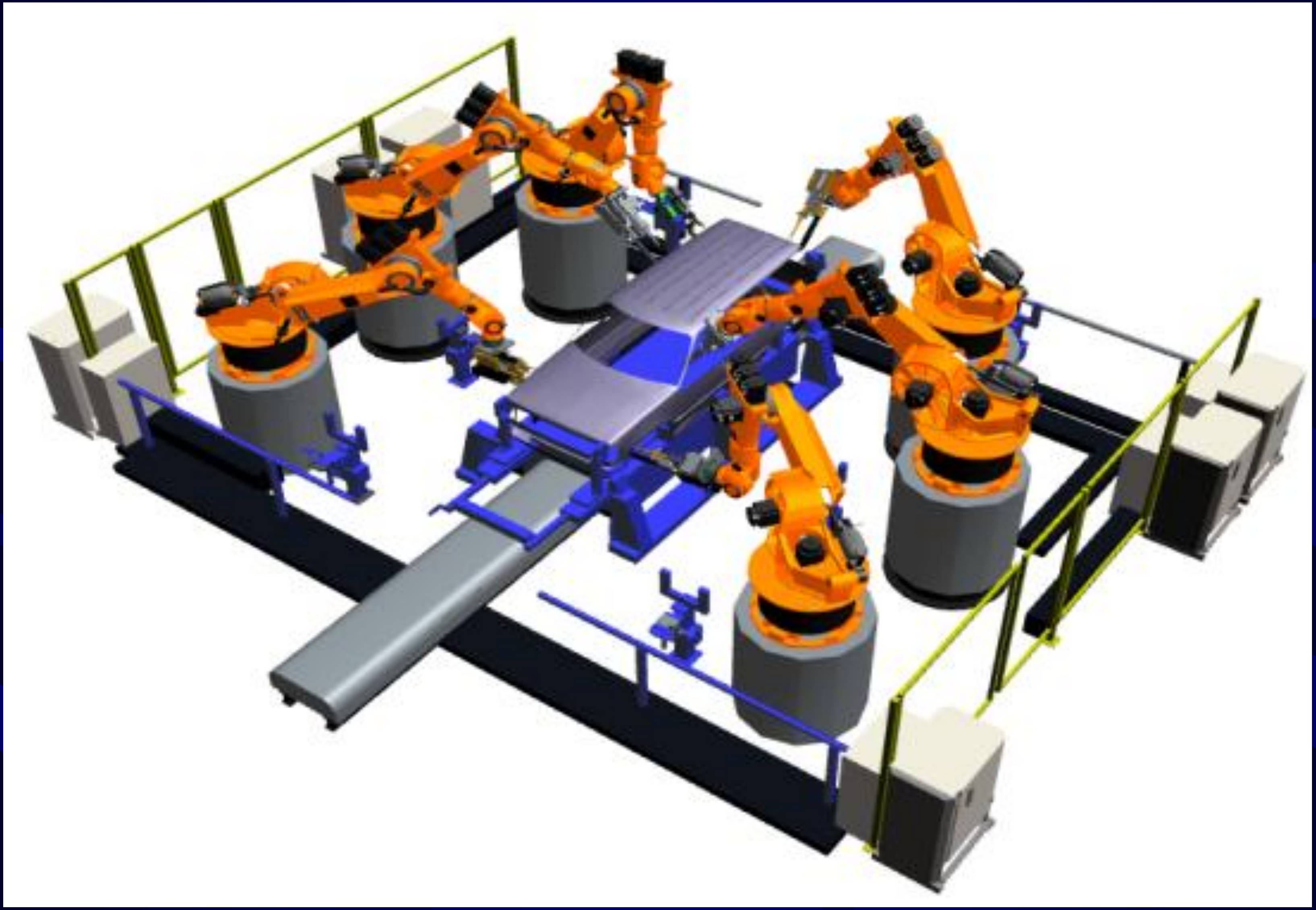

Source: http://www.kuka.be/kukasim/

Industrial Robot Manufacturers KUKA (German)

Robotic Arms

VIDEO: https://www.youtube.com/watch?v=p6NwH3G0V6Y /

Industrial Robot Manufacturers KUKA (German)

Robotic Arms

Source: https://www.pilz.com/en-AU/company/news/articles/073932

Industrial Robot Manufacturers
KUKA (German)

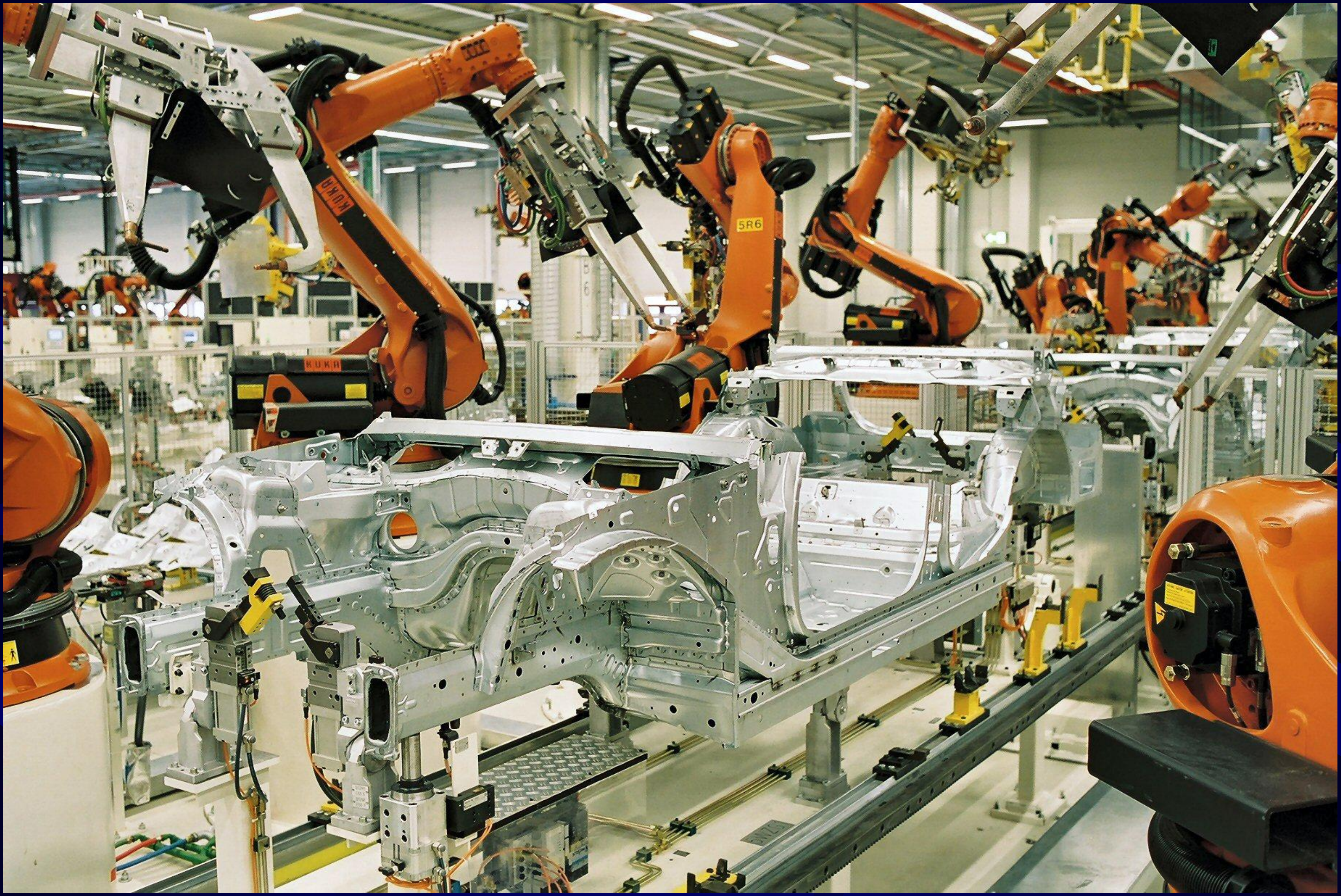

Source: https://en.wikipedia.org/wiki/KUKA

Industrial Robot Manufacturers KUKA (German)

Robotic Arms

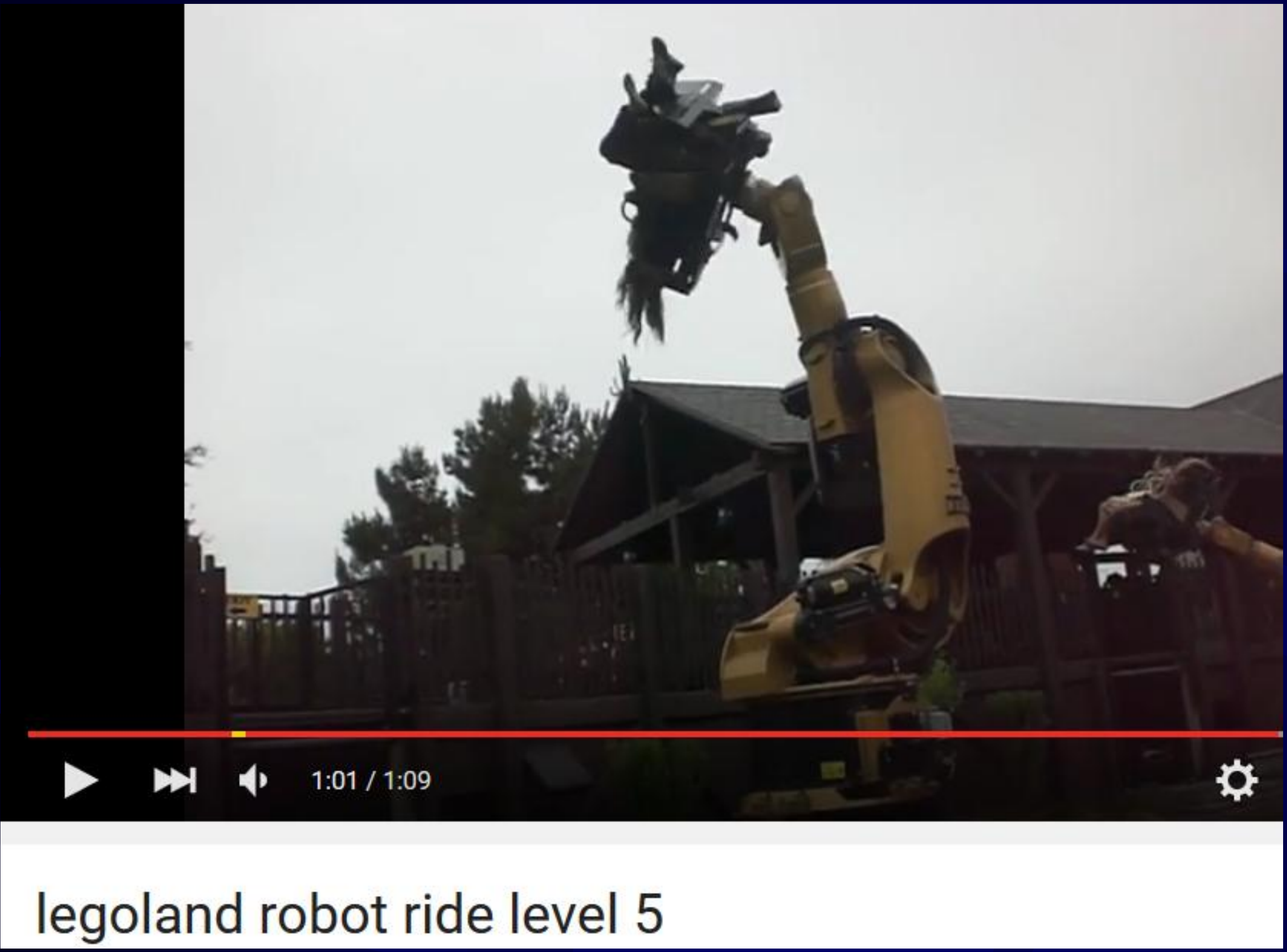

At Legoland in San Diego, CA

You pick level 1 to 5 to ride. And people squirt water canons at you while you ride

Dr. Wunderlich rode at level 4

VIDEO: https://www.youtube.com/watch?v=CVmX-NDSo2c

Industrial Robot Manufacturers KUKA (German)

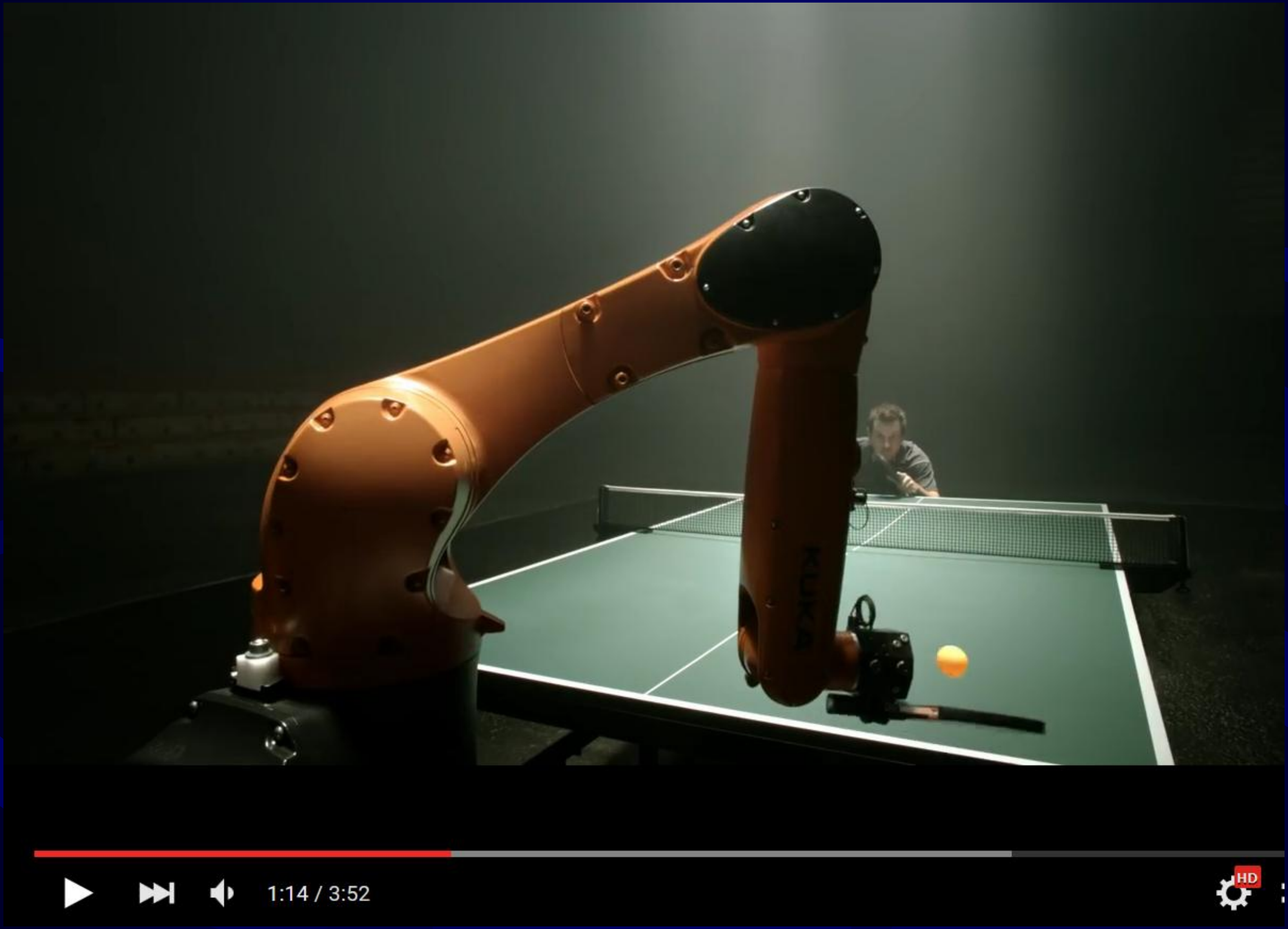

VIDEO: https://www.youtube.com/watch?v=tIIJME8-au8

Industrial Robot Manufacturers

Fanuc (Japanese)

Robotic Arms

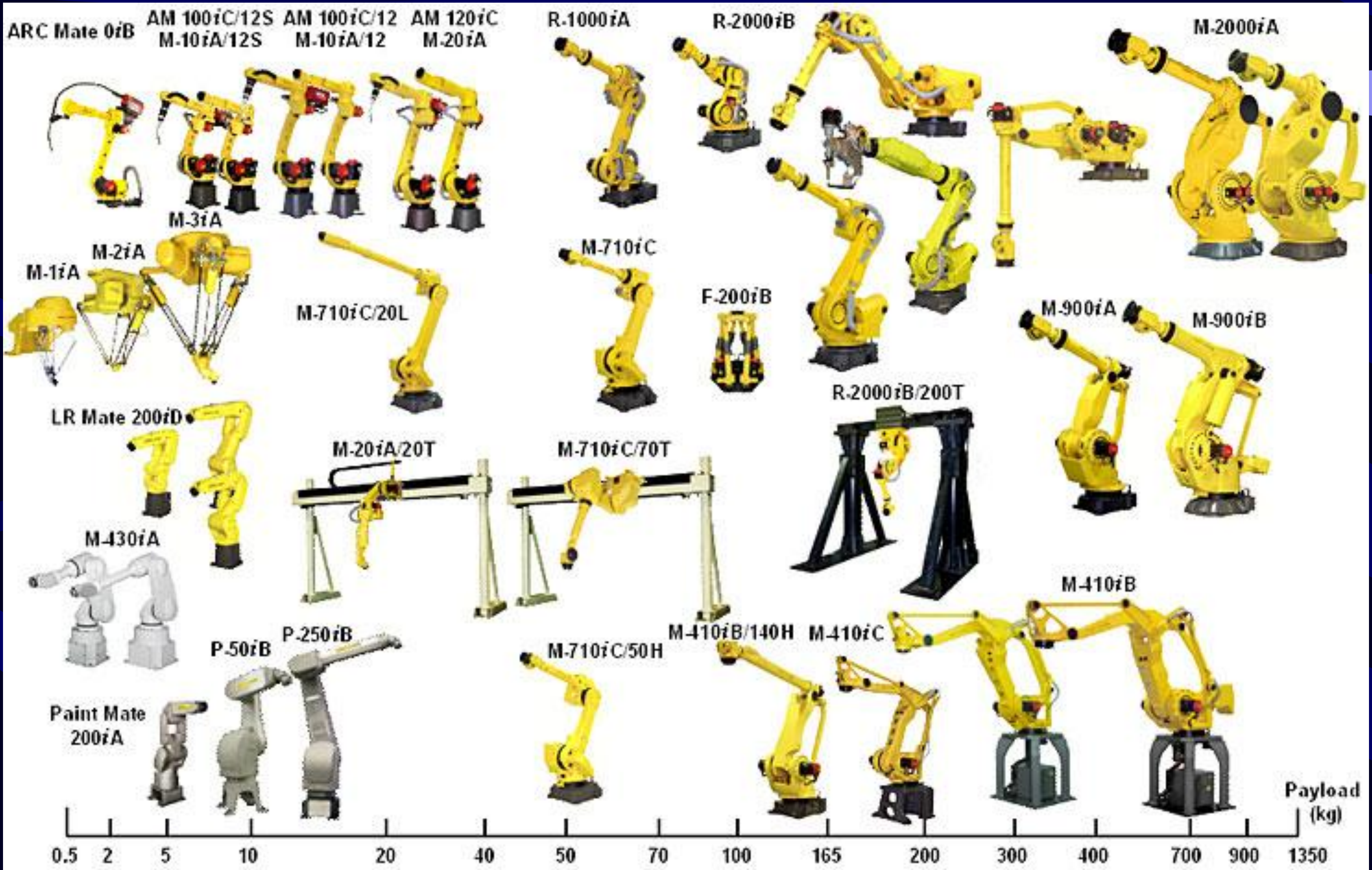

Source: http://www.fanuc.co.jp/en/product/robot/

Industrial Robot Manufacturers
Fanuc (Japanese)

Source: http://cdlms-inc.com/products.html

Industrial Robot Manufacturers

Fanuc (Japanese)

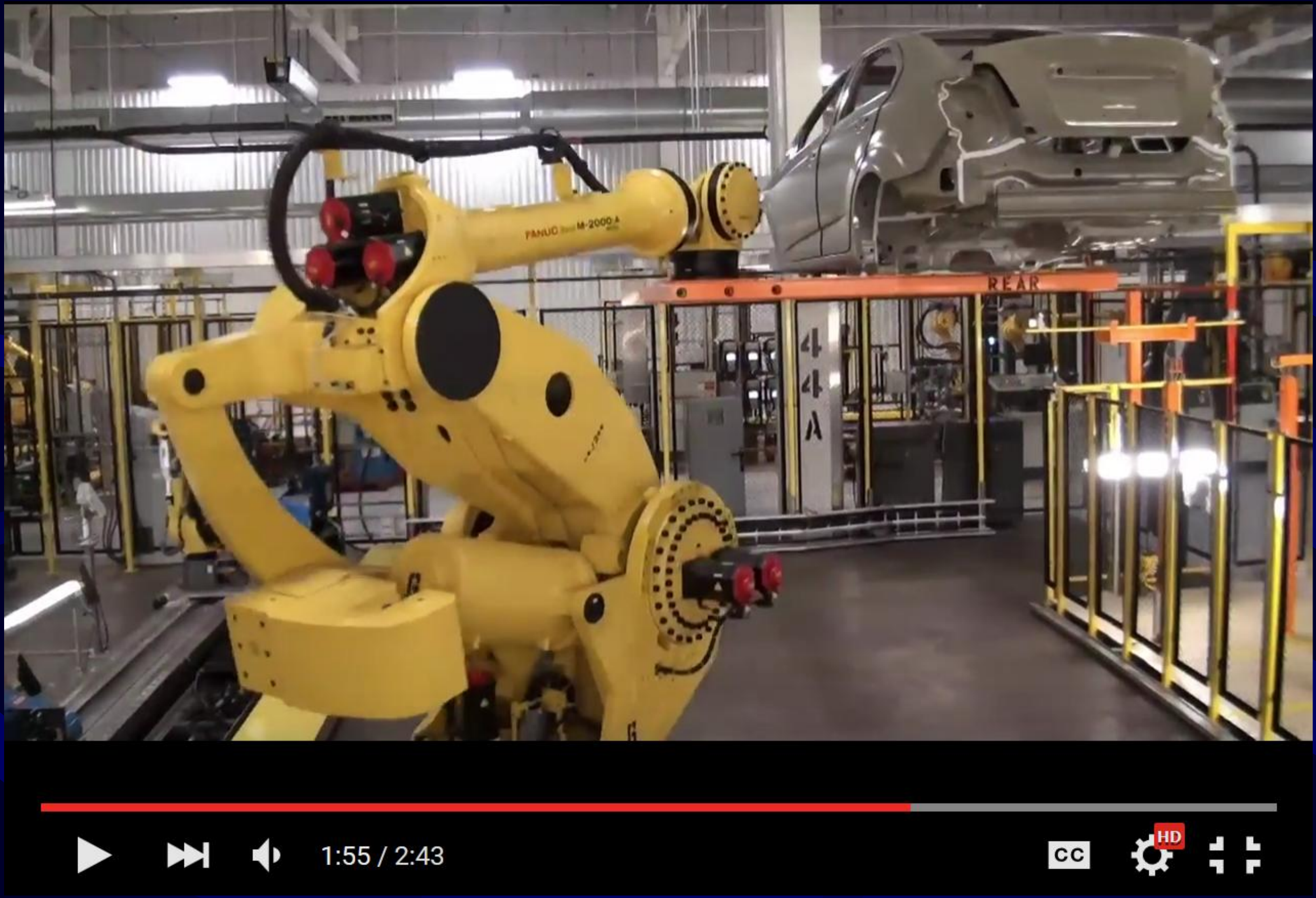

VIDEO: http://cdlms-inc.com/products.html

Industrial Robot Manufacturers

Fanuc (Japanese)

$250,000 Robot offered by Funuc to Etown College and J. Wunderlich after he visited Detroit Fanuc plant

Terms:

1) *College pays $25,000*
2) *Dr. Wunderlich to teach Fanuc Training to local industry*

Source: http://advatecllc.com/education/